Thesis-1985-R923a

Ruffini, John Lawrence, 1960-

Page Number 127

- ☐ Images
- ☐ Foldouts
- ☐ Maps

- ☐ Scanned
- ☐ Clean-up
- ☐ PDF

☐ Archive ☐ Projects

JS — Verified

8/25 — Date

THE APPLICABILITY OF HYDRODYNAMICALLY DERIVED MUSKINGUM FLOOD ROUTING COEFFICIENTS

By

JOHN LAWRENCE RUFFINI

Bachelor of Engineering

Darling Downs Institute of Advanced Education

Toowoomba, Australia

1983

Submitted to the Faculty of the
Graduate College of the
Oklahoma State University
in partial fulfillment of
the requirements for
the Degree of
MASTER OF SCIENCE
December, 1985

THE APPLICABILITY OF HYDRODYNAMICALLY DERIVED

MUSKINGUM FLOOD ROUTING COEFFICIENTS

Thesis Approved:

Thesis Adviser

C.E. Rice

Dean of the Graduate College

PREFACE

The author wishes to extend sincere appreciation to the following people and organizations for the role they played in facilitating this study:

Oklahoma State University, Oklahoma, for providing a research assistantship.

Dr. Bruce Wilson for his help and guidance as my thesis adviser.

The members of my research committee for their positive attitude and help with respect to my research and thesis, Dr. B. Wilson, Assistant Prof. Agric. Engineering, OSU, Dr. C. T. Haan, Prof Agric. Engineering, OSU, Dr. C. E. Rice, Research Leader, USDA Hydraulic Research Laboratory, Stillwater, OK.

My parents Raul and Vivienne Ruffini and my brothers and sisters for their love and and support. My freinds both here and at home.

TABLE OF CONTENTS

Chapter Page

LIST OF TABLES

LIST OF FIGURES

CHAPTER I

INTRODUCTION

From the earliest times man has endeavoured to survive by mastering his surroundings. He has continually improved the quality of his life by utilizing the natural resources of his planet. Water is one such resource. It is an essential part of our existance. We drink it, bath in it, grow our food with it and dispose of our waste in it. A large percent of our useable water is conveyed in rivers and channels. The movement of water in these rivers and channels therefore affects our lives beneficially or adversely.

In a river basin rainfall can produce runnoff. In periods of low rainfall, a stream or river flows at its lowest rate resulting in a reduced water supply, a poorer quality of water, and a less navigable channel. In periods of high rainfall, flooding can occur causing damage to valuable agricultural property and expensive river basin structures . The ability to predict water conveyance is therefore important.

Mathematical models are used to evaluate the impacts of water movement. The models simulate the depths and rates of flow in a channel as the result of rainfall and runoff

within a river basin. An important component in these simulations is the movement of flood waves through channels. This component is predicted with flood routing techniques. Water resources engineers use flood routing techniques in the planning, design, regulation and management of structures, rivers and channels in river basins.

One the most widely used hydrologic flood routing methods is the Muskingum flood routing technique. The Muskingum method is a simple, lumped parameter model based on the assumptions of a linear system. The accuracy of this method depends on the values of the parameters K and x. Empirical techniques are available to determine K and x for gaged rivers. Physically based techniques, however, are needed for ungaged rivers. Since most rivers and streams are ungaged, the evaluation of the Muskingum parameters with physically based techniques is an important problem. Dooge et al. (1982) have addressed this problem by relating the Muskingum parameters K and x to the hydraulic parameters of the channel system.

Objectives

The purpose of this study was to evaluate the accuracy of Dooge et al.'s approach and to examine conditions for its use on streams by:

(a) Comparing the simulation results from Dooge et al.'s linear Hydrodynamic Muskingum routing method to the simulation results obtained from a finite element solution

to the Saint Venant equations.

(b) Comparing the simulation results from Dooge et al.'s nonlinear Hydrodynamic Muskingum routing method to the simulation results obtained by a finite element solution to the Saint Venant equation.

(c) Conducting sensitivity analysis.

Scope of the Study

A flow model was developed using the techniques proposed by Dooge et al. (1982) . A finite element solution to the St. Venant equations was used to evaluate the accuracy of this approach. Predicted results from the linear Hydrodynamic Muskingum method were compared to simulated results from the Saint Venant equations for varying lengths, slopes, roughness coefficients, and channel geometries.

A nonlinear feature was incorporated into the flow model by allowing K and x to vary with distance downstream. The predicted results from the nonlinear model were compared to simulated results from the Saint Venant equations for varying lengths, slopes, roughness coefficients, inflow hydrographs, and channel geometries. The models sensitivity to variations in subreach length, time step, and reference flow value were examined. Finally, an observed inflow hydrograph was routed through a natural channel using the nonlinear Hydrodynamic Muskingum method and the finite element solution to the Saint Venant equations. The predicted outflow hydrographs from the two methods were

compared to observed values in a natural channel.

CHAPTER II

LITERATURE REVIEW

Introduction

Flood routing techniques are used to predict the movement of flood waves through irregular shaped channels. These techniques are divided into two general categories: hydrologic routing and hydraulic routing. Hydrologic routing techniques are based on a mass balance equation for an entire reach length. Flow rate functions are evaluated using either empirical data or idealized water surface profiles. In contrast, hydraulic routing techniques are based on a mass balance equation applied to infinitesimally small reach length within a channel reach. Flow rate functions in these models are usually evaluated using the equation of motion. The hydrologic routing methods are relativily easy to solve and are not limited by extensive input data. On the other hand, hydraulic routing methods are based on established and sound physical principles and are generally more applicable to a wider range of situations. Hydrologic routing should only be used when backwater effects and surges are unimportant, such as a flood wave moving down a long river.

In the following sections hydraulic models will be

discussed using the one-dimensional unsteady flow equations of open channel flow. The discussion on hydrologic models will be limited to those techniques corresponding to the Muskingum method.

One-Dimensional Unsteady Flow Equatons

This section will describe three different hydraulic routing models: the complete dynamic wave model, the kinematic wave model and the diffusion wave model. All three models use the equation of continuity in a similar manner, but differ in their use of the momentum equation. These differences will be illustrated in this secton.

Dynamic Wave Model

The partial differential equations describing open channel flow were first developed by Barre de Saint Venant in 1871 and are usually called the Saint Venant equations. More recently Chow (1964), Gilcrest (1950) and Henderson (1966) have derived these equations by considering the momentum balance and forces acting on a cross-section of flow. Strelkoff (1969) has presented a more rigorous derivation by using the point form of the equations of continuity and energy for incompressible flow. Kouiss (1975) has also given a similar derivation. Fread (1973) has shown that the Saint Venant equations form a system of two nonlinear, first order, first degree partial differential equations of the hyperbolic kind for which no analytical

solutions are known. Numerical solutions, however, are possible for given initial and boundary conditions.

Strelkoff (1969), Fread (1973), Kouiss (1975) have based their derivations on the following assumptions as summarized by Weinmann (1977):

- the flow is one dimensional,
- the flow is incompressible and homogeneous in density,
- the bed of the channel is fixed,
- the longitudinal axis of the channel can be approximated by a straight line,
- the bottom slope of the channel is small,
- the flow is gradually varied with hydrostatic pressure prevailing at all points in the flow, such that the vertical acceleration of water may be neglected,
- the water surface is horizontal and the velocity constant across any section perpendicular to the longitudinal axis (i.e. the velocity distribution coefficient = 1),
- the resistance coefficient for steady uniform flow is considered applicable and an empirical resistance equations such as Manning's equation describes the resistance effects,
- the effects of wind resistance on the water surface and of the Coriolis force can be neglected.

The equations for gradually varied, unsteady channel flow with lateral inflow can be written as:

Continuity,

$$\frac{\partial Q}{\partial X} + \frac{\partial A}{\partial t} = q \qquad (2.1)$$

Momentum,

$$\frac{\partial V}{\partial t} + V\frac{\partial V}{\partial X} + \frac{\partial V}{\partial A}.q + g\frac{\partial y}{\partial X} = g(S_o - S_f) \qquad (2.2)$$

where,

Q =volumetric flow rate [L^3/T],

q =lateral inflow per unit length of channel [L^2/T],

A =cross-sectional area [L^2],

S_o =bed slope [L/L],

Sf =friction slope [L/L],

V =mean velocity [L/T],

g =acceleration of gravity [L/T^2],

t =time [T],

X =distance down the channel [L],

y =depth of flow [L],

Differences between the dynamic wave model and the other hydraulic flood routing methods can be illustrated with a velocity-resistance equation. As an example, flow rate for nonuniform flows can be approximated using Manning's formula as,

$$Q = \frac{1}{n} R^{2/3} A S_f^{1/2} \qquad (2.3)$$

where n is the roughness coefficient, R is the hydraulic radius.

For uniform flow or normal flows (Qn) flow rate can also be predicted from Manning's formula, or,

$$Q_n = \frac{1}{n} A R^{2/3} S_o^{1/2} \qquad (2.4)$$

Thus,

$$Q = Q_n \frac{S_o^{1/2}}{S_f^{1/2}} \tag{2.5}$$

Neglecting lateral inflow, eq 2.2 can be expressed as

$$\underset{\text{friction}}{S_f} = \underset{\text{gravity}}{S_o - \frac{\partial y}{\partial X}} \underbrace{- \frac{V}{g}\frac{\partial V}{\partial X} - \frac{1}{g}\frac{\partial V}{\partial t}}_{\text{inertia}} \quad \underset{\text{pressure}}{} \tag{2.6}$$

By substituting eq 2.5 into 2.6, the differences in the three hydraulic models can be illustrated as;

$$Q_o = \sqrt{Q_n \left(1 - \frac{1}{S_o}\frac{\partial y}{\partial X} - \frac{V}{g.S_o}\frac{\partial V}{\partial X} - \frac{1}{g.So}\frac{\partial V}{\partial t}\right)} \tag{2.7}$$

Kinematic

Diffusion

Dynamic

Equation 2.7 illustrates the differences between the complete dynamic equation and the simpler diffusion and kinematic wave models. If the inertia terms are neglected the dynamic equation is reduced to the diffusion wave model. If both the inertia and pressure terms are neglected, the dynamic equation is further simplified to the kinematic wave model. Details of the kinematic and diffusion wave models are given in the following sections.

Kinematic Wave Model

Lighthill and Whitham (1955) have shown that kinematic waves (i.e. motion in time and space disregarding mass and force) exist when the flood wave movement can be described

by the equation of continuity and Kleitz-Seddon law. Kinematic waves travel without attenuation. The shape of the entire flood wave, however, does change because of variation in travel speed with flow rate (Weinmann, 1977).

Kinematic waves have only one characteristic and its speed can be expressed in terms of the Kleitz-Seddon law (Henderson, 1966), or,

$$c_k = \frac{dQ}{dA} = \frac{dX}{dt} \qquad (2.8)$$

where c_k =wave celerity.

By using the continuity equation (eq 2.1) and Kleitz-Seddon law (eq 2.8) and neglecting lateral inflow the following equation can be written,

$$\frac{\partial Q}{\partial t} + c_k \frac{\partial Q}{\partial X} = 0 \qquad (2.9)$$

The kinematic wave model uses a single value rating curve and only provides for translational effects. Its application is restricted to cases where attenuation is not significant. The model successfully simulates well confined, moderately steep channels and overland flow.

Diffusion Wave Model

The diffusion wave model was obtained by Lighthall and Whitham (1955) by adding a diffusion term to the kinematic wave model. The diffusion wave can also be derived by linearizing the Saint Venant equations and neglecting the

inertia terms (Ponce, 1978). The standard diffusion equation can be written as,

$$\frac{\partial Q}{\partial t} + c_k \frac{\partial Q}{\partial X} = D \frac{\partial^2 Q}{\partial X^2} + c_k q \qquad (2.10)$$

where D = hydraulic diffusivity.

Ponce (1981) showed that the diffusion wave models are applicable for a wider range of bed slopes and wave periods than the kinematic wave model. The diffusion wave model breaks down when acceleration effects or downstream disturbances become important. Ponce et al. (1982) developed the following criteria to determine when the diffusion wave will predict acceptable results.

$$T_r S_o \left[\frac{g}{y_o}\right]^{1/2} >= 15 \qquad (2.11)$$

where T_r = time to peak of the inflow hydrograph, g is the gravitational acceleration and y_o is the depth of flow at reference flow rate. The accuracy of the diffusion wave model improves as the left hand side of equation 2.11 becomes larger.

Numerical Solutions of Dynamic Wave Equations

Finite Difference Models

Weinmann and Laurenson (1977) discuss the various finite difference schemes used to convert the momentum equation and the continuity equation into algebraic

(difference) equations. These equations may be solved for y and V at finite incremental values of X and t. The solution schemes can be categorized into four groups:

- finite difference schemes that solve the characteristic equations for y and V at (X,t) values defined by the characteristic grid,
- explicit finite difference schemes that solve the characteristic equations using a rectangular X-t grid,
- explicit finite difference schemes for the original equations using a rectangular X-t grid,
- implicit finite difference scheme for the original equations using a rectangular grid.

Isaacson et al. (1966) pioneered this work by applying an explicit finite difference scheme to flood routing in the Ohio River. Amein and Fang (1970) used an implicit scheme to simulate floods in natural channels in North Carolina. Pinder and Saver (1971) predicted flood wave attenuation from bank storage using an explicit scheme. Fread (1973) used implicit four-point and weighted four-point finite difference schemes to investigate routing problems. Chaudry and Contractor (1973), Ligget and Woolhiser (1967),Viessmann et al. (1972) and many others have presented implicit and explicit finite difference solutions to approximately solve the Saint Venant equations. Explicit methods must meet a stability condition which relates the size of the time step to the size of the distance step (Amein and Fang, 1970). An implicit scheme is usually preferred over an explicit scheme

. Implicit schemes are inherently more stable.

Finite Element Methods

The finite element method discretizes the distance or region into elements in which polynomials are fitted to minimize error between exact and approximate solutions. This differs from the finite difference method which discretizes the governing differential equation directly. The finite element method therefore has an advantage over the finite difference method when complex geometries are being modelled (Myers 1971).

Cooley and Moin (1976) applied a finite element technique to the space derivatives of the Saint Venant equations. Difficulties were encountered in the error analysis stage because finite difference approximations were still used for the time derivatives. Nwaogazie and Tyagi (1984) presented finite element solutions for the complete dynamic model, the diffusion model, and the kinematic model using weighted implicit and explicit schemes. The time derivatives were approximated using a finite difference technique. The author found an error in the Nwaogazie and Tyagi (1984) finite element formulation of the momentum equation. The correct formulation is given in Appendix E.

The United States Army Corps of Engineers have incorporated a finite element solution to the St. Venant equations in their Stream Hydraulics Package based on work

by Smith (1979). The finite element solution uses Galerkin's weighted residual method (Zienkiewicz, 1977). A linear function is used to approximate the depth of flow and a quadratic function is used to describe unit width flow rate. Thus, a three node element is used to model flow in a subreach with values of flow being defined at both ends and at the middle, and depth at the ends only. The time dependent terms are modelled using an implicit finite difference scheme. The Newton Raphson method is used to reduce the nonlinear set of simultaneous equations (resulting from the Galerkin method) to a purely simultaneous form. An iteration technique is then used to reach a converged solution of the simultaneous equations. Gauss elimination is used in the intermediate steps to solve the matrix equations.

Classical Muskingum's Method

Original Formulation

McCarthy (1938) is credited with developing the Muskingum method around 1934 (Viessman et al, 1972). The Muskingum method is based on a spacially lumped continuity equation and an assumed storage-discharge relationship (Gilcrest, 1950). A general derivaton is given below.

(a) Continuity Equation. The continuity equation is the cornerstone of all hydrologic routing. The Muskingum method uses the continuity equation in a spacially lumped form,

$$Q_1(t) - Q_2(t) = \frac{dS}{dt} \qquad (2.12)$$

where,

Q1(t) = inflow rate into the reach

Q2(t) = outflow rate from the reach

$\frac{dS}{dt}$ = the rate of change of storage within the reach

(b) Storage-Discharge Relationship. Equation 2.12 is a single equation with two unknowns (Q_2 and S). To solve this equation a storage-discharge relationship must be specified. A number of authors [e.g. Chow, 1959, Crass and Johnstone, 1949, Knappen et al, 1952 and Puls, 1959] have suggested ways to represent the storage-discharge relationship using simplified methods, Chow (1959) mentions the use of semigraphical techniques , nomographs and circular computers.

McCarthy's formulation assumed that storage is a linear function of $Q_1(t)$ and $Q_2(t)$,

$$S = K\,(x\,Q_1(t) + (1-x)\,Q_2(t)) \qquad (2.13)$$

where,

K = the storage time constant for the reach

x = the weighting factor which varies from 0 to 0.5 for a given river section.

K and x are determined from the channel characteristics of the particular channel of interest.

Parameters for Gaged Streams

The accuracy of the Muskingum method depends on the accuracy of its parameters K and x. These parameters can be estimated for a given reach if inflow-outflow data is known. The parameters are usually determined graphically (Viessmen et al. 1972). McCann and Singh (1980) evaluated methods of optimizing Muskingum parameters using least squares analysis, method of moments, method of accumulants, graphical methods and direct optimization.

Parameters for Ungaged Streams

The parameters K and x are more difficult to estimate on ungaged streams. Viessman et al. (1972) suggest a K value equal to the travel time in the reach and an average x value of 0.2 or 0.25.

Mockus (1962) developed a method for estimating K and x based on a 'wedge' and 'prism' storage concept,

$$K = L/V \qquad (2.14)$$

$$x = 0.5V/(1.7+V) \qquad (2.15)$$

where V is the steady state velocity at reference flow rate.

Attempts have been made to rewrite the hydraulic routing methods into the Muskingum format. This allows K and x to be expressed in terms of hydraulic parameters (Cunge, 1969, Dooge, 1982).

Diffusion Method of Flood Routing

Cunge (1969) showed that the Muskingum method approximated a convection-diffusion equation. Ponce (1981)

developed a linear and non-linear form of the method.

The Soil Conservation Service (Reily, 1985) is currently developing a range of unsteady flow routing models varying from simple coefficient methods to the numerical solution of the Saint Venant equations. The linear diffusion method , developed by Ponce (1981), is being strongly considered as a coefficient method. The method relates the coefficients K and x to the frictional and cross-sectional characteristics of the channel and to the computational grid dimensions. The method is consistant as the computational algorithm reproduces similar results for varying degrees of substepping.

Linear Diffusion Model. The linear diffusion model is based on the convection-diffusion equation (eq 2.10). For zero lateral inflow this equation can be rewritten as (Ponce and Yevjevich, 1978),

$$\frac{\partial Q}{\partial t} + c_k \frac{\partial Q}{\partial X} = D \frac{\partial^2 Q}{\partial X^2} \qquad (2.16)$$

where the hydraulic diffusivity, D, is expressed in terms of physical properties of the system,

$$D = \frac{Q_o}{2 B S_o} \qquad (2.17)$$

where Q_o is the reference flow value, B is the channel top width at Q_o, S_o is the water surface slope for steady equilibrium flow conditions. The other terms are previously defined.

Ponce (1981) obtained the following hydrodynamic estimates of the Muskingum parameters by first discretizing the left hand side of equation 2.16 on the x-t plane,

$$\frac{x(Q_j^{n+1} - Q_j^n) + (1-x)(Q_{j+1}^{n+1} - Q_{j+1}^n)}{\delta t} + \frac{c(Q_{j+1}^n - Q_j^n + Q_{j+1}^{n+1} - Q_j^{n+1})}{2\delta X} = 0 \qquad (2.18)$$

where, x =weighting factor, j= space index, n =time index, δX =space step and δt =time step.

Equation 2.18 can be rewritten as,

$$\frac{Q_j^n + Q_j^{n+1}}{2} - \frac{Q_{j+1}^n + Q_{j+1}^{n+1}}{2} =$$

$$\frac{[\ \delta X\ ]}{c_k}\ \frac{(\ x.Q_j^{n+1} + (1-x)\ Q_{j+1}^{n+1})}{\delta t} - \frac{[\ \delta X\ ]}{c_k}\ \frac{(x.Q_j^n + (\ 1-x)\ Q_{j+1}^n)}{\delta t} \qquad (2.19)$$

An examination of equation 2.19 indicates that it is similar to the hydrologic continuity equation (i.e. inflow-outflow = rate of change in storage). The storage in the reach can be approximated by the Muskingum equation,

$$S^n = K\ [\ x\ Q_j^n + (1-x)\ Q_{j+1}^n\ ] \qquad (2.20)$$

By comparing equations 2.19 and 2.20 an expression for the parameter K can be written as,

$$K = \frac{\delta X}{c_k} \qquad (2.21)$$

Substituting equation 2.21 into equation 2.19 and by rearranging the terms the Muskingum-Cunge version of the flood routing equation can be derived as,

$$Q_{j+1}^{n+1} = C_1 Q_j^n + C_2 Q_j^{n+1} + C_3 Q_{j+1}^n \qquad (2.22)$$

where,

$$C_1 = \frac{\delta t/K + 2x}{\delta t/K + 2(1-x)} \qquad (2.23)$$

$$C_2 = \frac{\delta t/K - 2x}{\delta t/K + 2(1-x)} \qquad (2.24)$$

$$C_3 = \frac{2(1-x) - \delta t/K}{\delta t/K + 2(1-x)} \qquad (2.25)$$

Ponce (1981) derives a numerical diffusion coefficient by expanding the grid function Q(j δX,n δt) in terms of a Taylor series about the grid point (j δX,n δt) , or,

$$D_n = c_k \delta X (0.5 - x) \qquad (2.26)$$

where,

D_n =numerical diffusion coefficient

The hydraulic diffusivity can now be set equal to the numerical diffusion coefficient. Equating equations 2.17 and 2.26 yields the following expression for x,

$$x = 0.5 \left(1 - \frac{Q_o}{B S_o c \delta X}\right) \qquad (2.27)$$

The Courant and the Reynolds numbers can be defined as;

$$C = c_k \frac{\delta t}{\delta X} \qquad (2.28)$$

$$D = \frac{q}{S_o c_k \delta X} \qquad (2.29)$$

where $q = Q_o/B$ is the reference unit width flow rate, C is Courant number and D is the cell Reynolds Number. By using

the definitions for C and D the routing coefficients for the linear diffusion model of Ponce (1981) can be written as,

$$C_1 = \frac{1+ C- D}{1+ C+ D} \tag{2.30}$$

$$C_2 = \frac{-1 +C +D}{1 +C +D} \tag{2.31}$$

$$C_3 = \frac{1 -C +D}{1 +C +D} \tag{2.32}$$

The above equations for K and X can be derived by rearranging the diffusion and Muskingum's models in a number of different ways (see Koussis, 1978; Gill, 1979; Wilson et al., 1983). All of these approaches give the same values for K and x.

Nonlinear Diffusion Model. In the linear diffusion model, Muskingum constants C_1, C_2 and C_3 are calculated at the start of routing and then held constant until the entire hydrograph is routed through the reach (i.e. independant of time and space). The accuracy of the method therefore depends on the correct selection of the reference hydraulic values (i.e., Q_o, S_o, and B in equation 2.28). Ponce and Yevjevich (1978) have shown, through numerical experimentation, that reference flows based on base flow values tend to predict a slower movement of the floodwave than expected. On the other hand, reference flows based on peak flow values tend to overpredict floodwave movement. The linear coefficients also failed to account for steepening of the rising limb of the hydrograph as it moved downstream.

This occurs because different flows travel at different celerities. Applying the linear model to short reaches reduces the effects of these problems.

Ponce and Yevjevich (1978) have presented a variable parameter diffusion model that remains within the computational framework of the linear diffusion model. The parameters c_k and D, and thus routing coefficients (C_1, C_2, C_3), are defined in terms of local flow conditions. For each computational cell consisting of four grid points, δt is fixed and δX and S_o are specified. The values of the floodwave celerity, c_k, and the unit width discharge q, are determined for each computational cell. The celerity, c_k, and discharge q are defined at grid point (j,n) by:

$$c = \left.\frac{dQ}{dA}\right|_{j,n} \tag{2.33}$$

$$q = \left.\frac{Q}{B}\right|_{j,n} \tag{2.34}$$

The celerity and unit discharge are calculated by using a four-point average and iterating until covergence. The intial value at (j+1,n+1) is obtained by a three point average of (j,n), (j+1,n) and (j,n+1).

Non-linear diffusion models account for wave steepening. Their disadvantages include a substantial increase in computer time and a slight tendency not to conserve mass.

Dooge et al. Approach. Dooge et al. (1982) has taken the

Saint Venant equations for unsteady flow and the Muskingum method in their conventional forms and transferred them into a space-state formulation. The hydrodynamic equation of motion is written for a state space trajectory system. This result is solved by neglecting second order variations in the space state variables, and then linked to an equivalent Muskingum model. Muskingum's K and x are obtained in terms of the hydraulic properties of the channel system. The results are written for any cross-sectional shape and any type of friction law. Details of this derivation are given in chapter three.

CHAPTER III

FLOW MODEL DEVELOPMENT

Introduction

This chapter contains the derivation of a physically-based model for Muskingum's parameters formulated on the method proposed by Dooge et al. (1982). A discussion of the theoretical limitations of the method is presented. A nonlinear form of Dooge's hydrodynamic Muskingum method is given.

Hydrodynamic Muskingum's Method

The Muskingum method described in the previous chapter is a linear, spacially lumped model with two parameters K and x. This section will relate these parameters to the physical properties of the system. Dooge et al. (1982) developed their theory using space state trajectory techniques. Their theory is reformated in this section following the more traditional approach given by Lighthill and Whitham (1955). This format makes it easier to compare Dooge et al.'s approach to those based on the diffusion wave model. A summary of this format is presented here.

The equation of motion for one-dimensional unsteady open channel flow without lateral inflow can be written as (

Dooge et al., 1982),

$$\frac{\partial Q}{\partial t} = -gy\ (1 - F^2)\ \frac{\partial A}{\partial X} - \frac{2Q}{A}\ \frac{\partial Q}{\partial X} + gA\ (S_o - S_f) \qquad (3.1)$$

where

$$F^2 = \frac{Q^2\ T}{g\ A^3} \qquad (3.2a)$$

and

$$S_f = \frac{K_o\ Q^2}{A^b} \qquad (3.2b)$$

and

$$y = \frac{A}{T} \qquad (3.3)$$

The symbols Q is the volumetric flow rate, A is the cross-sectional area, g is the acceleration of gravity, S_o is the bed slope, t is time, x is the distance downstream, F is the Froude number as defined by equation 3.2a, y is an average flow depth, K_o is a constant that can be defined from uniform flow conditions, T is the top width and b is a constant equal to 3 for Chezy's equation and 3.333 for Manning's equation.

The continuity equation (2.1) and momentum equation (2.2) are the Saint Venant equations. These equations form a nonlinear spacially varied system of equations. If a comparison with the Muskingum method is to be made, the Saint Venant equations must be transformed into a linear lumped system.

Equation 3.1 can be linearized using a general

approach given by Lighthill and Whitham (1955). In this approach, it is assumed that variables Q and A can be written using small perturbation as,

$$Q = Q_o + Q' \tag{3.4a}$$

$$A = A_o + A' \tag{3.4b}$$

where Q_o and A_o are the flow rate and cross-sectional area, respectively, at reference flow condition corresponding to steady uniform flow, and Q' and A'are the small perturbation about this flow condition.

By substituting these relationships into equation 3.1, by eliminating appropriate reference flow condition terms, and by neglecting insignificant perturbation terms (e.g., Q'^2), equation 3.1 is linearized as,

$$\frac{\partial(Q')}{\partial t} = -gy_o\,[1 - F_o^2]\,\frac{\partial(A')}{\partial X} - \frac{2Q_o}{A_o}\,\frac{\partial(Q')}{\partial X} + gS_o\,[bA' - \frac{2A_o}{Q_o}\,Q'] \tag{3.5}$$

In equation 3.5 the energy slope term is expanded using a binomial expansion with b as an integer value.

The time derivative of equation 3.1 can be expressed as a space derivative using the kinematic wave approximation in conjunction with the continuity equation. This approximation allows $\partial(Q')/\partial t = c_k\,\partial Q/\partial x = bQ_o/(2A_o)\,\partial Q/\partial x$

from equation 3.2. A linearized form of the equation of motion can now be written as,

$$gy_o\,[1 - F_o^2]\,\frac{\partial(A')}{\partial X} + \frac{(4-b)Q_o}{2A_o}\,\frac{\partial(Q')}{\partial X} = gS_o\,[bA' - \frac{2A_o\,Q'}{Q_o}] \qquad (3.6)$$

The next step is to use equation 3.6 in formulating a spacially lumped model. In a spacially lumped model the conditions are only known at the inlet and outlet of the reach. Therefore, the derivative terms are approximated as,

$$\frac{\partial(A')}{\partial X} = \frac{A_2' - A_1'}{L} \qquad (3.7a)$$

and

$$\frac{\partial(Q')}{\partial X} = \frac{Q_2' - Q_1'}{L} \qquad (3.7b)$$

where L is the reach length.

Equation 3.6 can be applied to any point within the channel reach. Once again for a lumped system, the logical locations to use this equation are at the upstream and downstream points. By using equations 3.7a and 3.7b, the upstream point can be evaluated as,

$$g\,y_o\,(1-F_o^2)\,\frac{(A_2' - A_1')}{L} + \frac{(4-b)Q_o}{2A_o}\,\frac{(Q_2' - Q_1')}{L}$$

$$= g\,S_o\,(b\,A_1' - \frac{2A_o\,Q_1')}{Q_o} \qquad (3.8a)$$

and the downstream point can be evaluated as,

$$g\,y_o\,(1-F_o^2)\,\frac{(A_2' - A_1')}{L} + \frac{(4-b)Q_o}{2A_o}\,\frac{(Q_2' - Q_1')}{L}$$

$$= g\,S_o\,(b\,A_2' - \frac{2A_o\,Q_2')}{Q_o} \qquad (3.8b)$$

A reasonable estimate of the storage perturbation in the channel reach as a result of perturbation in flow rates can be defined as,

$$S' = 0.5\ (A_1' + A_2')\ L \tag{3.9}$$

where S' is the perturbation of storage in the reach.

Finally, by rearranging equations 3.8a and 3.8b for A1' and A2' and by substituting these values into equation 3.9, a storage equation in the form of Muskingum's equation can be obtained as,

$$S' = K\ [x\ Q_1' + (1-x)Q_2'] \tag{3.10}$$

where

$$K = \frac{L}{c_k} \tag{3.11}$$

and

$$x = 1 - \frac{y_o}{bS_oL}\ [1 - (\frac{b}{2} - 1)^2\ F_o^2] \tag{3.12}$$

where c_k is the kinematic wave speed of the reference flow rate, L is the reach length, y_o is the depth at reference flow rate calculated from steady state condtions, b is the power friction slope and F_o is the Froude number at reference flow conditions.

To summarize, the Muskingum parameters are derived by linearizing the Saint Venant equations and evaluating derivative and storage terms using only the endpoint

conditions. These steps resulted in an equation of the form used in the classical Muskingum method. By making a one to one correspondence between terms in the Muskingum equation (2.13) and the terms given by equation 3.10, the parameters K and x are related to the physical properties of the flow system. This approach is not based on the traditional "prism" and "wedge" storage concepts, but built on the equation of motion for open channel flow. Dooge et al.'s approach will be referred to as the hydrodynamic Muskingum method to distinguish it from the classical Muskingum procedure. Appendix A contains a computer printout of the linear hydrodynamic Muskingum model.

Disscusion of Theory

The expected accuracy of Dooge et al.'s (1982) method depends on the validity of their assumptions. There are three major assumptions used in the method:

(a) A reference flowrate can be found such that the perturbation terms are small (i.e. equations 3.4a 3.4b).

(b) The derivative terms at the endpoints can be approximated by a straight line between these points (i.e. equations 3.7a and 3.7b).

(c) Kinematic wave theory can be used to approximate $\partial Q'/\partial t$.

The reference flowrate, Q_o, should be selected to minimize Q'. Several possible alternatives exist to select

Q_o, such as the peak flow rate, base flow rate, 1/2 or 3/4 the difference between peak flowrate and base flow rate, or a volume weighted average. Dooge et al. (1982) also implied a time varying Q_o could be used. This would give the Muskingum method a non-linear feature.

The derivative approximations using endpoint conditions are more reasonable when the wavelength (in distance) of the inflow hydrograph is large compared to the reach length. This approximation may lead to problems in early stages of the run. The $\partial Q'/\partial X$ is initially equal to zero (assuming uniform flow initially) at the outlet of the reach until the leading edge of the flood wave reaches this point. The error associated with this condition can be reduced by selecting a larger time increment or by subdividing reach into smaller reach lengths.

Kinematic wave theory is used to approximate the temporal rate of change in flow rate. Although an approximation, this approach is still superior to the approach taken by Koussis (1978), Gill (1979), Ponce (1982) and others who manipulate the diffusion wave model to obtain Muskingum K and x values. In the diffusion wave model, the inertia terms are neglected completely. Therefore, in theory, Dooge et al.(1982) would have a larger range of applicability than those models based on the diffusion wave approach.

Nonlinear Hydrodynamic Muskingum Method

A nonlinear feature is incorporated into the model by using a space varying Q_o. Q_o is evaluated at the end of each subreach as a fraction, Q_{ref}, of the peak outflow value minus the base flow value,

$$Q_o^{j+1} = (Q_p^{j} - Q_b) Q_{ref} + Q_b \tag{3.13}$$

where Q_b is the base flow and j+1 is the subreach of interest.

This allows Q' to be minimized over the entire reach length. The nonlinear model should perform better than the linear model in cases were the inflow hydrograph attenuates significantly on its travel down the reach. Appendix A contains a computer printout of the Hydrodynamic Muskingum model.

The outflow values for each subreach are calculated from,

$$Q_2 = C_1 I_1 + C_2 I_2 + C_3 I_3 \tag{3.14}$$

where $C_3 = 1 - C_1 - C_2$. (3.15)

The nonlinear Hydrodynamic method is an easy method to apply. It requires far less computational time than the finite element solution to the Saint Venant equations. The finite element solution to the Saint Venant equations also requires precise values for the initial and boundary conditions to ensure stability of the solution algorithm.

The nonlinear Hydrodynamic Muskingum method is far more robust and allows a degree of flexibility in the selection of input parameters. This feature will be discussed in later chapters.

The Hydrodynamic Muskingum method divides the channel reach into a number of subreaches. This should theoretically produce better results as the assumptions made in the derivation become better as the length over which they are applied becomes smaller (e.g., approximation of derivatives by a straight line between end points). This differs from the classical Muskingum method which is applied to the whole channel reach.

CHAPTER IV

DESCRIPTION OF VALIDATION PROCEDURES

Introduction

Dooge et al.'s (1982) method of estimating K and x was evaluated for three different types of channel geometries. Tests were conducted on rectangular channels (Series I, II, III,IV,VII), triangular channels (Series V), and a natural channel (Series VI). For all tests, the predicted values using the nonlinear hydrodynamic Muskingum method were compared to those predicted with the Saint Venant equations. The linear Hydrodynamic Muskingum method was applied to Series I tests only. In addition, an actual observed hydrograph was also used for the natural channel. Series I,II,IV,V,VI and VII used a reference flow rate fraction (Q_{ref}) of a half.

The Saint Venant equations were solved using a finite element algorithm developed by the Corp of Engineers (Smith, 1979). The Corp of Engineers program is written to handle a variety of real world problems such as irregular channel geometries and variations of Manning's n with distance and flow depth. Additional information about finite element methods is given in Appendix F. Data format is similar to Corp of Engineer's HEC II simulation program.

To check numerical error, δt and δX values were reduced by two, and the extreme tests were again simulated. The changes in predicted values were insignificant. A steady state rating curve was used as the downstream boundary condition. Series I,II,III,IV,V and VII used uniform flow initial conditions. Series VI used a backwater curve to calcualte the initial flow conditions.

Inflow Hydrographs

A total of six different inflow hydrographs were available as the upstream boundary condition. An observed inflow hydrograph at the upstream gaging station of the natural channel was used in a simulation. This allowed a comparison to be made between the observed downstream hydrograph and the predicted downstream hydrographs. For the rectangular and triangular channels, five synthetic hydrographs were used to provide a range of different hydrograph shapes. The peak flow rates and base flow rates were selected to represent a range of flow conditions for the given channel geometry using the data reported by Leopold et al (1963). Inflow hydrographs two to five have the same total volume of flow in the first forty-eight hours. All five synthetic inflow hydrographs were predicted from the following equation (used by Weimann, 1977 and Ponce, 1982),

$$Q_i = Q_b + Q_p \ (t\ )^r \exp[\ (t_p-t)/(t_p-t_g)\ ]$$

(4.1)

TABLE I

SIMUALTION PARAMETERS FOR THE INFLOW HYDROGRAPHS

Inflow Hydrograph	Q_b cms	Q_p cms	t_p secs	t_g secs
one	50	100	14400	21600
two	10	100	14400	21600
three	5	30	43200	131000
four	5	40	7200	95000
five	5	60	28800	46500

TABLE II

SUMMARY OF CONDITIONS USED IN SERIES I TESTS

Length m	Slope	Manning's n	Inflow Hydrograph	Number of Runs
5000	0.01	0.05 0.10	one two	4
	0.001	0.05 0.10	one two	4
	0.0001	0.05 0.10	one two	4
10000	0.01	0.05 0.10	one two	4
	0.001	0.05 0.10	one two	4
	0.0001	0.05 0.10	one two	4
15000	0.01	0.035 0.05 0.10	one two	6
	0.001	0.035 0.05 0.10	one two	6
	0.0001	0.035 0.05 0.10	one two	6

where

$$r = t_p/(t_g-t_p) \tag{4.2}$$

where Q_i, Q_b, and Q_p are the inflow, base and peak volumetric flow rates, respectively, t_p and t_g are the time to peak and time to center of gravity, respectively, and t is the time. The actual values for these parameters are summarized in Table I.

Series I Tests

Series I tests were conducted on rectangular channels. The rectangular channels had a constant width of twenty meters. Runs were made for different combinations of reach length, bed slope, roughness coefficient and base flow rate. A summary of conditions considered is given in Table II. Overall forty-two simulation tests were conducted for comparison between the Saint Venant equations, the linear hydrodynamic Muskingum method and the nonlinear hydrodynamic Muskingum method (see Table VII).

The linear model was only used in this Series of tests. Theoretically the nonlinear model is superior to the linear model, therefore it will be examined in more detail than the linear model. Other justifications for this decision will be given in Chapter V.

Series II Tests

Series II tests were conducted to examine the effects

of varying the ratio, $\delta X/\delta t$, subreach length, δX, and time step, δt, on the nonlinear hydrodynamic Muskingum method. Six simulations from Series I tests were chosen using three different bed slopes, two different inflow hydrographs and a constant roughness coefficient.

Initially, the time step was selected so as to adequately describe the inflow hydrograph (i.e. $\delta t < Tp/5$ Ponce and Theurer, 1982). All time steps used satisfied this criteria. The total reach length was then divided into subreaches using the criteria recommended by Weinmann (1977), where the subreach $\delta X = \delta t\ c_k$. The ratio, $\delta X/\delta t$, was held constant while δX and δt were varied simultaneously by a factor ranging from 0.1 to 10. Another set of tests were conducted to evaluate the sensitivity of the predicted results to δX. The subreach length, δX, was varied from $\delta X/10$ to $10\delta X$ for a constant δt. The time step was again selected to adequately describe the inflow hydrograph. In the third set of tests, the time step, δt, was varied from $2\delta t$ to $\delta t/100$ with a constant δX of $\delta X = \delta t\ c_k$, where δt was selected to adequately describe the inflow hydrograph. A more detailed description of parameter values is given in Chapter V.

Series III

Series III tests were preformed to evaluate the effect of varying the reference flow value, Q_o. The best and the worst run for each slope value were selected from Series I.

The reference flow rate was then varied from base flow rate to peak flow rate in twenty-five percent increments, for each case. An additional run using a slope of 0.0001, a Manning's n of 0.05 and inflow hydrograph four was also performed. A total of thirty-five simulation runs were conducted for the nonlinear hydrodynamic Muskingum method. Table III contains a summary of the conditions used.

Series IV

Series IV tests were used to evaluate the model's performance under the influence of different types of inflow hydrographs. A rectangular channel with a constant roughness coefficient, width and length of 0.05, 20 meters and 15000 meters respectively, was used. Five inflow cases were used in conjunction with three different bed slopes Some of the tests were identical to Series I tests.

Series V

To evaluate the effect of different channel geometries, tests were also conducted with a triangular shaped channel. This channel had a constant single sideslope of 2:1, a reach length of 15000 meters, bed slopes of 0.001 and 0.0001 and Manning's roughness coefficients of 0.05 and 0.1. These channel parameters were used for all five hydrograph shapes given in Table I. Table IV summarizes the conditions used. The simulation runs were conducted for both the Saint Venant and the nonlinear hydrodynamic Muskingum method.

TABLE III

SUMMARY OF CONDITIONS FOR SERIES III

Slope	Manning's n	Inflow Type	Q_{r-of} 0	.25	.50	.75	1	Number of Runs
0.01	0.05	one	x	x	x	x	x	5
	0.05	two	x	x	x	x	x	5
0.001	0.05	one	x	x	x	x	x	5
	0.05	two	x	x	x	x	x	5
0.0001	0.05	one	x	x	x	x	x	5
	0.05	two	x	x	x	x	x	5
	0.05	four	x	x	x	x	x	5

TABLE IV

SUMMARY OF SERIES V TESTS FOR TRIANGULAR CHANNELS WITH A 2:1 SIDESLOPE

Slope	Manning's n	Inflow Type	Number of Runs
0.001	0.05	one two three four five	5
	0.10	one two three four five	5
0.0001	0.05	one two three four five	5

Series VI

Series VI tests were conducted to compare predicted results of the nonlinear hydrodynamic Muskingum model and the Saint Venant equations against the observed movement of a flood wave through a channel. The Illinois River in Oklahoma was selected as the natural channel. Data for this channel was obtained from Nwaogazie and Tyagi (1984). The reach length of interest was between the Watts and Tahlequah gaging stations. The reach length was 81100 meters, and the bed slope was 0.0009. The roughness coefficient for this channel was expressed as a function of flow rate by Nwaogazie and Tyagi (1984). This function was used in the finite element simulation. An average roughness coefficient of 0.055 was used for the hydrodynamic method. The observed hydrograph of April 14th, 1979, at Watts was used as the inflow hydrograph. Numerical results from both models were compared to the observed outflow hydrograph at the Tahlequah gaging station.

Series VII

Series VII runs were conducted to examine in more detail the effects of slope on the predictive response of the nonlinear Hydrodynamic Muskingum methods. Table V contains a summary of these runs.

TABLE V

MISCELLANEOUS RUNS FOR A RECTANGULAR CHANNEL OF LENGTH 15000 METERS

Slope	Inflow Type	Manning's n
0.01	four	0.05
0.001	four	0.05
0.0005	four	0.05
0.0001	four	0.05

CHAPTER V

RESULTS AND DISCUSSION

Introduction

This chapter contains the results for Series I through VII. A discussion on each Series is presented in separate sections. A summary of all the results is then given.

In this chapter SV and NHDM mean Saint Venant equation model and nonlinear Hydrodynamic Muskingum method, respectively. This is done to present the results more simply.

Series I

Series I tests were used to evaluate the sensitivity of the linear Hydrodynamic Muskingum method and the nonlinear Hydrodynamic Muskingum method to variations in slope, roughness, and reach length. The sensitivity of high and low base flow rates was also considered.

The time step was selected so as to adequately describe the inflow hydrograph, as discussed in Chapter IV. The total reach length was divided into subreaches using the criteria recommended by Weinmann (1977), where the subreach length $\delta X = \delta t \, c_k$. The outflow hydrograph from the subreach is used as the inflow hydrograph for the next subreach.

This process is continued until an outflow hydrograph at the outlet of the reach is obtained. Adopting this subreach approach reduces the importance of the channel length as an input parameter. The longer the channel the greater the accumulation of numerical error, if the subreach is kept constant for the different runs. The significance of this error was evaluated by examining results for the 5000 and 10000 meter runs.

The linear flow model performed well over the range of runs conducted in Series I tests. The different reach lengths showed no significant trend in accumulation of error from the 5000 meter channel to the 15000 meter channel for the same subreach length. Predicted peak outflow rates for the 15000 meter reach length simulations are tabulated in Table VI. Overall the linear model does an excellent job of approximating the Saint Venant equations for those runs with relatively small attenuation in the peak flow rate (Q_p = 100 cms) of the inflow hydrograph. As shown in Table VI, the predicted peak flow rates between the two models were reasonably close for the 0.01 and 0.001 slope simulations. In these simulations the downstream peak flow rate was 85 cms or greater, which corresponds to an attenuation of less than 15% in the inflow peak flow rate. For the 0.0001 slope simulations, however, the deviations between the Saint Venant and the Hydrodynamic Muskingum method were more noticeable (see Table VI Runs A13-A18), especially for a Manning's n of 0.1. These runs corresponded to a greater

TABLE VI

SIMULATED PEAK OUTFLOW RATES FOR RECTANGULAR CHANNELS OF OF SERIES I TESTS USING A TOTAL REACH LENGTH OF 15000 M

Run	Slope	Manning's n	Inflow Type	Simulated Peak Outflow		
				Saint Venant	Hydrodynamic Muskingum Nonliner	Method Linear
	m/m			m^3/sec	m^3/sec	m^3/sec
A1	0.01	0.035	one	99.5	99.9	99.9
A2		0.050	one	99.5	99.9	99.9
A3	(moderate)	0.100	one	98.8	99.2	99.5
A4		0.035	two	99.1	99.9	99.9
A5		0.050	two	99.1	99.8	99.8
A6		0.100	two	97.6	99.6	99.7
A7	0.001	0.035	one	97.9	98.9	98.9
A8		0.050	one	95.8	97.5	97.9
A9	(mild)	0.100	one	90.4	92.9	93.8
A10		0.035	two	96.2	98.0	98.2
A11		0.050	two	92.5	94.0	96.2
A12		0.100	two	82.1	87.3	87.6
A13	0.0001	0.035	one	77.3	80.6	81.2
A14		0.050	one	78.6	80.3	81.0
A15	(almost)	0.100	one	73.7	84.0	84.5
A16	level	0.035	two	67.7	62.0	63.7
A17		0.050	two	58.9	57.9	60.9
A18		0.100	two	44.6	63.6	65.7

attenuation in peak flow rate. With the exception of Manning's n of 0.10, the peak flow rates for this slope were still adequately predicted by the linear model.

One possible reason for the relatively poor predictive accuracy of the linear Hydrodynamic Muskingum method at the mild slopes was the procedure used to define the reference flow rate. A constant Q_o value was used for all subreaches. This value was reasonable when the attenuation of the hydrograph was small (less than 15%). However, for those reaches with large attenuations, the outflow hydrograph varies noticeablely between each subreach. A more reasonable approach would be to use a different Q_o value for each subreach.

The nonlinear hydrodynamic Muskingum method incorporated a space varying Q_o as described in Chapter Three. In general the nonlinear hydrodynamic Muskingum model more accurately simulated the results of the Saint Venant equations than the linear hydrodynamic Muskingum method. This can best be seen by examining the peak flow rates in Table VI for Runs A7 to A12. Although the difference between linear and nonlinear models is small, there is still an improvement in simulated values.

The nonlinear hydrodynamic Muskingum method also simulates the Saint Venant equations well for the those runs with attenuations in the inflow hydrograph of less than fifteen percent. Runs A1 to A12 in Table VI highlight the excellent agreement in predicted peak flow rates. For the

0.0001 slope the predicted peak flow rates were fairly close (less than 8% error) for the Manning's ns of 0.035 and 0.05 values between the two models (see Table VI Runs A13,A14 and A16,A17). The largest difference between the two models occurred with the combination of smallest slope and largest roughness coefficient (0.10) for both inflow cases (Table VI Runs A15 and A18).

Typical fits between the Saint Venant and nonlinear hydrodynamic Muskingum methods for each slope using inflow hydrographs one and two are shown in Figure 1, Figure 2 and Figure 3, respectively. The overall shape of the outflow hydrograph, time to peak and peak flow rates of the nonlinear Hydrodynamic Muskingum method were reasonably close to the Saint Venant results for the 0.01 and 0.001 slope simulations. Figure 1 and Figure 2 demonstrate this point. The 0.0001 slope simulations, however, showed a tendency to rise too quickly causing differences in the time to peak and in the shape of the rising limb of the outflow hydrograph. Figure 3 demonstrates this point. The early rise of the rising limb of the inflow hydrograph goes against the trend present in the lower slope simulations where the time to peak was delayed as the slope decreased for constant roughness coefficient and inflow type. This oddity will be examined further in Series VII.

For the nonlinear model, no significant trend can be seen in the accumulation of error, as the reach length was varied from 5000 meters to 15000 meters for a constant

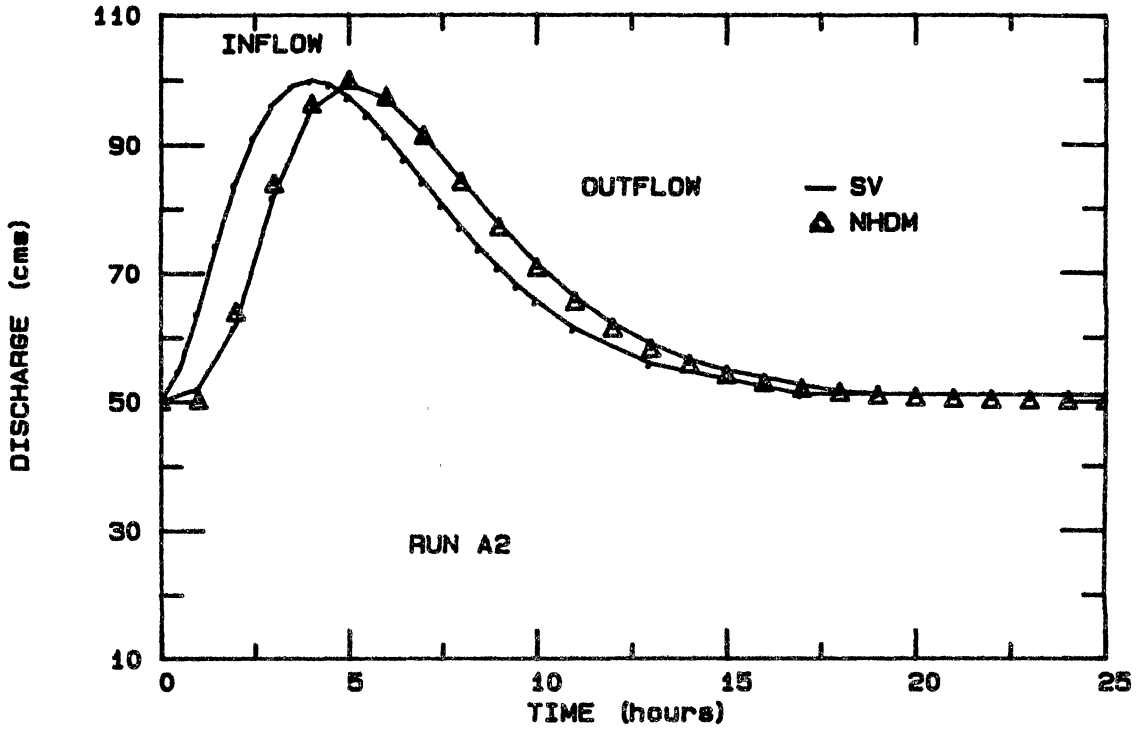

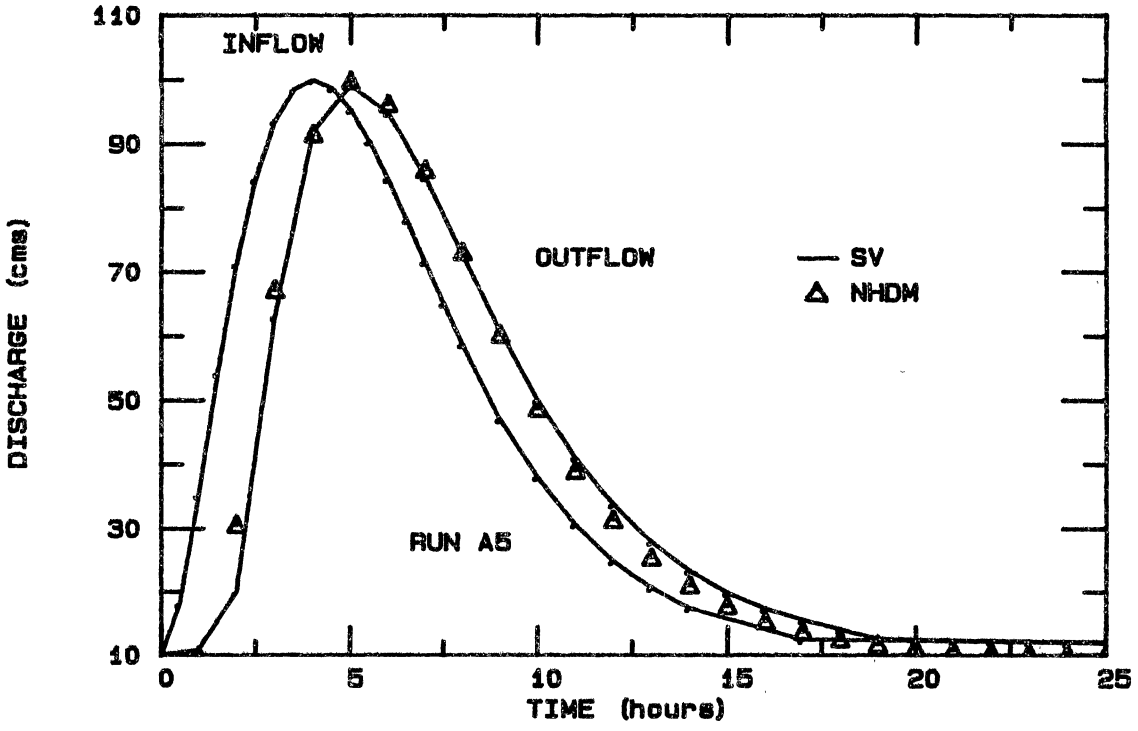

Figure 1. Typical Fits for Series I Tests with a Slope of 0.01

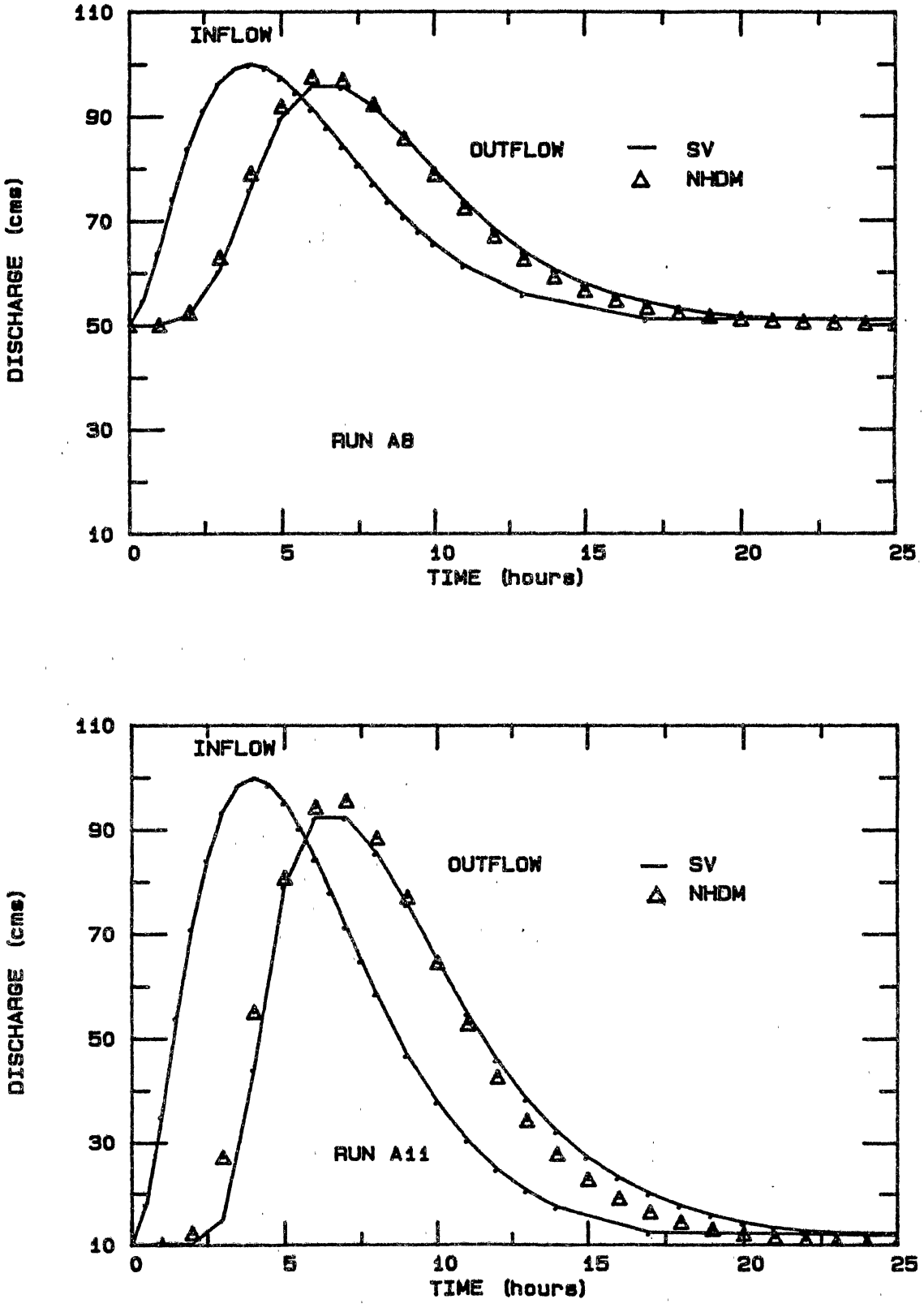

Figure 2. Typical Fits for Series II Tests with a Slope of 0.001

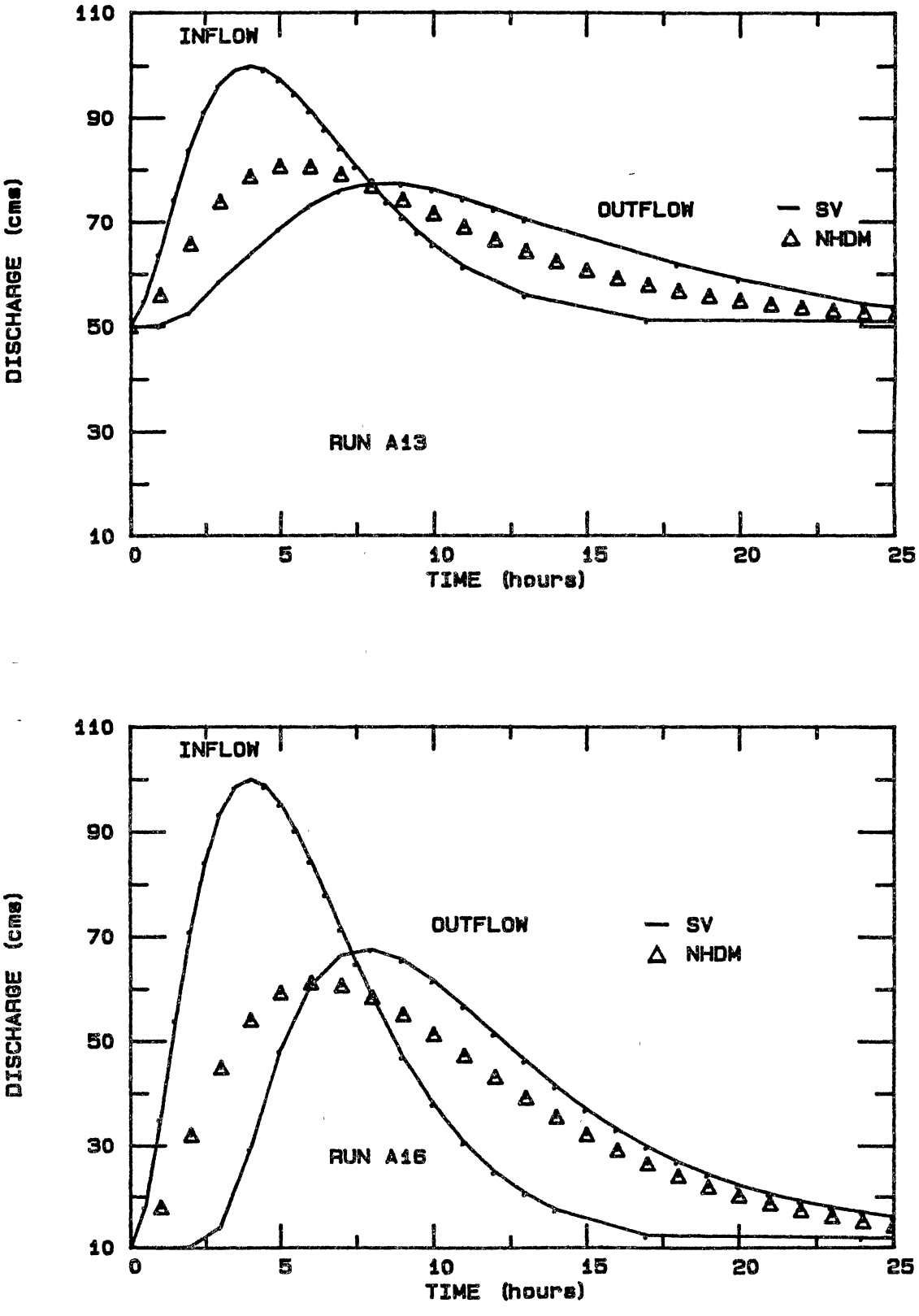

Figure 3. Typical Fits for Series III Tests with a Slope of 0.0001

subreach length. Appendix B contains all the nonlinear 15000 meter runs.

Series II

The Series II tests were conducted to evaluate the nonlinear Hydrodynamic Muskingum method's sensitivity to subreach length, ∂X, time step, ∂t and ratio $\partial X/\partial t$. The subreach length ∂X was varied from 15m to 15000m, the time step was varied from 60 seconds to 3600 seconds and the ratio $\partial X/\partial t$ was varied from 0.004 to 250.

Table VII contains a summary of the results. In Table VII, the results with an * beside the δt represent the runs which used the criteria $\delta X = \delta t\ c_k$ (Weinmann, 1977), where δt was selected to adequately describe the inflow hydrograph as described in Chapter IV. It can be seen from these results that a wide range of $\delta X/\delta t$ was examined. Only a small change in the predicted peak flow rate and time to peak was noticed. Figure 4 and Figure 5 demonstrate this point in graphic fashion. The values plotted were normalized against the standard* values for each slope and inflow case. The 0.01 and 0.001 slope results showed a decrease in peak flow values with increasing $\delta X/\delta t$ ratio. This trend was not as evident in the 0.0001 slope cases.

From these results, it would seem that the method will still produce reasonable estimates of time to peak and peak flow values as long as the ratio is within an order of magnitude above or three orders of magnitude below the

TABLE VII

SUMMARY OF RESULTS FOR SERIES II TESTS

Run	Slope	δX	δt	Inflow Type	$\frac{\delta X}{\delta t}$	Qp	tp
	m/m	m	secs		m/sec	cms	hrs
B1*	0.01	1667	400	one	4.166	99.98	5
B2	"	16.7	400	"	0.0417	99.98	5
B3	"	15000	400	"	37.5	99.75	5
B4	"	15000	60	"	250.0	99.74	5
B5*	"	1500	400	two	3.75	99.88	5
B6	"	15	3600	"	0.0042	100.00	5
B7	"	150	400	"	0.375	99.89	5
B8	"	1500	100	"	15.0	99.86	5
B9	"	5000	100	"	50.0	99.80	5
B10	"	15000	100	"	150.0	99.32	5
B11*	0.001	1154	600	one	1.923	97.54	6
B12	"	15	3600	"	0.0042	98.20	6
B13	"	15	600	"	0.025	97.88	6
B14	"	150	600	"	0.25	97.55	6
B15	"	15000	600	"	25.0	97.50	6
B16*	"	682	400	two	1.725	95.60	7
B17	"	100	3600	"	0.028	96.90	7
B18	"	1000	100	"	10.0	95.60	7
B19	"	15000	60	"	250.0	94.05	6
B20*	0.0001	536	600	one	0.888	80.30	5
B21	"	32	3600	"	0.00889	80.30	5
B22	"	536	60	"	8.888	80.25	5
B23	"	5000	60	"	83.0	80.48	5
B24*	"	469	600	two	0.78	57.9	5
B25	"	30	600	"	0.05	57.9	5
B26	"	15000	400	"	37.5	59.1	6
B27	"	7500	60	"	125.0	60.7	6

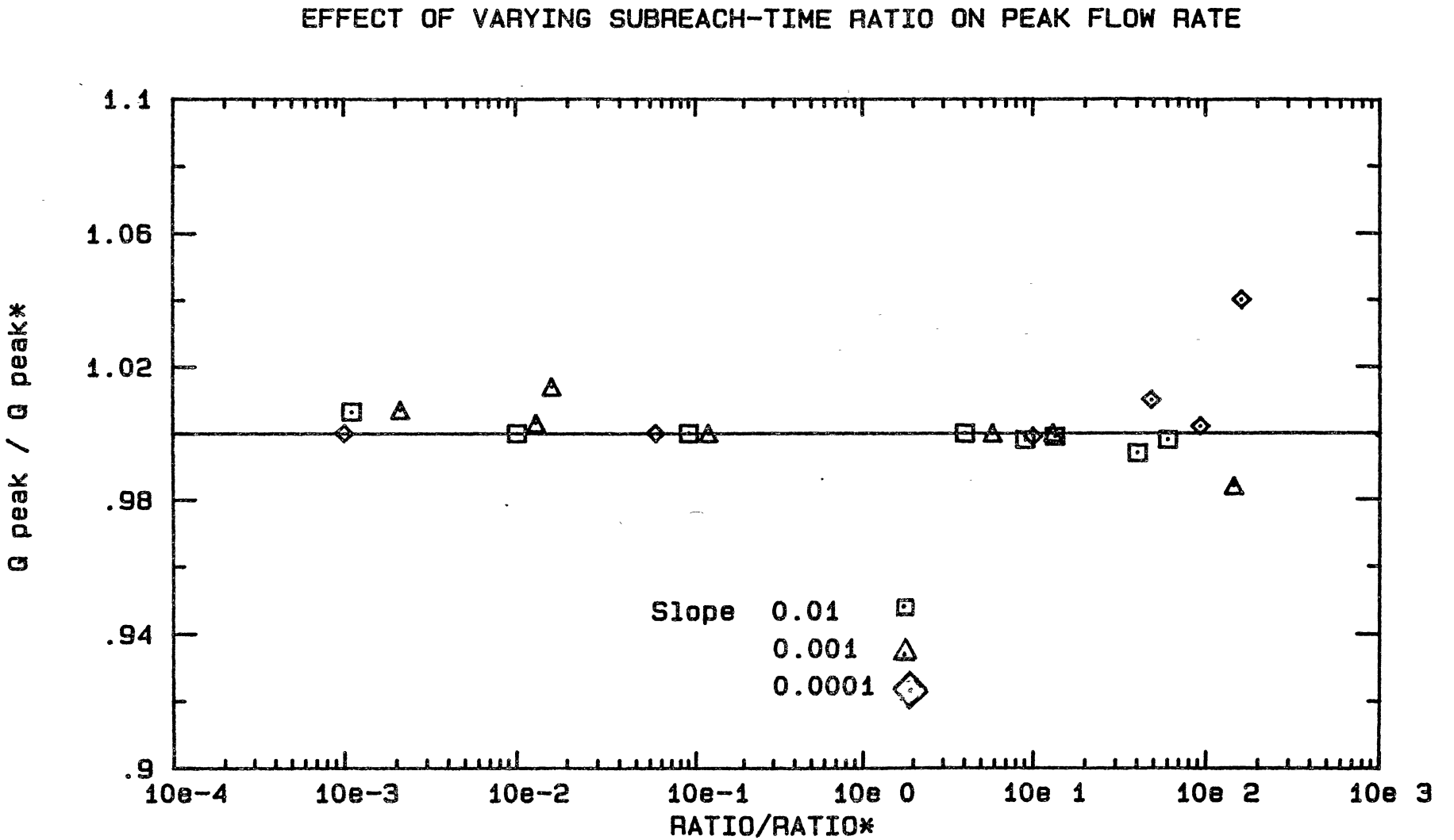

Figure 4. Illustration of the Effect of Varying Subreach Length and Time Step on Peak Flow Rate

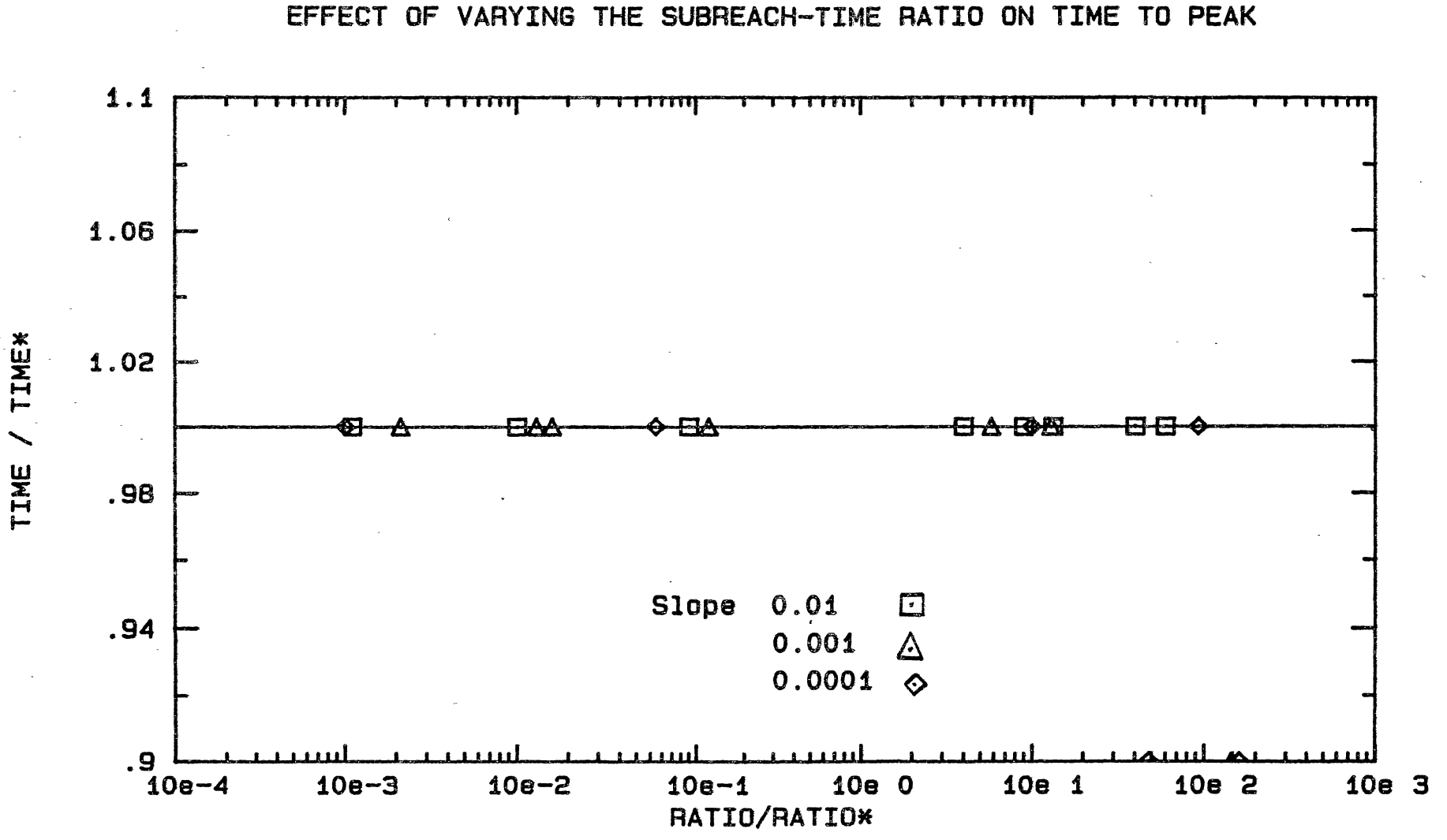

Figure 5. Illustration of the Effect of Varying Subreach Length and Time Step on Time to Peak

standard* value. In general, the method proved to be flexible in the selection of time step and distance step, as long as the time step selected adequately described the inflow hydrograph. This feature allows the engineer a great deal of latitude in selecting the distance step and time step.

Series III

Series III tests were performed to examine the sensitivity of the nonlinear hydrodynamic Muskingum method to the reference flow fraction Qref. In general, there was a trend for the peak flow values to increase as Qref was varied from zero to one (i.e., Q_o varied from Q_b to Q_p in equation 3.13). A value of 0.5 for Q_{ref} produced the best prediction of peak flow in most cases. Both these trends can be seen in Table VIII. The only run that showed a wide variation in peak flow values for different Qref values was the 0.0001 slope, inflow two case (Table VIII, Runs C26-C30). All the other runs were within plus or minus five percent of the peak values predicted by the finite element solution to the Saint Venant equation. The time to peak was later at Qref equal to zero in all cases other than the 0.0001 slope, inflow two case. In all cases the time to peak remained the same for Qref equal to 0.5 or greater. Data shown in Table VIII highlight these points.

Figure 6 illustrates the effect on the overall shape of the hydrograph of varying the reference flow fraction. The higher values of Qref produced a steeper rise in the rising

TABLE VIII

SUMMARY OF RESULTS FOR SERIES III TESTS FOR A RECTANGULAR CHANNEL OF CONSTANT ROUGHNESS OF N = 0.05

Run	Slope m/m	Qref	Inflow Type	Peak Flow Rate (cms)	%error	Time to Peak NHDM	SV
C1	0.01	0.00	one	99.8	+ 0.35	5	5
C2	"	0.25	"	99.9	+ 0.42	5	
C3	"	0.50	"	99.9	+ 0.47	5	
C4	"	0.75	"	99.9	+ 0.47	5	
C5	"	1.00	"	99.9	+ 0.46	5	
C6	"	0.00	two	98.8	- 0.37	6	5
C7	"	0.25	"	98.8	- 0.38	5	
C8	"	0.50	"	99.8	+ 0.60	5	
C9	"	0.75	"	99.9	+ 0.83	5	
C10	"	1.00	"	99.9	+ 0.77	5	
C11	0.001	0.00	one	97.7	+ 2.00	7	6
C12	"	0.25	"	97.7	+ 2.04	6	
C13	"	0.50	"	97.5	+ 1.85	6	
C14	"	0.75	"	98.2	+ 2.50	6	
C15	"	1.00	"	98.2	+ 2.55	6	
C16	"	0.00	two	93.4	+ 1.03	9	7
C17	"	0.25	"	96.1	+ 3.92	7	
C18	"	0.50	"	94.1	+ 1.70	6	
C19	"	0.75	"	96.1	+ 3.98	6	
C20	"	1.00	"	96.2	+ 4.02	6	
C21	0.0001	0.00	one	77.7	- 1.07	5	8
C22	"	0.25	"	79.1	+ 0.70	5	
C23	"	0.50	"	80.0	+ 2.25	5	
C24	"	0.75	"	81.3	+ 3.50	5	
C25	"	1.00	"	82.2	+ 4.62	5	
C26	"	0.00	two	44.6	-24.30	10	8
C27	"	0.25	"	51.5	-12.52	7	
C28	"	0.50	"	57.8	- 1.79	5	
C29	"	0.75	"	63.0	+ 6.98	5	
C30	"	1.00	"	66.7	+13.25	5	

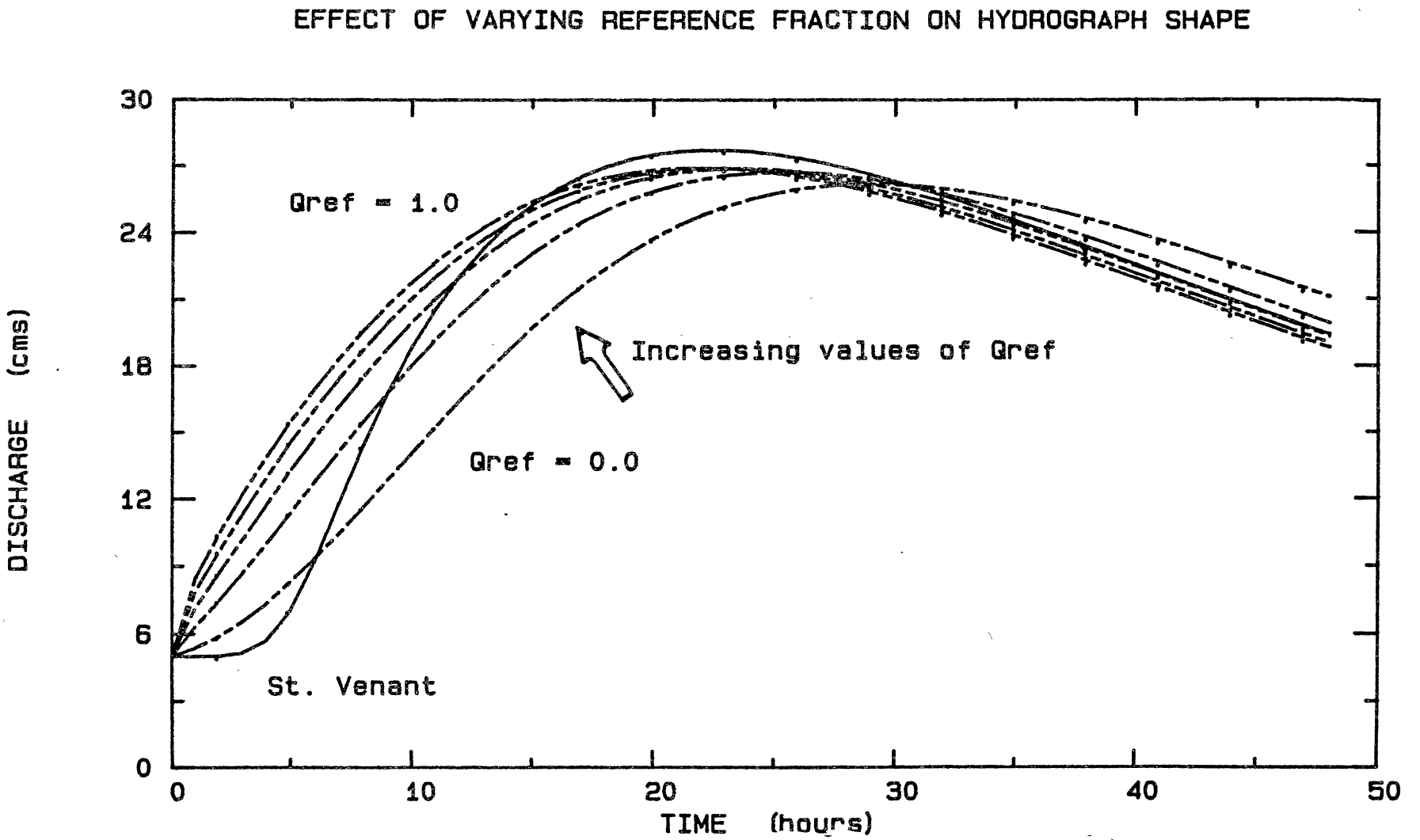

Figure 6. Illustration of the Effect of Varying Qref on Hydrograph Shape

limb of the outflow hydrograph. The lower values of Q_{ref} cause a delay in the arrival of the time to peak. Figure 6 was used to demostrate the trend of varying Q_o on the hydrograph shape. Although the same trend exists on the other runs the differences are much smaller, as can be seen in Table VIII.

In general the method is not overly sensitive to the selection of Q_{ref}.

Series IV

Series IV tests were conducted to assess the nonlinear Hydrodynamic Muskingum method's behaviour under the influence of different types of inflow hydrographs. A summary of the results are presented in Table IX. Figure 1 and Figure 2 contain typical plots for inflow one and two and have previously been discussed in this chapter. Figure 7 and Figure 8 contain typical plots for inflows three, four and five. The good agreement between the nonlinear Hydrodynamic Muskingum method and the Saint Venant equations can be seen here. From Table IX it can be seen that the predicted peak flow rates and the predicted time to peaks compare favorably with the values from the finite element solution to the Saint Venant equations for all five inflow types. The runs using inflows three, four and five proved to be more accurate in their prediction of time to peak. In general the lower peak flow values of the inflow hydrograph produced marginally better results. The method was able to

TABLE IX

SUMMARY OF RESULTS USED IN SERIES IV TESTS. ALL SIMULATIONS SIMULATIONS USED 15000 METER RECTANGULAR CHANNELS

Run	Slope	Manning's n	Inflow Type	Saint Venant Equation Q_p cms	Saint Venant Equation t_p hrs	Nonlinear Hydrodynamic Muskingum Q_p cms	Nonlinear Hydrodynamic Muskingum t_p hrs
D1	0.01	0.05	one	99.5	5	99.9	5
D2		0.05	two	99.1	5	99.8	5
D3		0.05	three	29.9	14	29.9	14
D4		0.05	four	39.5	3	39.7	5
D5		0.05	five	59.8	9	59.8	9
D6	0.001	0.05	one	95.8	6	97.5	6
D7		0.05	two	92.5	7	94.1	6
D8		0.05	three	29.9	15	29.9	16
D9		0.05	four	38.8	7	39.5	6
D10		0.05	five	59.0	11	59.5	11
D11	0.0001	0.05	one	78.6	8	80.0	5
D12		0.05	two	58.9	8	57.9	5
D13		0.05	three	27.7	22	26.9	23
D14		0.05	four	30.6	15	29.0	15
D15		0.05	five	46.2	14	42.0	14

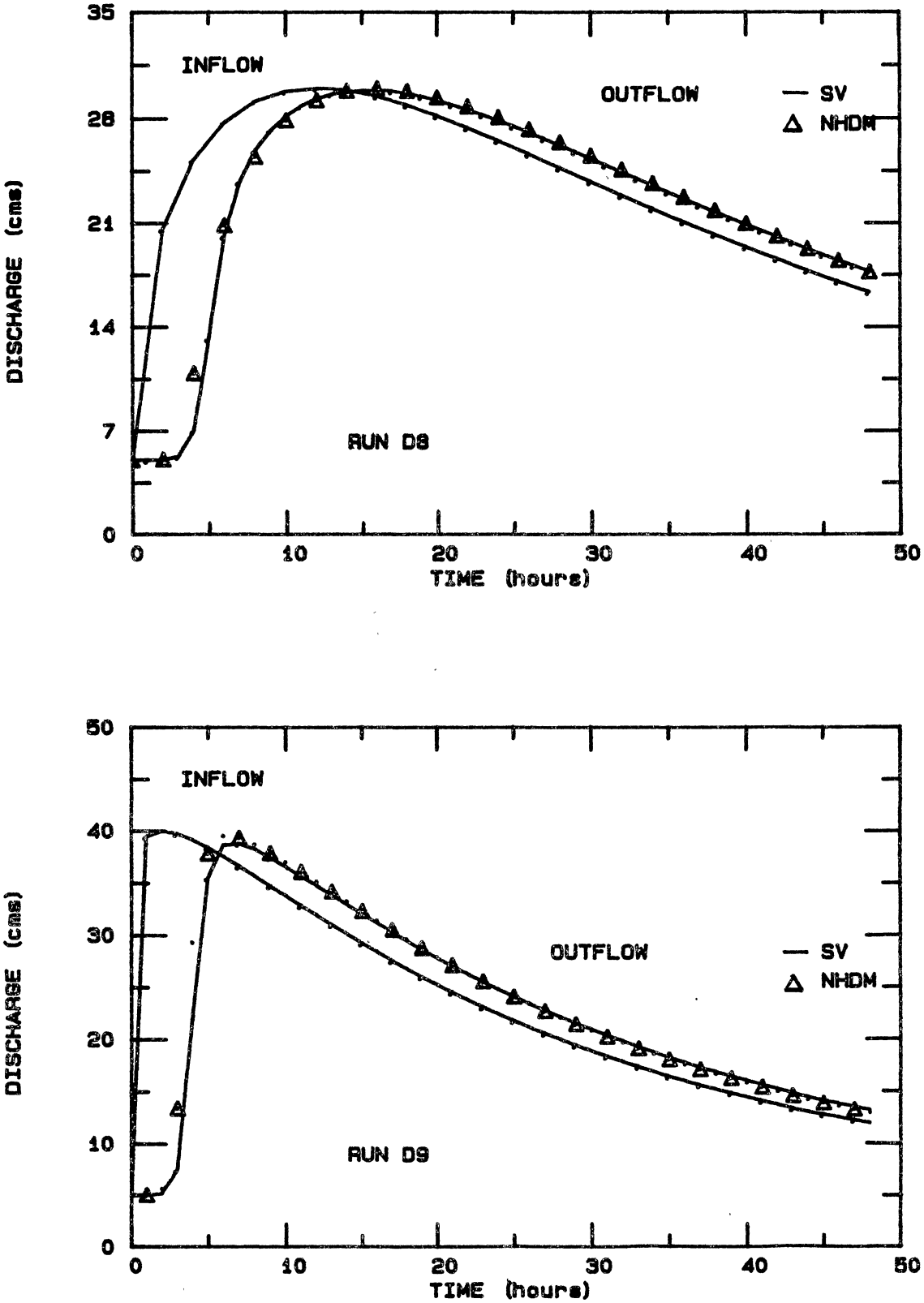

Figure 7. Outflow Hydrographs for Inflow Three (Top) and Inflow Four (Bottom) for a Standard Condtion

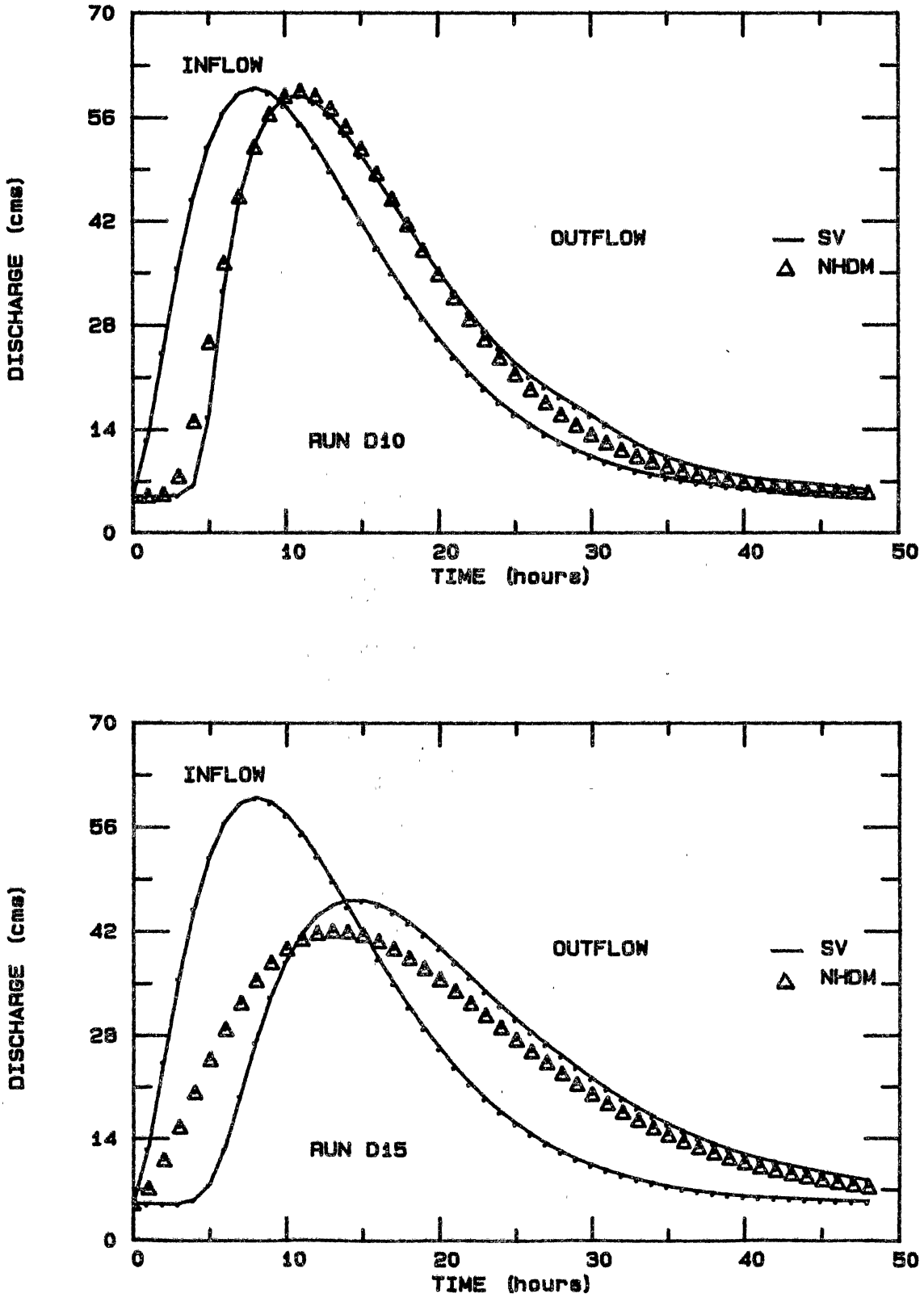

Figure 8. Outflow Hydrographs for Inflow Five for the Standard Condtion (Top) . Poorest Fit (bottom)

successfully handle all inflow types used in this series of tests. Appendix D contains plots of all the runs simulated in Series IV.

Series V

Series V tests were made to evaluate the nonlinear hydrodynamic Muskingum method's performance on a non-rectangular channel geometry. A summary of the results with their corresponding slope and Manning's n for triangular channels is presented in Table X. Overall the results for the triangular channels were good for the runs with a roughness coefficient of 0.05. The predicted peak flow values for the higher roughness coefficients were not as good as the others. Typical hydrograph for Runs E5 and E6 are presented in Figure 9. As shown by these figures the nonlinear Hydrodynamic Muskingum method also adequately predicted the shape of the outflow hydrograph.

The worst outflow hydrograph for the triangular channel at a slope of 0.001 and the coresponding hydrograph for the rectangular channel for the same slope, length, and roughness coefficient are shown in Figure 10 . As shown by this figure, the predictive accuracy of the hydrodynamic Muskingum method is less accurate for the triangular channel. In these runs the Saint Venant solution was relatively independant of geometry whereas, for the triangular channel the response with the hydrodynamic Muskingum method was quicker with less attenuation in peak

TABLE X

SUMMARY OF RESULTS USED IN SERIES V TESTS. ALL SIMULATIONS USED 15000 METER TRIANGULAR CHANNELS WITH A 2:1 SIDE SLOPE

	Slope	Manning's n	Inflow Type	Simulated Peak Outflow Rate	
				Saint Venant m^3/sec	Nonlinear Hydrodynamic Muskingum m^3/sec
E1	0.001	0.05	one	96.2	98.7
E2		0.05	two	93.1	97.4
E3		0.05	three	29.85	29.9
E4		0.05	four	38.5	39.8
E5		0.05	five	58.9	59.7
E6		0.10	one	90.6	96.5
E7		0.10	two	82.5	94.0
E8	0.0001	0.05	one	78.0	82.6
E9		0.05	two	57.7	65.9
E10		0.05	three	27.4	28.4
E11		0.05	four	27.7	32.1
E12		0.05	five	45.1	48.5

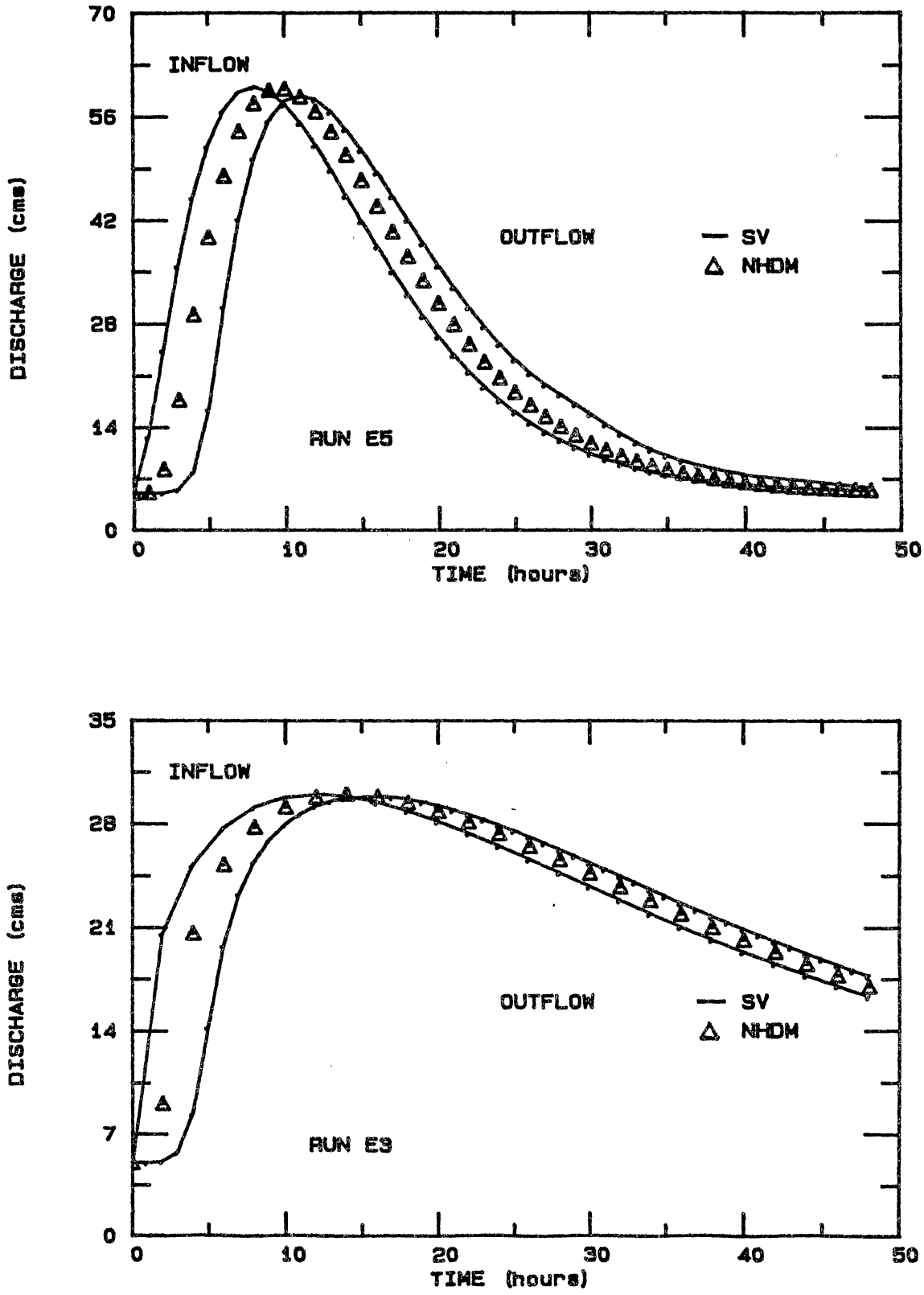

Figure 9. Typical Fits For Series V Tests for Triangular Channels. Inflow Five Run E5 (Top) and Inflow Three Run E3 (Bottom)

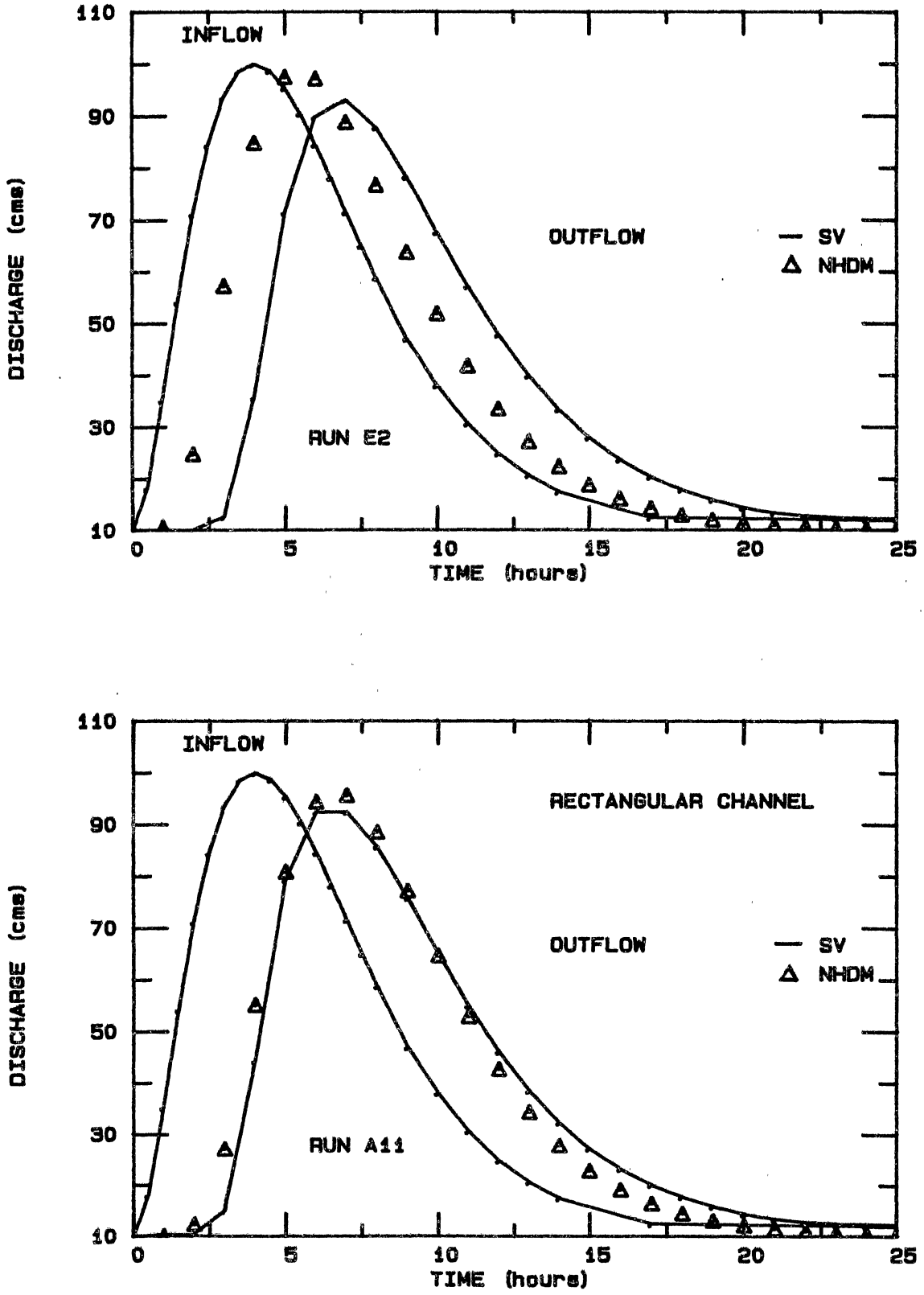

Figure 10. Poorest Fit for a Triangular Channel with a Slope of 0.001 (Top). Series I Result for a Rectangular Channel under same conditions (Bottom)

flow rate.

Series VI

Series VI test was used to examine predicted results for a natural channel reach. In addition, an observed outflow hydrograph was also available for this channel reach. In Figure 11, the observed outflow and those predicted by the nonlinear hydrodynamic Muskingum methods are shown. In comparison to the observed values, the nonlinear Hydrodynamic Muskingum method does a good job of predicting the outflow hydrograph. Figure 11 also highlights the fact that the Saint Venant equations only approximate the actual movement of a flood wave.

Series VII

Series VII was conducted to examine the effect of varying the slope from 0.01 to 0.0001 for a constant inflow type and roughness coefficient. Figure 12 shows the same trend found in all the Series I simulations. The 0.0001 slope simulation tended to rise too quickly resulting in a difference in time to peak and in the shape of the rising limb of the outflow hydrograph. This early rise goes against the trend in the other slope simulations. In these simulations the time to peak was delayed as the slope was decreased from 0.01 to 0.0001 (see Figure 12). As discussed in Chapter III, there are three major assumptions which could account for the relatively poor results for the 0.0001

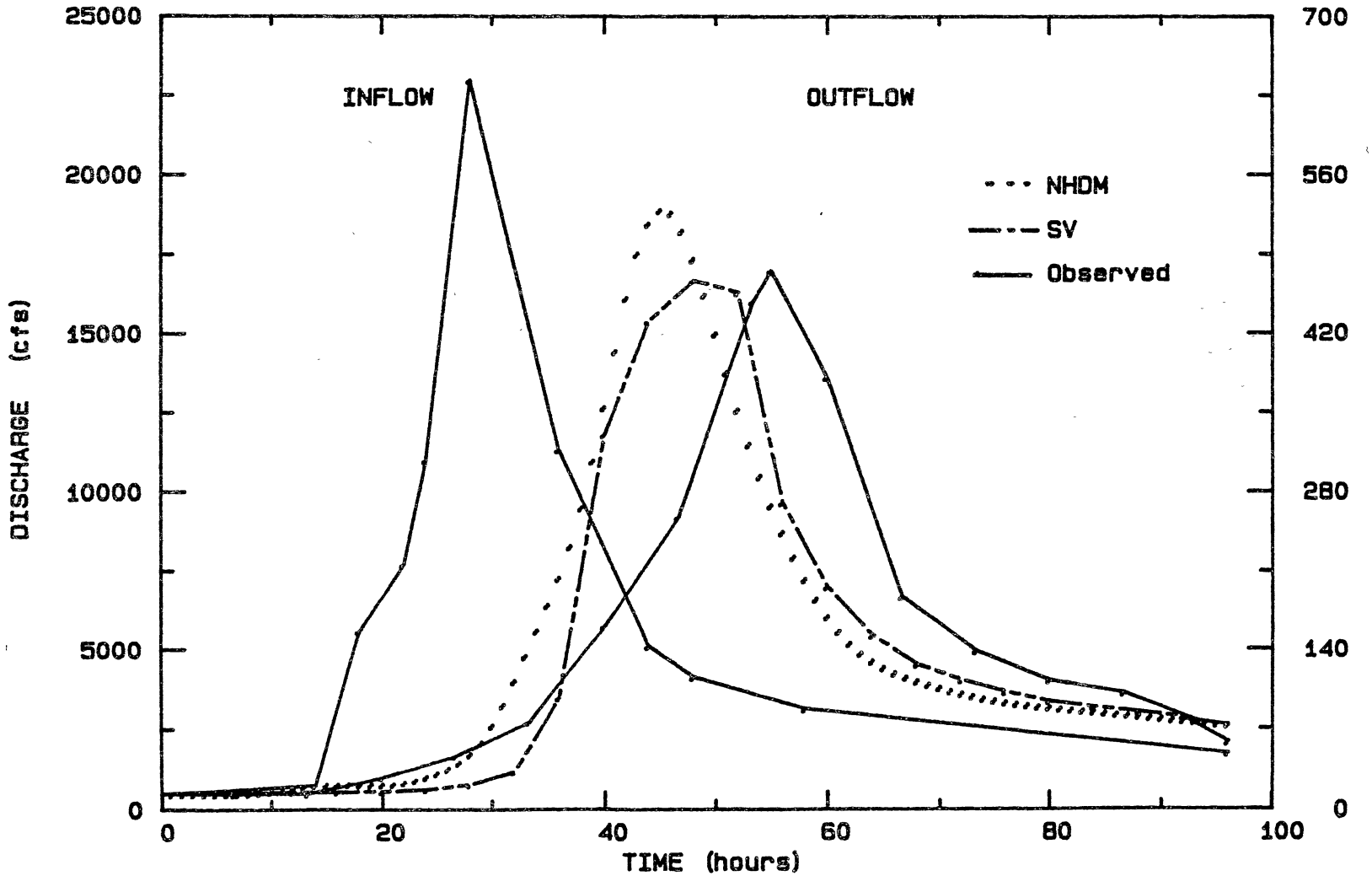

Figure 11. Comparison of NHDM and SV Simulated Results to an Observed Outflow Hydrograph Measured at Tahlequah, Oklahoma on April 10th 1979

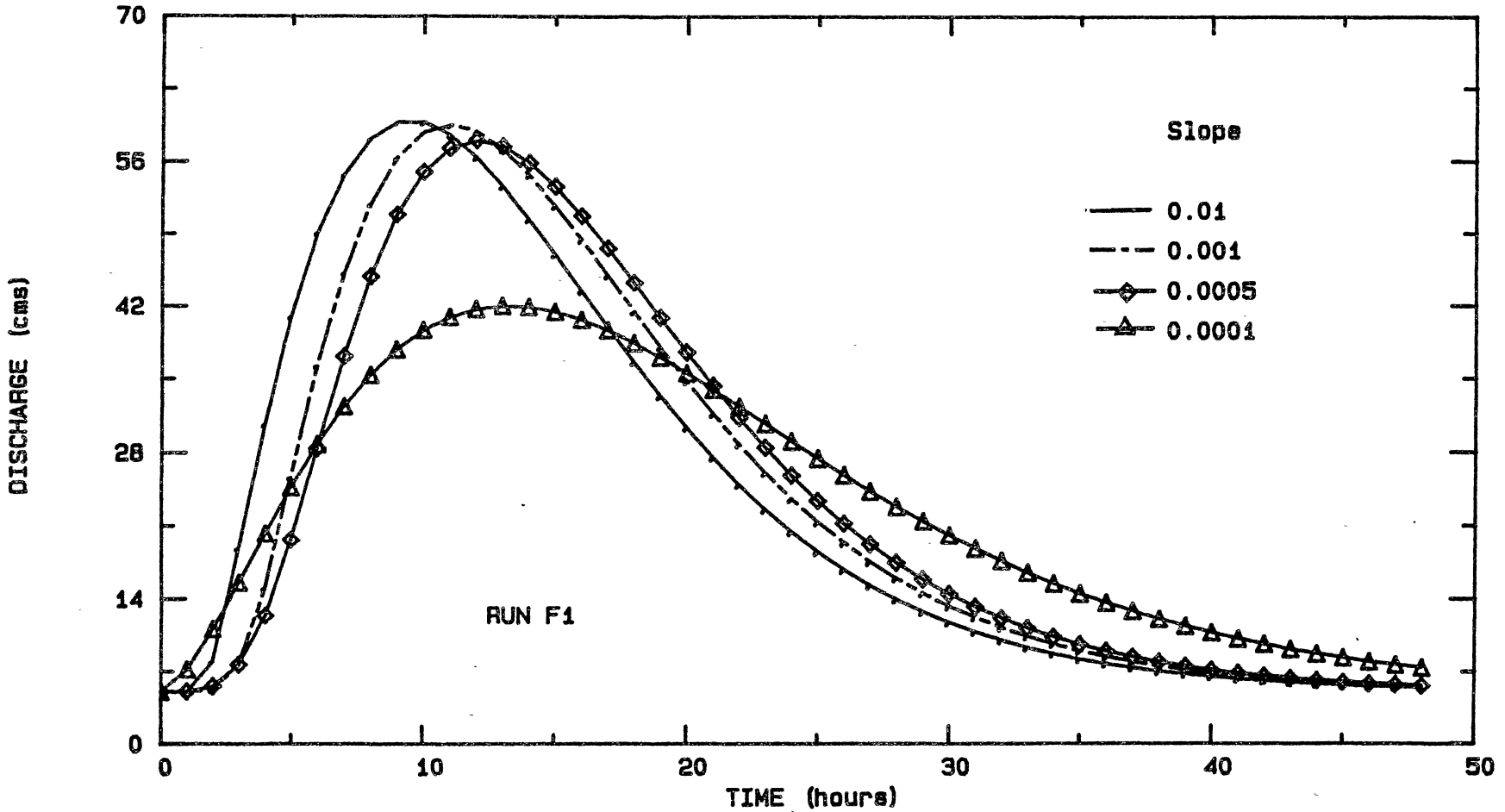

Figure 12. The Effect of Varying Slope on the Outflow Hydrograph for Constant Inflow Type, Manning's n and Channel Geometry

slope. Numerical error could also be a possible source of the discrepency in the observed trend.

A possible reason for this difference may be the fact that the time derivative is approximated with a space derivative in the derivation of the method. This approximation was examined by looking at the values for $\partial Q/\partial t$ and $-c\ \partial Q/\partial X$ for the 0.001 slope, inflow two, 0.05 roughness coefficient and the 0.0001 slope, inflow two, 0.10 roughnes coefficient . The 0.001 slope value showed a difference of approximately 10% between the two terms compared to a difference of approximately 30% for the 0.0001 slope value. The differences between the two terms were calculated from printout of the finite element program. This early rise may be a problem for the model at slopes of 0.0001 or less.

Table X contains a summary of the distribution of bed slopes for 188 Oklahoma streams (Sauer, 1979). It can be seen from Table X that only three percent of the Oklahoma streams examined had a bed slope of less than 0.005, while ninety percent had slopes of 0.001 or greater. The nonlinear hydrodynamic Muskingum method when compared to the Saint Venant equations performed excellently when the slope values were greater than 0.0001, and only failed to model the rising limb of the outflow hydrograph for the 0.0001 slope runs. From this it would seem that the poor performance at the 0.0001 slope values of the nonlinear Hydrodynamic Muskingum method would not be a drawback when

TABLE XI

DISTRIBUTION OF BED SLOPES FOR OKLAHOMA STREAMS

Range of Bed Slopes	Percentage of Total %	Number of Channels
> 0.03	0	0
0.03 - 0.01	15	28
0.01 - 0.005	21	40
0.005 - 0.001	53	100
0.001 - 0.005	8	15
0.005 - 0.0001	3	5
< 0.0001	0	0

applying the method to Oklahoma streams.

Summary

Overall, the results presented in this chapter have shown that Dooge et al's (1982) Hydrodynamic Muskingum Method is a useful technique for determining Muskingum's K and x. The nonlinear Hydrodynamic Muskingum method proved to be a slightly better model than the linear Hydrodynamic Muskingum method. In general, however, conclusions drawn from the nonlinear model also apply to the linear model.

The nonlinear Hydrodynamic Muskingum method predicted the peak flow rates excellently for those runs with attenuations of less than fifteen percent over the fifteen kilometer reach. The model predicted peak flow rates better at lower values of Manning's n and higher slope values . These trends were illustrated in Series I, IV and V tests.

The nonlinear Hydrodynamic Muskingum method predicted the time to peak accurately for all the 0.01 and 0.001 runs of Series I tests. The 0.0001 slope cases of Series I tests tended to have an earlier time to peak. Series IV tests showed excellent agreement between time to peak of the Nonlinear Hydrodynamic Muskingum and the Saint Venant equations for all slope values. Series V tests showed an earlier time to peak in all cases. In general there was a good agreement between time to peak of the nonlinear Hydrodynamic Muskingum method and the Saint Venant equations.

The overall shape of the outflow hydrographs predicted by the nonlinear Hydrodynamic Muskingum method was good when compared to the Saint Venant equations (see Series I, IV and V tests). The 0.0001 slope values in all cases showed an earlier rise in the rising limb of the outflow hydrograph when compared to the Saint Venant Equations (Series VII tests). The selection of time step, subreach length and subreach-time step ratio was not critical as long as the time step was selected to adequately describe the inflow hydrograph (see Series II tests). The nonlinear Hydrodynamic Muskingum method showed some sensitivity to the selection of reference flow fraction Q_{ref} . The peak flow rate increased and the time to peak decreased with increasing reference flow fraction. Q_{ref} set equal to 0.5 produced the best results for peak flow values, time to peak and overall shape.

In most cases, the predicted results with the nonlinear Hydrodynamic Muskingum method compared quite well to those with a finite element solution to the Saint Venant equation. The method showed some sensitivity to roughness coefficient, baseflows and inflow hydrograph, performing slightly better at lower roughness coefficients, higher baseflows and lower peak inflow flow values. The larger slope values produced better results. The method has applications to non-rectangular channels.

CHAPTER VI

SUMMARY AND CONCLUSIONS

A study was conducted to evaluate the validity of Dooge et al.'s (1982) hydrodynamically derived Muskingum flood routing coefficients. The objectives of the study were to (a) compare the simulation results from Dooge et al.'s (1982) Hydrodynamic Muskingum routing method to the simulation results obtained from a finite element solution to the Saint Venant equations and to (b) compare the simulation results from Dooge et al.'s nonlinear Hydrodynamic Muskingum routing method to the simulation results obtained by a finite element solution to the Saint Venant equations.

The Muskingum's flood routing coefficients K and x were derived by reducing the Saint Venant equations to a linear, spacially lumped system following a procedure similar to that used by Dooge et al. (1982). A flow model was developed using this derivation and a nonlinear feature incorporate. Seven series of tests were conducted to evaluate the flow model for a range of slopes, inflow hydrographs , roughness coefficients and channel geometries. The method's sensitivity to time step, subreach length and

subreach length-time step ratio was also studied.

Based on the results presented in Chapter V the following conclusions can be drawn:

1. The nonlinear Hydrodynamic model performs slightly better than the linear Hydrodynamic model.

2. The nonlinear Hydrodynamic model predicts the peak flow rates accurately when compared to the Saint Venant equations. The model predicted peak flow rates better at lower values of Manning's n and higher slope values.

3. The nonlinear Hydrodynamic model predicts time to peak accurately when compared to the Saint Venant equations. The 0.0001 slope cases showed a tendancy to predict earlier time to peaks.

4. The overall shape of the outflow hydrographs predicted by the nonlinear Hydrodynamic Muskingum method is good. The 0.0001 slope cases showed an earlier rise in the rising limb of the hydrograph.

5. The smaller roughness coefficents and larger slopes produce slightly better results.

6. The nonlinear Hydrodynamic Muskingum method can be used for non-rectangular geometries with less accuracy.

7. The nonlinear Hydrodynamic Muskingum method was not sensitive to time step, subreach length or subreach-time step ratio as long as the time step adequately described the inflow hydrograph.

8. The nonlinear Hydrodynamic Muskingum method worked best with a reference flow value half way between the

baseflow and peak flow values (i.e. $Q_{r_{ef}} = 0.5$).

9. The nonlinear Hydrodynamic Muskingum method was not sensitive to inflow type. It performed slightly better at higher baseflows and lower peak flows.

10. The nonlinear Hydrodynamic Muskingum method predicted the outflow hydrograph for the Illinois River reasonablely well when compared to the observed outflow hydrograph.

Overall the model is robust, simple and accurate for the range of runs considered in this study. Its has the potential to be a cheap useful engineering model.

Recommendations for Future Research

1. Perform runs on a more diverse set of channel geometries.

2. Evaluate model using observed inflow and outflow data for actual channels.

3. Perform more runs in the 0.0005 to 0.0001 slope range to determine the point where the model starts to predict an early rise in the rising limb of the outflow hydrograph.

4. Evaluate the models performance under different boundary conditions.

5. Compare the model against other Muskingum routing methods for ungaged streams.

REFERENCES CITED

Amein, M. and C. S. Fang. 1970. Implicit flood routing in natural channels. Journal of Hydraulic Research, 96(12):24.

Butler, S. S. 1957. Engineering hydrology. Prentice-Hill, Inc., N.J.

Chaudhry, Y. M. and D. N. Contractor. 1973. Application of implicit methods to surges in channels. Water Resources Research, 9(6):1605-1612.

Cunge, J. A. 1969. On the subject of a flood propagation computation method (Muskingum method). Journal of Hydraulic Research, 7(2):205-230.

Davis, V. C. 1952. Handbook of applied hydraulics. McGraw-Hill, Inc., New York

Dooge, J. C., W. B. Strupczewski and J. J. Napiorkowski. 1982. Hydrodynamic derivation of storage parameters of the Muskingum model. J. Hydrol., 54:371-387.

Gill, M. A. 1979. Critical examination of the Muskingum method. J. Hydrol., 10:261-270.

Henderson, F. M. 1966. Open channel flow. MacMillan, Inc., New York.

Johnstone, D. and W. P. Cross. Elements of applied hydrology. McGraw-Hill, Inc., New York.

Koussis, A. 1978. Theoretical estimation of flood routing parameters. Journal of the Hydraulics Division, ASCE, 104(4):109-115.

Liggett, J. A. and D. A. Woolhiser. 1967. Difference solution of shallow water equations. J. Eng. Mech. Div., ASCE, 95(2):39-71.

Lighthill, M. J. and G. B. Whitham. 1955. On kinematic waves I. Flood movement in long rivers. Proc. of the Royal Society of London,

A229:281-316.

Linsley, R. M., M. A. Kohler and J. L. H. Paulus. 1975. Hydrology for Engineers. McGraw-Hill, Inc. New York.

Mockus, J. 1962. SCS National Engineering Handbook. Soil Conservation Service, pp. 17.1-17.32.

Meyers, G. L. 1971. Analytical methods in conduction heat transfer. McGraw-Hill, Inc. New York.

Nwaogazie, F. I. L. and A. K. Tyagi. 1984. Unified streamflow routing by finite elements. Journal of Hydraulics Division, ASCE, 108(11): 1595-1611.

Pinder, G. F. and S. P. Sauer. 1971. Numerical simulation of flood wave modification due to bank storeage effect. Water Resources Research, 7(1):63-70.

Ponce, V. M. and V. Yevjevich. 1978. Muskingum-Cunge mehtod with variable parameters. Journal of Hydraulics Division, ASCE, 104(12): 353-360.

Ponce, V. M. 1981. Development of an algorithm for the linearized diffusion method of flood routing. San Diego State University Civil Engineering Series, No. 81140.

Ponce, V. M. and F. D. Thevrer. 1982. Accuracy criteria in diffusion routing. Journal of Hydraulics Division, ASCE, 108(6):747-757.

Reily, R. 1984. Personal interview. Soil Conservation Service, Chickasha, Oklahoma, May 25.

Sauer, V. B. 1974. Flood characteristics of Oklahoma streams. U.S.G.S-WRI 52-73.

Singh, V. P. and R. C. McCann. 1980. Some notes on Muskingum method of flood routing. J. Hydrol., 48:343-361.

Smith, D. J. 1979. Stream hydraulics package computer program decription. U.S. Army Corps of Engineers, Hydrologic Engineering Center RMA 9020.

Weinmann, P. E. 1977. Comparison of flood routing

methods for natural rivers. Monash University Civil Engineering Research Report 2/1977, Clayton, Victoria, Australia.

Viessman, W., Jr., J. W. Knapp, G. L. Lewis and T. E. Harbaugh. 1972. Introduction to hydrology. Harper and Row Publishers, New York.

Zienkiewicz, o.c. 1977. The finite element method in engineering science. McGraw-Hill, Inc., New York.

APPENDIX A

COMPUTER PROGRAM FOR HYDRODYNAMIC MUSKINGUM MODEL

```
C
C
C       HYDRODYNAMIC MUSKINGUM METHOD PROGRAM
C
C       THIS PROGRAM CALCULATES HYDRODYNAMIC MUSKINGUM PARAMETERS
C       UTILIZING A METHOD PROPOSED BY DOOGE (1982).
C
C
        DIMENSION O(3000),OUT(3000),RIN(3000),A(5),WP(5)
C
C
C ****************************************************************
C QREF    0 - 1  THE FRACTIONAL VALUE OF (QP - QB) TO BE USED
C TO CALCULATE REFERENCE FLOWRATE ,0.5 SUGGESTED.
C ZE USED IN MANNING'S EQUATION ,1 OR 1.489 ,S.I. OR ENGLISH
C INTP PRINTOUT INTERVAL IN SECONDS
C AL CHANNEL LENGTH METERS OR FEET.    N NUMBER OF SUBREACHES .
C AS CHANNEL SLOPE.   AM THE POWER OF FLOWRATE IN ENERGY SLOPE EQ.
C AN  MANNING'S N VALUE
C A(1) - A(5) THE COEFFICIENTS 4TH POLYNOMIAL DESCRIBING AREA.
C WP(1)-WP(5) THE COEFFICIENTS 4TH POLYNOMIAL DESCRIBING WETTED PE
C TSIM TIME OF SIMULATION  ,T1 TIME STEP
C QP PEAK INFLOWRATE        ,YO GUESS AT INITIAL DEPTH
C QB BASEFLOW RATE CUBIC METERS/SEC OR FT^3/SEC
C ****************************************************************
C
      CHARACTER FILEI*12,FILEO*12,FILEO2*12
C
C **** OPEN DATA FILES FOR INPUT AND OUTPUT *****
C
      OPEN (UNIT=1,FILE='CON')
      WRITE(1,9990)
 9990 FORMAT(//5X,'LINEAR 1 OR NONLINEAR MODEL 2')
      READ(1,*) DLN
      WRITE(1,9995)
 9995 FORMAT(//5X,'ENTER FILE NAME FOR INPUT DATA')
      READ(1,9996) FILEI
 9996 FORMAT(A)
      OPEN (UNIT=5,FILE=FILEI)
      WRITE(1,9997)
 9997 FORMAT(//5X,'ENTER FILE NAME FOR OUTPUT DATA')
      READ(1,9996) FILEO
      OPEN (UNIT=6,FILE=FILEO)
      WRITE(1,9998)
 9998 FORMAT(//5X,'ENTER FILE NAME FOR OUTPUT PLOTTING')
      READ(1,9996) FILEO2
      OPEN (UNIT=7,FILE=FILEO2)
C
        READ(5,*) QREF,ZE
        READ(5,*) INTP,AL,AS,AM,AN,N
        READ(5,*)(A(I),I=1,5)
        READ(5,*)(WP(I),I=1,5)
        READ(5,*) TSIM,T1,YO,QP,QB
        QO=QB+(QP-QB)*QREF
```

```
      QP=QP-QB
      TP=0
      NTRIB=0
      TC=1
      AL=AL/N
      WRITE(6,*) T1,AL,'SET RATIO',(AL/T1)
      CALL PRAM(A,WP,AN,YO,AL,AS,C1,C2,C3,AM,QO,ZE,T1)
      I1=INT(TSIM/T1)
C
C     CALCULATE INITAL VALUES OF C1,C2,C3 AND THEN READ IN
C     INFLOW DATA.
C
      CALL INFLOW(O,RIN,K,X,T1,I1,TSIM,QB,C1,C2,C3,QP,TP,TC)
      READ(5,*) TRIB
      QR=0
      DO 8 I4=0,I1
      OUT(I4)=RIN(I4)
      RIN(I4)=O(I4)
      IF (QR.LT.RIN(I4)) QR=RIN(I4)
    8 CONTINUE
      DO 5 I2=2,N
      IF (DLN.LT.2) GO TO 18
      QR=QB+(QR-QB)*QREF
      CALL PRAM(A,WP,AN,YO,AL,AS,C1,C2,C3,AM,QR,ZE,T1)
   18 CALL ROUT(O,RIN,K,X,I1,TSIM,QB,C1,C2,C3)
      QR = 0
      DO 7 I3=0,I1
      IF (QR.LT.O(I3))  QR=O(I3)
      RIN(I3)=O(I3)
    7 CONTINUE
      IF ((INT(TRIB/AL)).NE.I2) GO TO 5
      CALL TRIBY(RIN,I1,T1,QO)
    5 CONTINUE
      TOP=0
      H=0
      H1=0
      DO 15 I=0,I1
      H=H+O(I)
      H1=H1+OUT(I)
      IF (TOP.GT.O(I)) GO TO 13
      TOP=O(I)
      TOPI=(I)
      TOPO=OUT(I)
   13 IF ((INT(I*T1/INTP)).NE.(I*T1/INTP)) GO TO 15
      WRITE(6,*) INT(I*T1/3600),OUT(I),O(I)
      WRITE(7,*) INT(I*T1/3600),',',O(I)
   15 CONTINUE
      WRITE(6,*) TOPI,TOPO,TOP
      WRITE(6,*) 'VOLUME IN',H1,'VOLUME OUT',H
      STOP
      END
C
C     THIS SUBROUTINE CALCULATES HYDRODYNAMIC ROUTING PARMETERS
C     C1,C2,C3 .
```

```
C
      SUBROUTINE PRAM(A1,WP,AN1,YO,ALC,SO,C1,C2,C3,AM1,QO,ZE,T1)
      DIMENSION A1(5),WP(5)
      INTER = 0
      Y1= 1.25*YO
      GO TO 858
  803 INTER = INTER + 1
      IF (INTER.LT.5000) GO TO 858
      WRITE(6,*) 'INTER ERROR QO Q1' ,QO,Q1
      GO TO 970
  858 AO=A1(1)+A1(2)*YO+A1(3)*YO**2+A1(4)*YO**3+A1(5)*YO**4
      WP1=WP(1)+WP(2)*YO+WP(3)*YO**2+WP(4)*YO**3+WP(5)*YO**4
      TO=A1(2)+2*A1(3)*YO+3*A1(4)*YO**3+4*A1(5)*YO**4
      Y=SQRT(SO)
      Q1=(ZE/AN1)*AO*((AO/WP1)**(0.666667))*Y
      IF (Q1.LT.(0.95*QO)) GO TO 873
      IF (Q1.GT.(1.05*QO)) GO TO 877
      GO TO 970
  873 AY = YO
      YO = YO + 0.5*ABS(Y1-YO)
      Y1 = AY
      GO TO 803
  877 AY = YO
      YO = YO - 0.5*ABS(Y1-YO)
      Y1 = AY
      GO TO 803
  970 DX=(QO/AO*AM1)
      WRITE(6,*) 'QO ,RATIO, SUBR',QO,DX,INT(T1*DX)
      K1=ALC/AM1/QO*AO
      FO=QO**2*TO/(32.2*AO**3)
      Z1=1-FO**2*(AM1*AO/TO/YO-1)**2
      X1=0.5-0.5/AM1*YO/SO/ALC*Z1
      KC=K1-K1*X1+0.5*T1
      C2=(K1*X1+0.5*T1)/KC
      C3=(K1-K1*X1-0.5*T1)/KC
      C1= 1-C2-C3
      CERROR = C1+C2+C3
      WRITE(6,*) 'K ,X,CERROR',K1,X1,CERROR
      WRITE(6,*) 'C1,C2,C3',C1,C2,C3
      WRITE(6,*)
      RETURN
      END
C
C THIS SUBROUTINE READS IN THE INFLOW HYDROGRAPH AND ROUTS
C DOWN THE FIRST SUBREACH. INFLOW CAN BE IN PAIRS OF POINTS
C OR DEFINED USING QP ...(PEAKFLOW - BASEFLOW) ,QB BASEFLOW
C TP TIME TO PEAK ,TG TIME TO CENTER OF GRAVITY USE (ID=3)
      SUBROUTINE INFLOW(OUT,RINF,K,X,T1,I1,TSIM,QO,C1,C2,C3,QP,TP,TC)
C
      INTEGER A,B
      DIMENSION OUT(I1),TND(2,30),RINF(I1)
      READ(5,*) ID
      OUT(0) =QO
      IF (ID.EQ.3) GO TO 7
```

```
      READ(5,*) TP,TC
      R1= TP/(TC-TP)
      DO 6 IT=0,I1
      G =(TP-IT*T1)/(TC-TP)
      RINF(IT) =QO +QP*(IT*T1/TP)**R1*EXP(G)
      IF (IT.EQ.0) GO TO 6
      OUT(IT)= C1*RINF(IT)+C2*RINF(IT-1) +C3*OUT(IT-1)
 6    CONTINUE
      GO TO  11
 7    READ(5,*) ND
      DO 70 J=1,ND
      READ(5,*) TND(1,J),TND(2,J)
      WRITE(6,*) TND(1,J),TND(2,J)
70    CONTINUE
      A=1
      B=2
      DO 80 J2=0,I1
85    TT=T1*J2
      IF (TT.LE.TND(1,B)) GO TO 90
      A=A+1
      B=B+1
      GO TO 85
90    RINF(J2)=(J2*T1-TND(1,A))/(TND(1,B)-TND(1,A))*(TND(2,B)-TND(2,A)
     1 )+TND(2,A)
      IF (J2.EQ.0) GO TO 80
      OUT(J2)=C1*RINF(J2)+C2*RINF(J2-1)+C3*OUT(J2-1)
80    CONTINUE
11    RETURN
      END
C
C THIS SUBROUTINE ROUTS THROUGH THE REMAINING SUBREACHES.
C C1,C2,C3 ARE EVALUATED AT THE BEGINNING OF EACH SUBREACH.
C
      SUBROUTINE ROUT(OUT,RINF,K,X,I1,TSIM,QO,C1,C2,C3)
      DIMENSION OUT(I1) ,RINF(I1)
      OUT(0)=QO
      L=I1
      DO 40 I=0,L
      OUT(I+1)=C1*RINF(I+1)+C2*RINF(I)+C3*OUT(I)
40    CONTINUE
      RETURN
      END
C
C THIS SUBROUTINE READS IN TRIBUTARY INFLOWS
C
      SUBROUTINE TRIBY(RINF,I1,T1,QO)
      INTEGER A,B
      DIMENSION TND(2,30) ,RINF(I1)
      READ(5,*) NTRIB
      DO 70 J=1,NTRIB
      READ(5,*) TND(1,J),TND(2,J)
70    CONTINUE
      A=1
      B=2
```

```
      DO 80 J2=0,I1
85    TT=T1*J2
      IF (TT.LE.TND(1,B)) GO TO 90
      A=A+1
      B=B+1
90    RINF(J2)=(TND(1,B)-T1*J2)/(TND(1,B)-TND(1,A))*(TND(2,B)-TND(2,A)
     1 )+TND(2,A)+RINF(J2)
80    CONTINUE
      QO=QO+TND(2,1)
      RETURN
      END
```

APPENDIX B

SERIES I LINEAR AND NONLINEAR PLOTS

LHDM - LINEAR HYDRODYNAMIC MUSKINGUM METHOD

NHDM - NONLINEAR HYDRODYNAMIC MUSKINGUM METHOD

SV - SAINT VENANT EQUATIONS

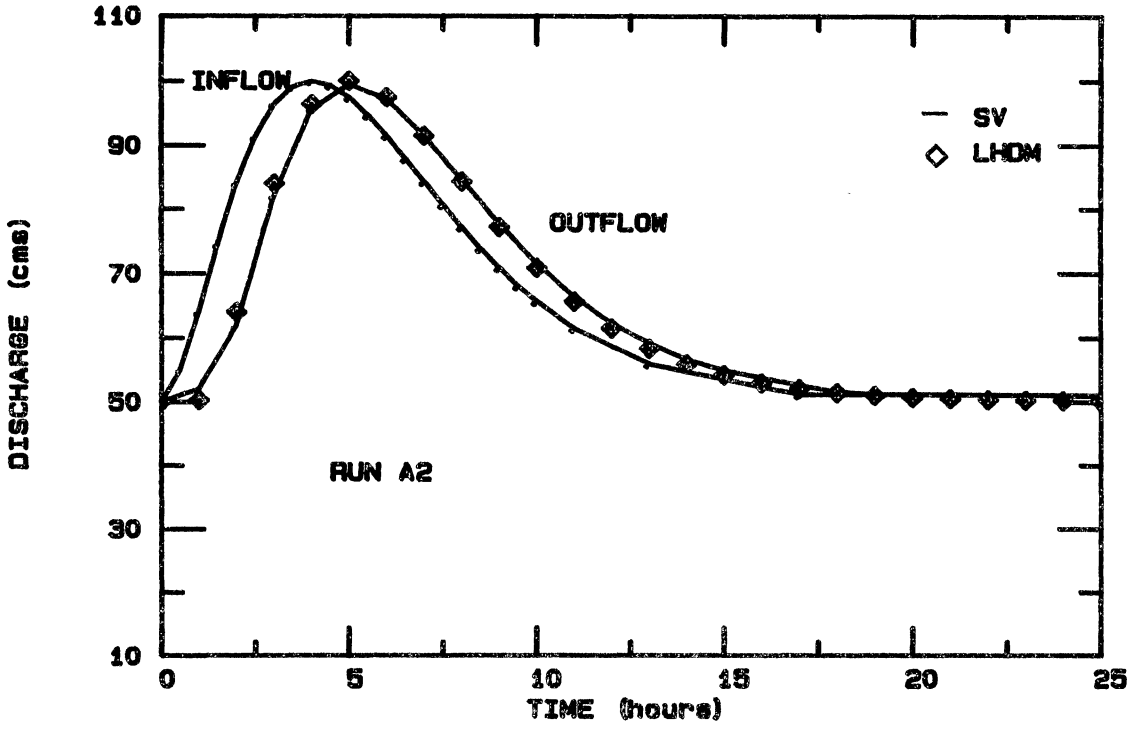
110
90
70
50
30
10
DISCHARGE (cms)
INFLOW
OUTFLOW
SV
LHDM
RUN A2
0
5
10
15
20
25
TIME (hours)

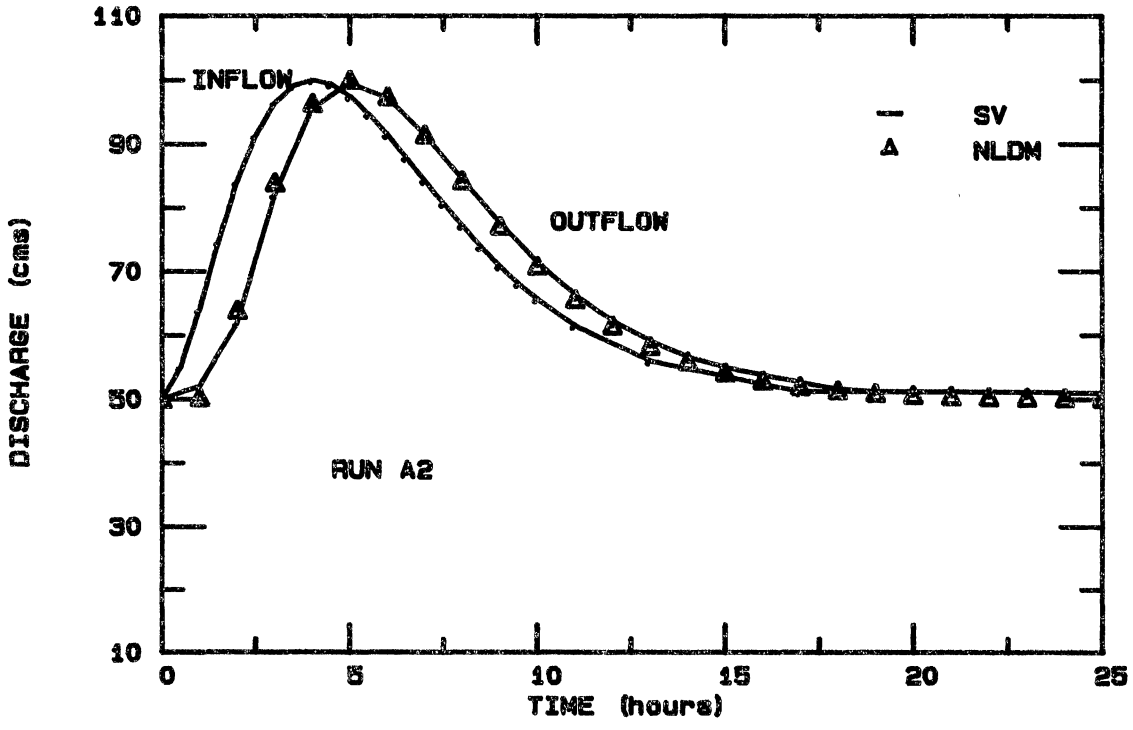
110
90
70
50
30
10
DISCHARGE (cms)
INFLOW
OUTFLOW
SV
NLDM
RUN A2
0
5
10
15
20
25
TIME (hours)

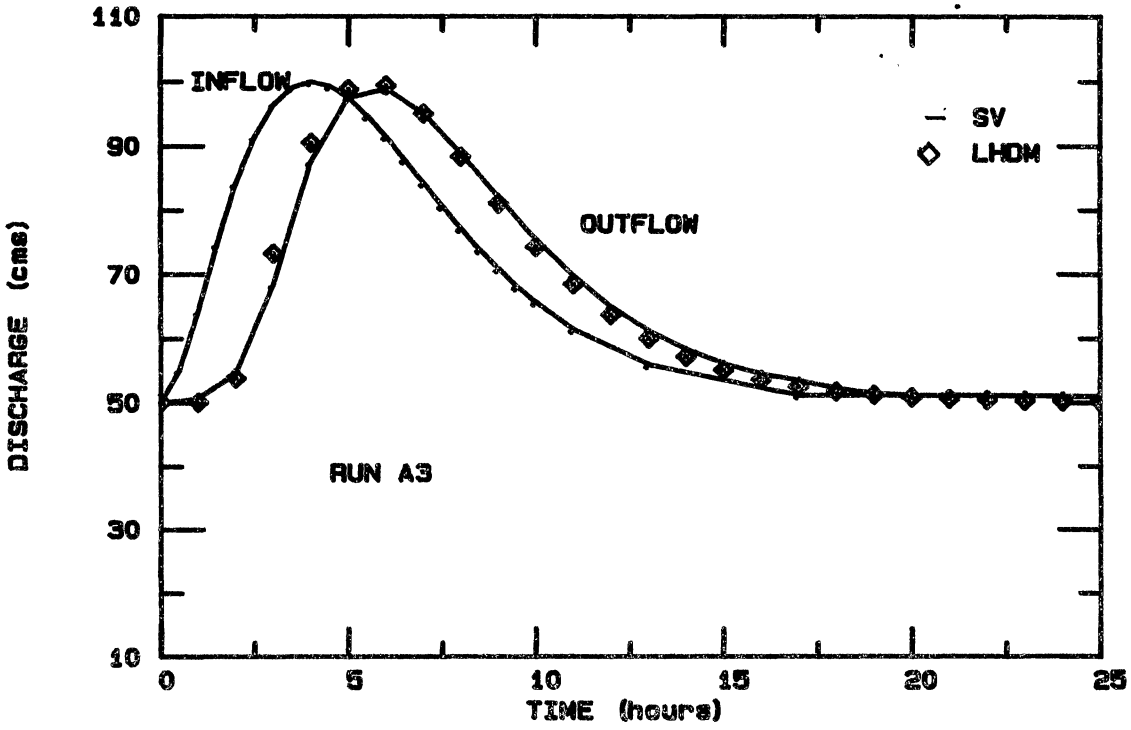
110
90
70
50
30
10
DISCHARGE (cms)
INFLOW
OUTFLOW
SV
LHDM
RUN A3
0
5
10
15
20
25
TIME (hours)

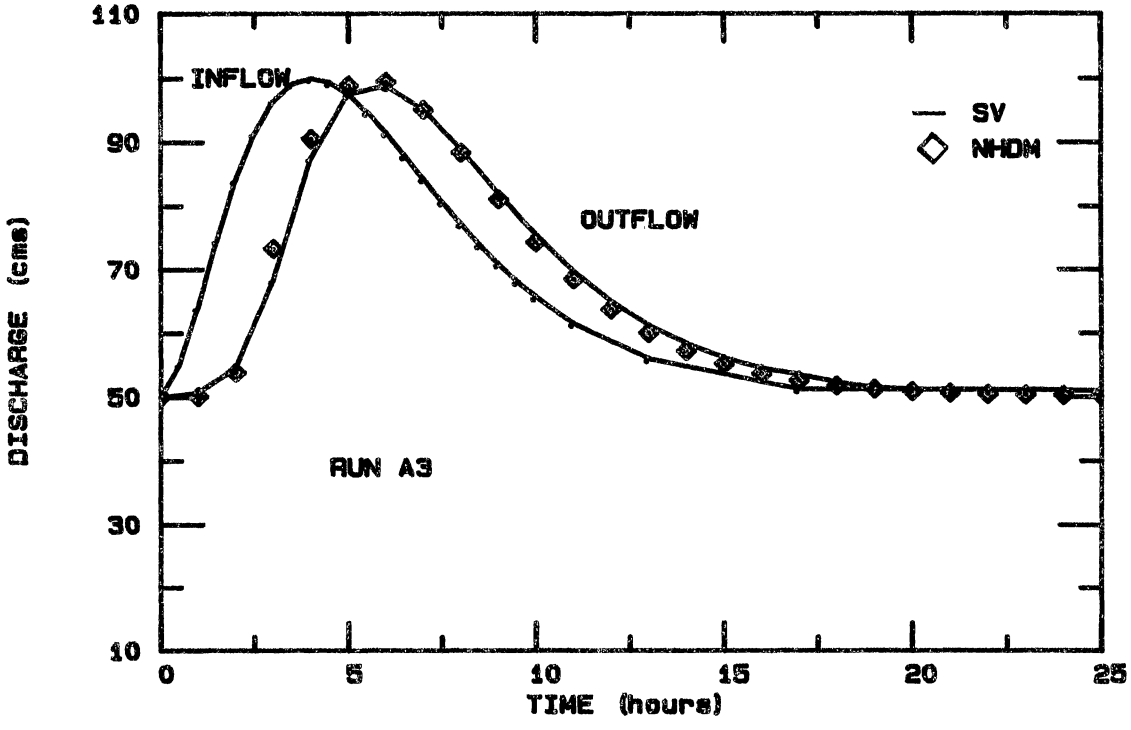
110
90
70
50
30
10
DISCHARGE (cms)
INFLOW
OUTFLOW
SV
NHDM
RUN A3
0
5
10
15
20
25
TIME (hours)

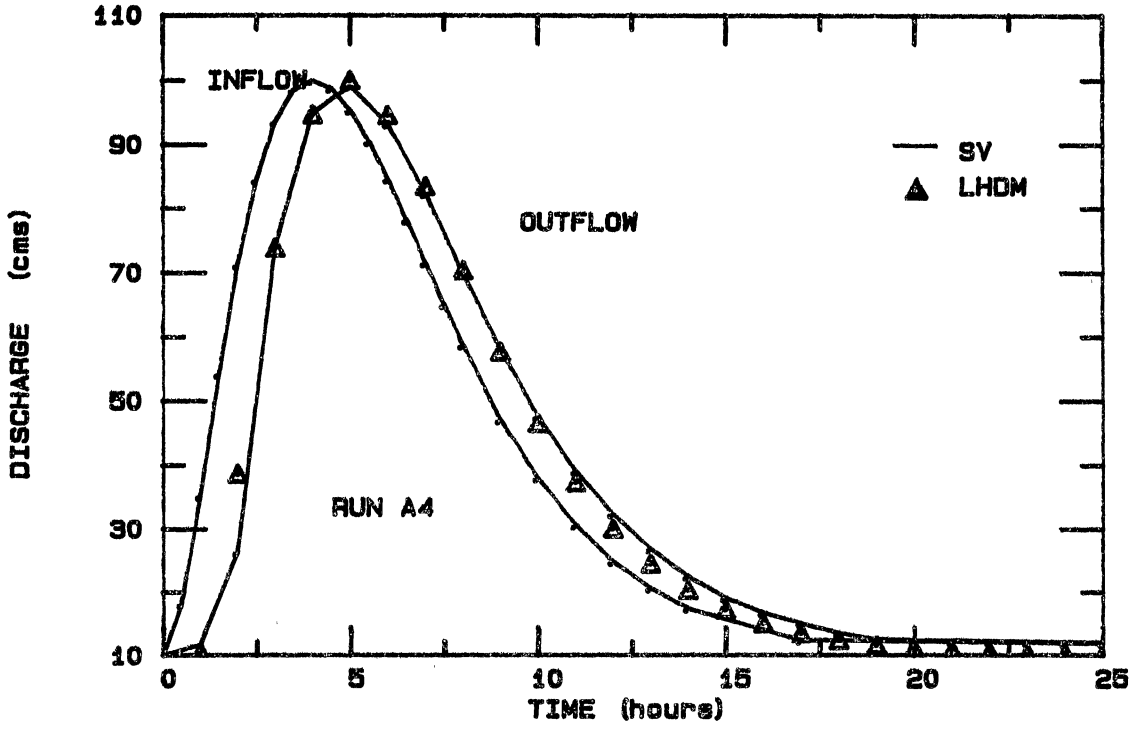
110
90
70
50
30
10
INFLOW
OUTFLOW
SV
LHDM
RUN A4
DISCHARGE (cms)
0
5
10
15
20
25
TIME (hours)

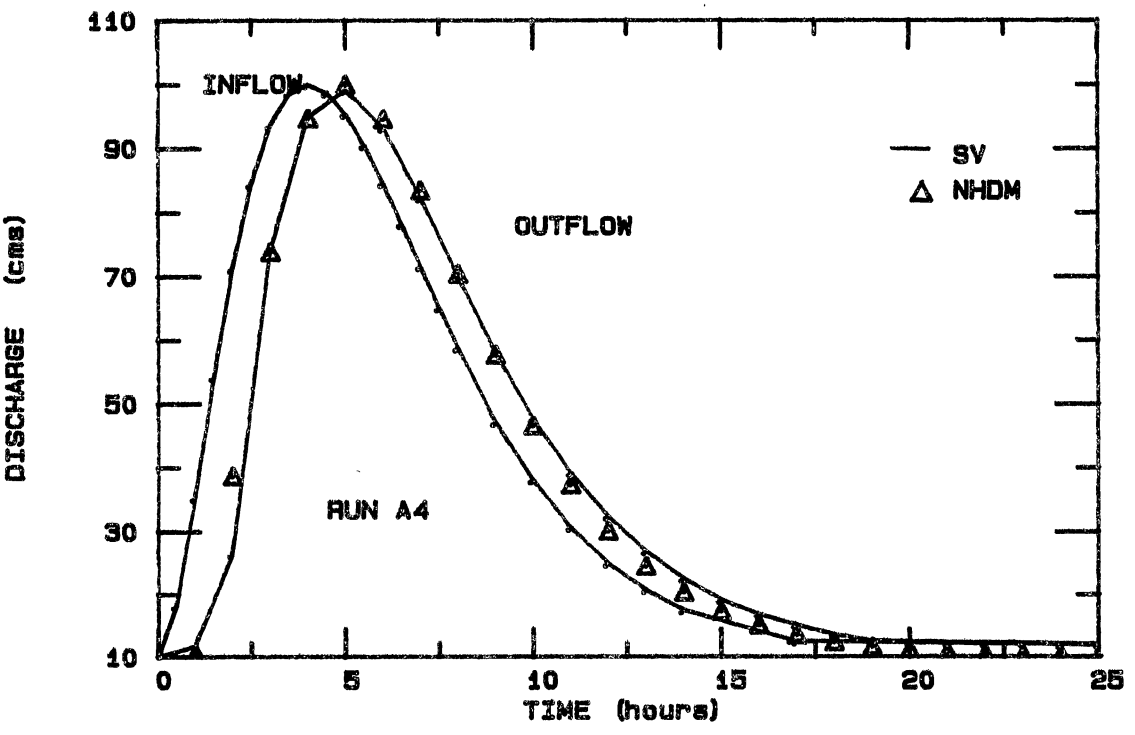
110
90
70
50
30
10
INFLOW
OUTFLOW
SV
NHDM
RUN A4
DISCHARGE (cms)
0
5
10
15
20
25
TIME (hours)

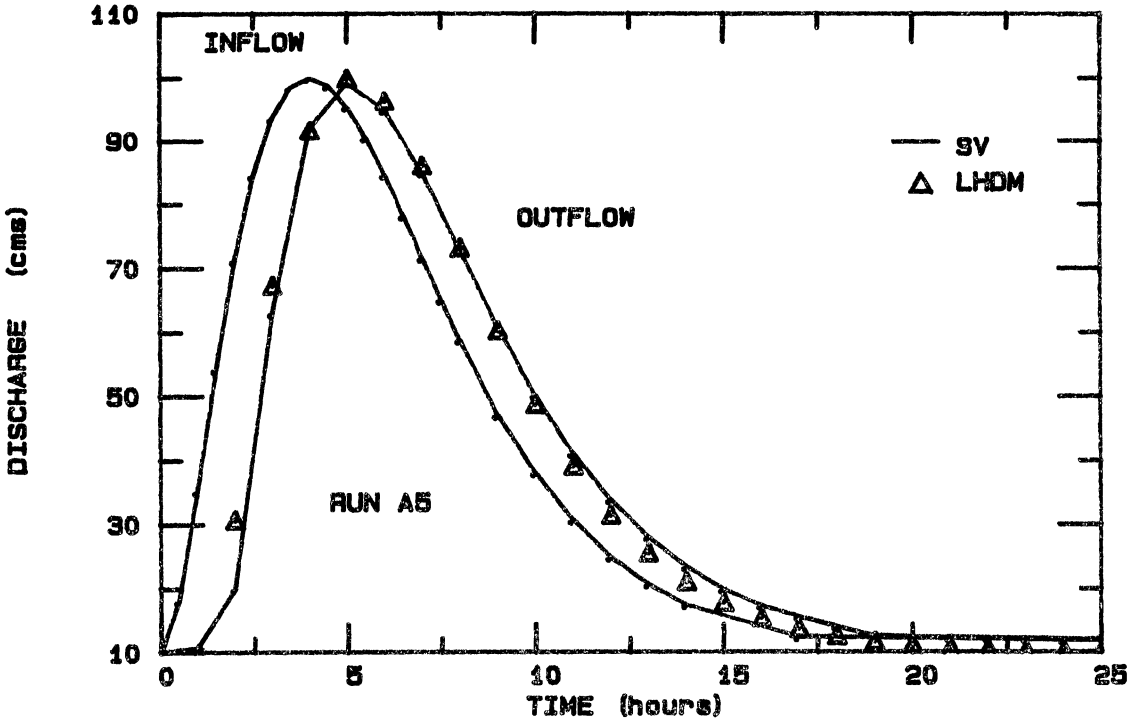
110
90
70
50
30
10
INFLOW
OUTFLOW
RUN A5
SV
LHDM
DISCHARGE (cms)
0
5
10
15
20
25
TIME (hours)

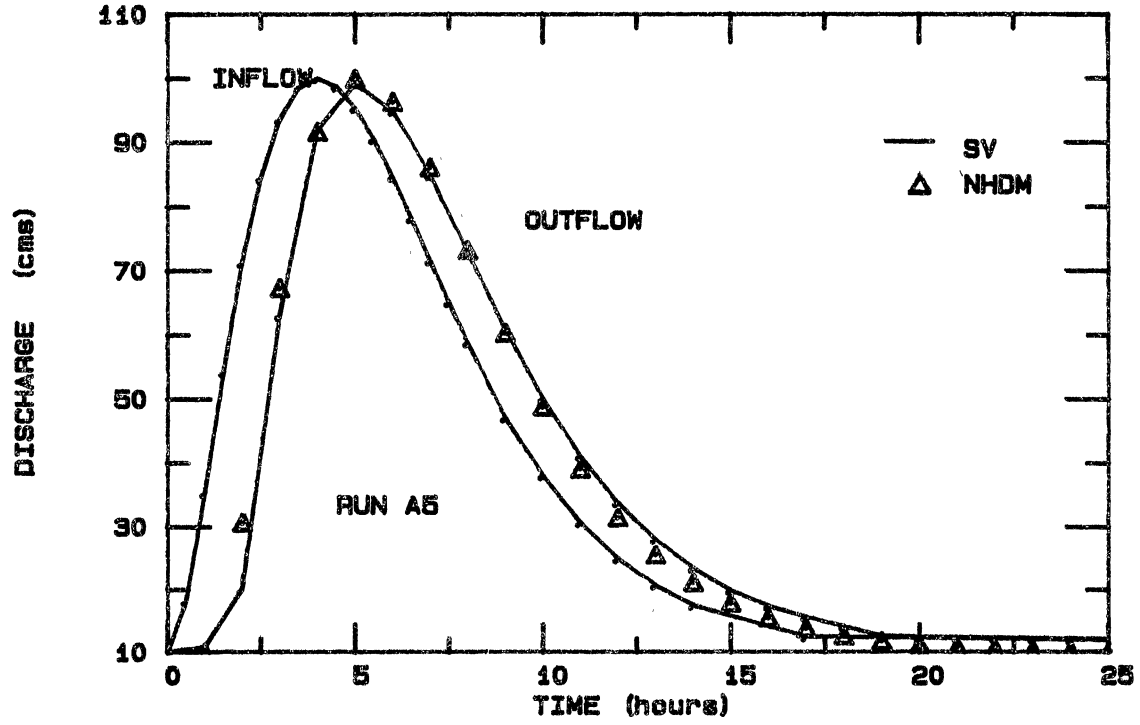
110
90
70
50
30
10
INFLOW
OUTFLOW
RUN A5
SV
NHDM
DISCHARGE (cms)
0
5
10
15
20
25
TIME (hours)

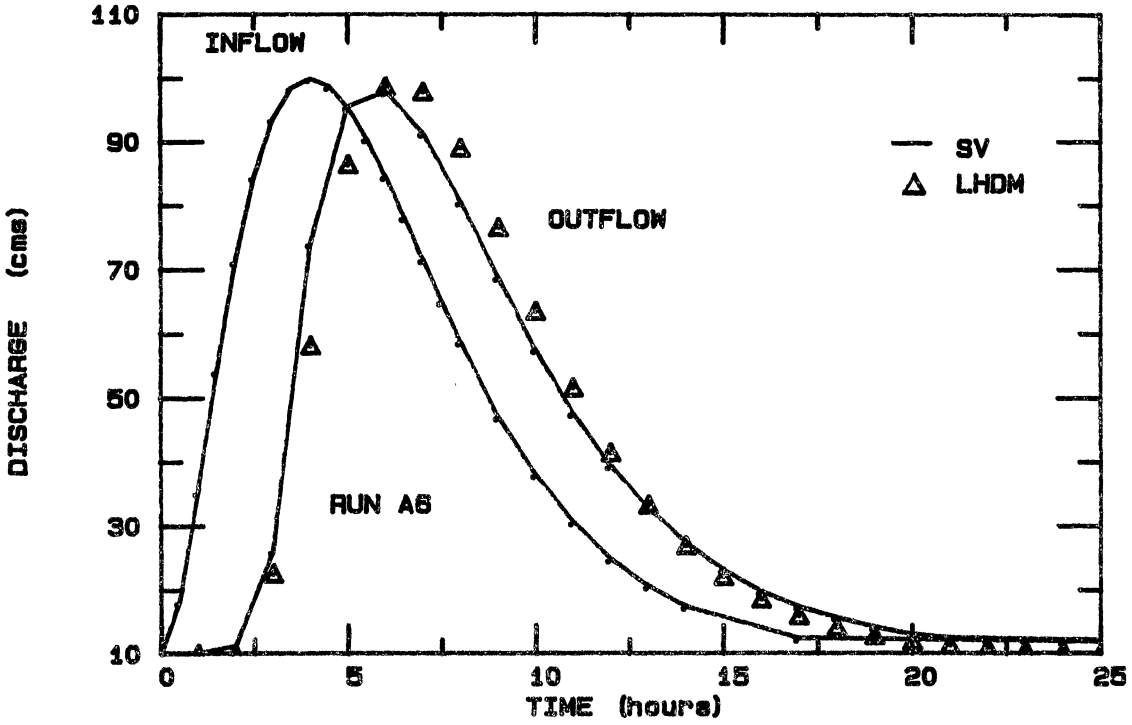
110
90
70
50
30
10
INFLOW
OUTFLOW
RUN A6
SV
LHDM
DISCHARGE (cms)
0
5
10
15
20
25
TIME (hours)

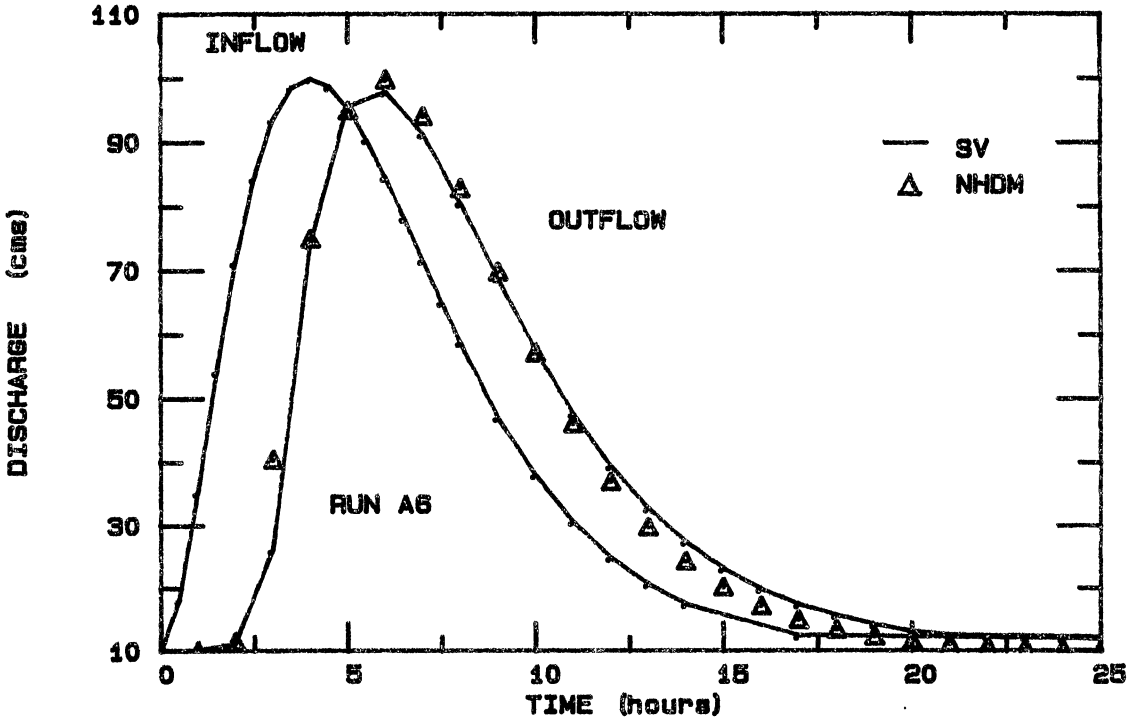
110
90
70
50
30
10
INFLOW
OUTFLOW
RUN A6
SV
NHDM
DISCHARGE (cms)
0
5
10
15
20
25
TIME (hours)

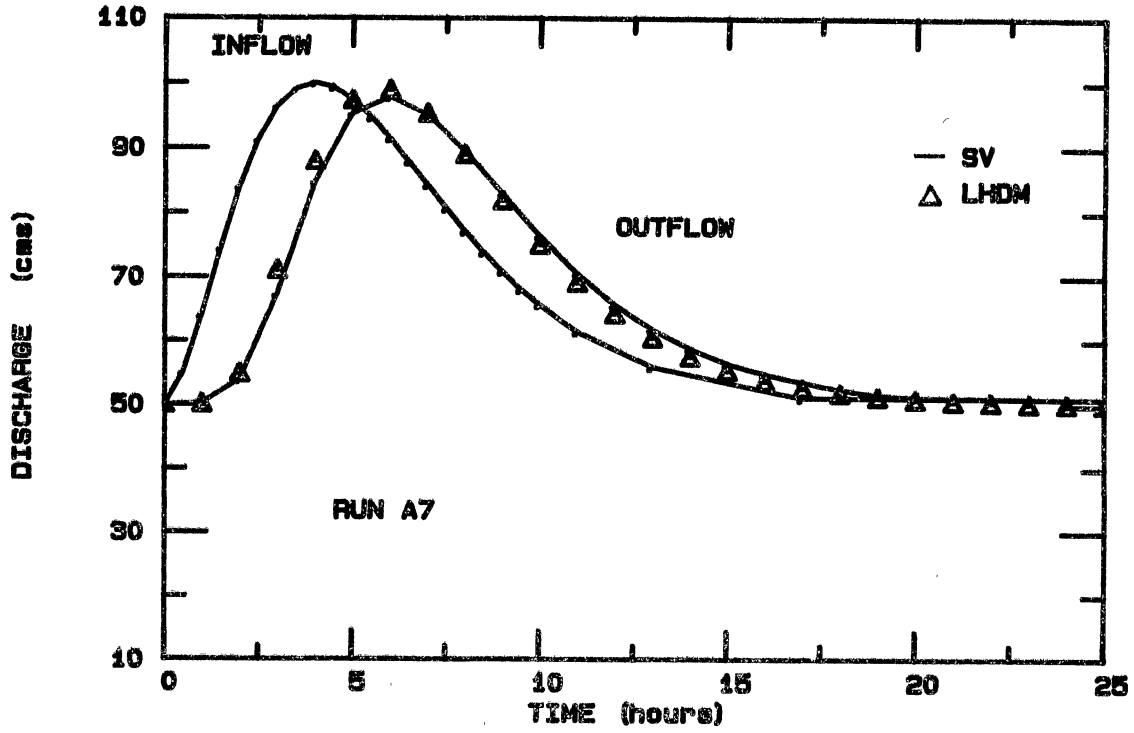
INFLOW
OUTFLOW
SV
LHDM
RUN A7
DISCHARGE (cms)
TIME (hours)
110
90
70
50
30
10
0
5
10
15
20
25

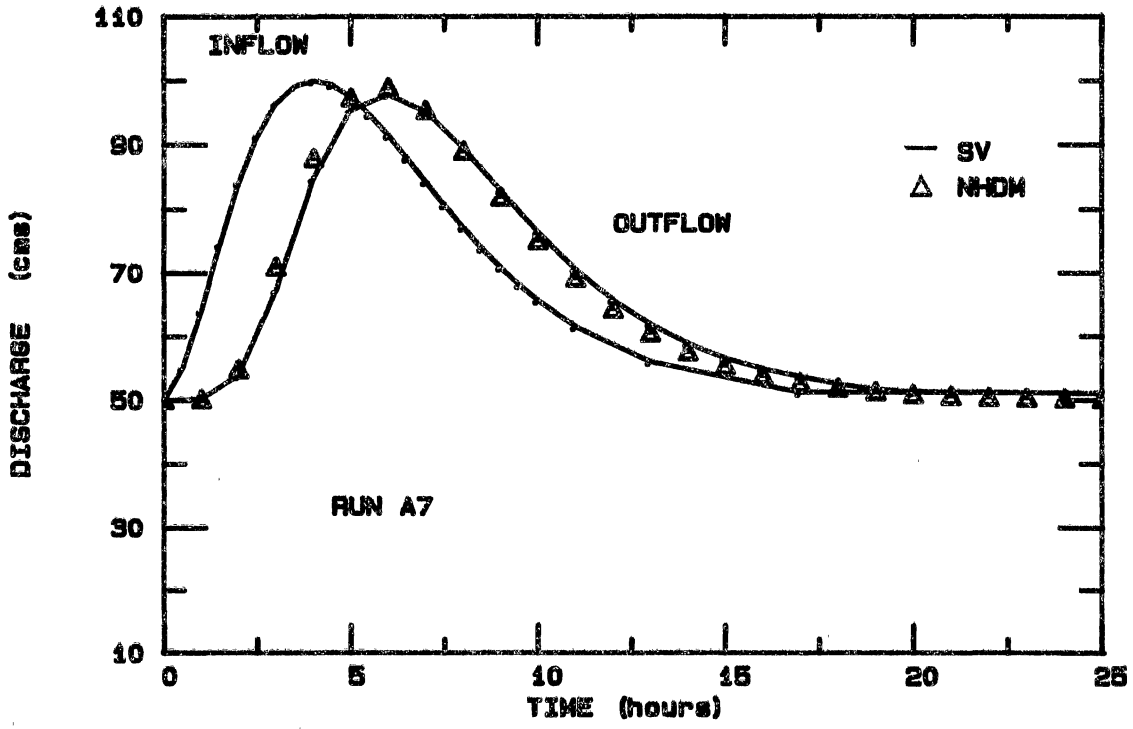
INFLOW
OUTFLOW
SV
NHDM
RUN A7
DISCHARGE (cms)
TIME (hours)
110
90
70
50
30
10
0
5
10
15
20
25

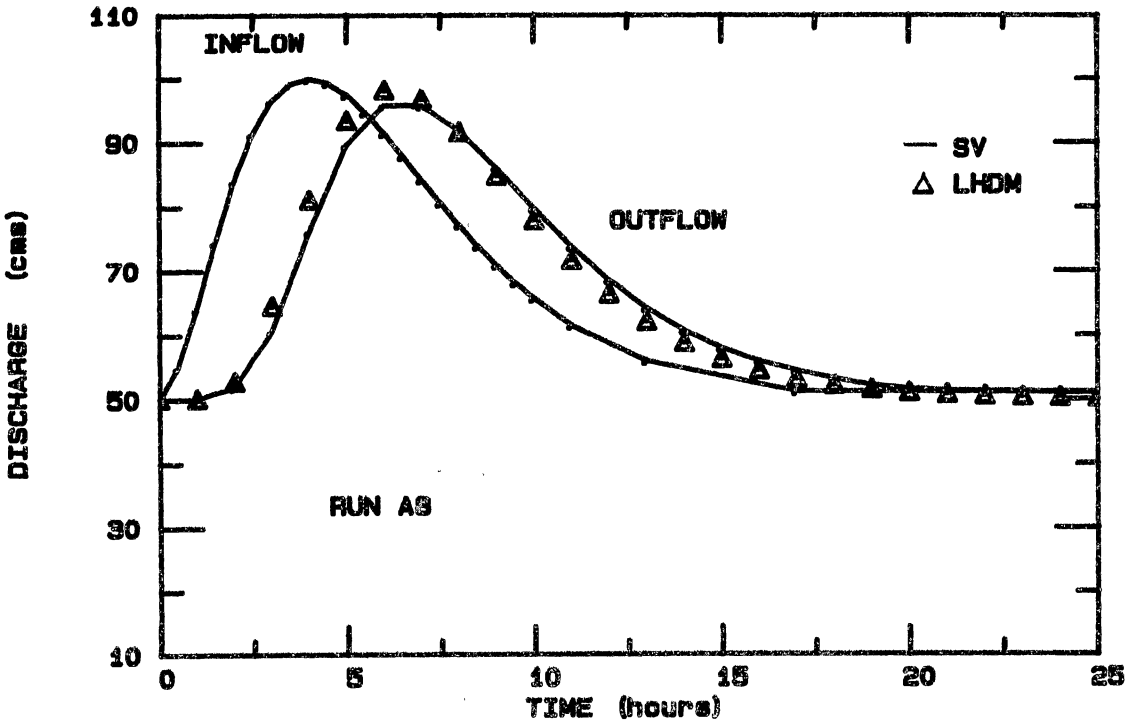
INFLOW
OUTFLOW
SV
LHDM
RUN A9
DISCHARGE (cms)
TIME (hours)
110
90
70
50
30
10
0
5
10
15
20
25

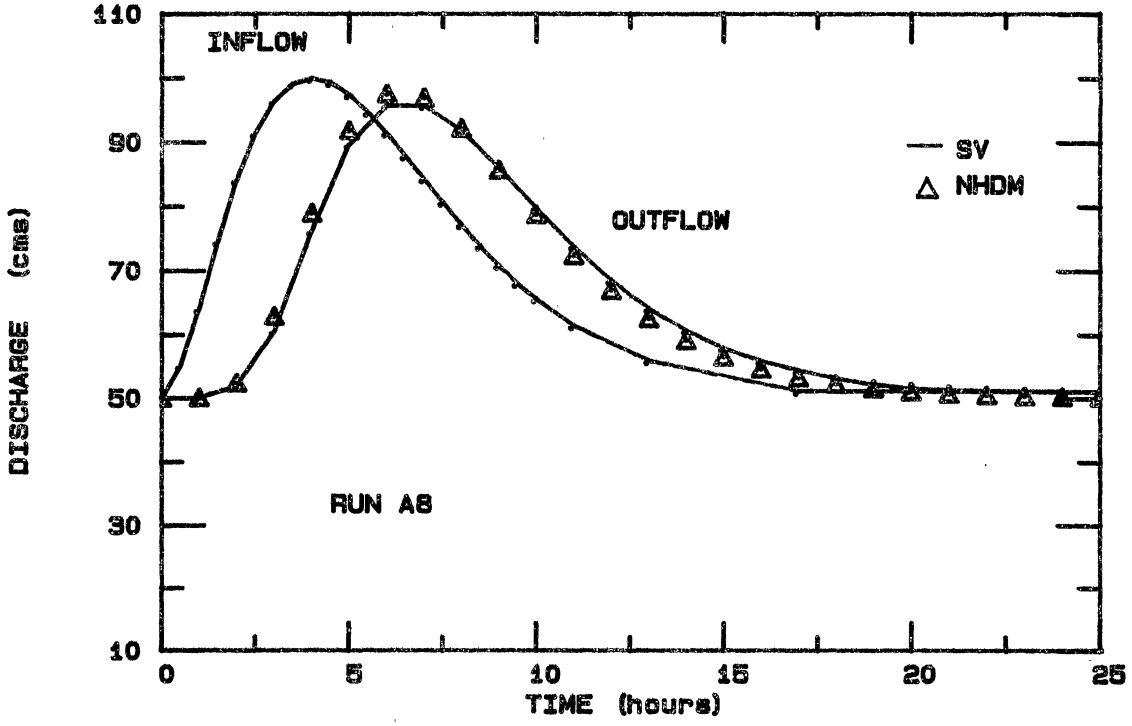
INFLOW
OUTFLOW
SV
NHDM
RUN A8
DISCHARGE (cms)
TIME (hours)
110
90
70
50
30
10
0
5
10
15
20
25

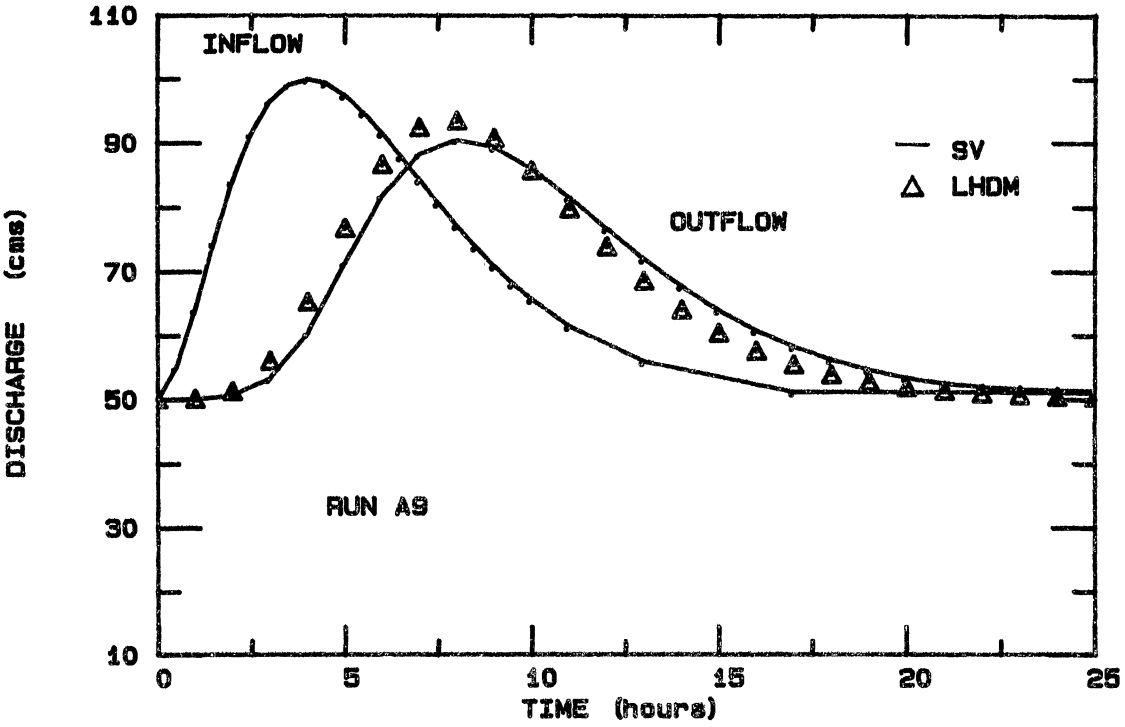
INFLOW
OUTFLOW
SV
LHDM
RUN A9
DISCHARGE (cms)
TIME (hours)
110
90
70
50
30
10
0
5
10
15
20
25

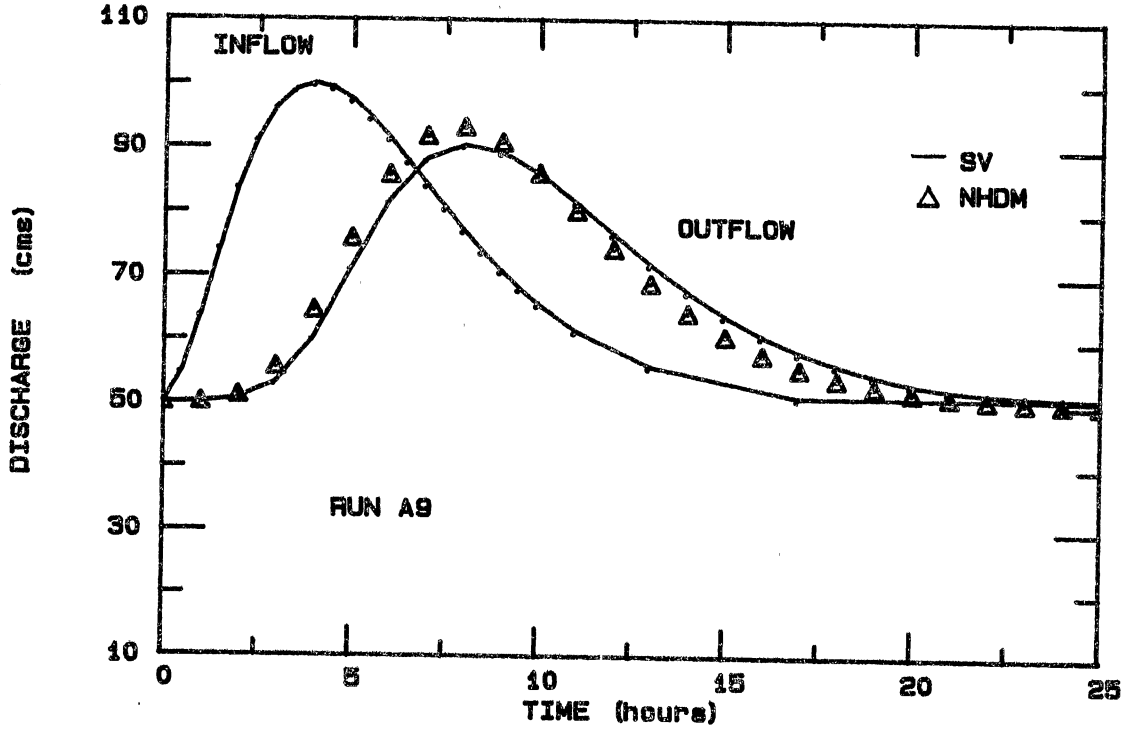
INFLOW
OUTFLOW
SV
NHDM
RUN A9
DISCHARGE (cms)
TIME (hours)
110
90
70
50
30
10
0
5
10
15
20
25

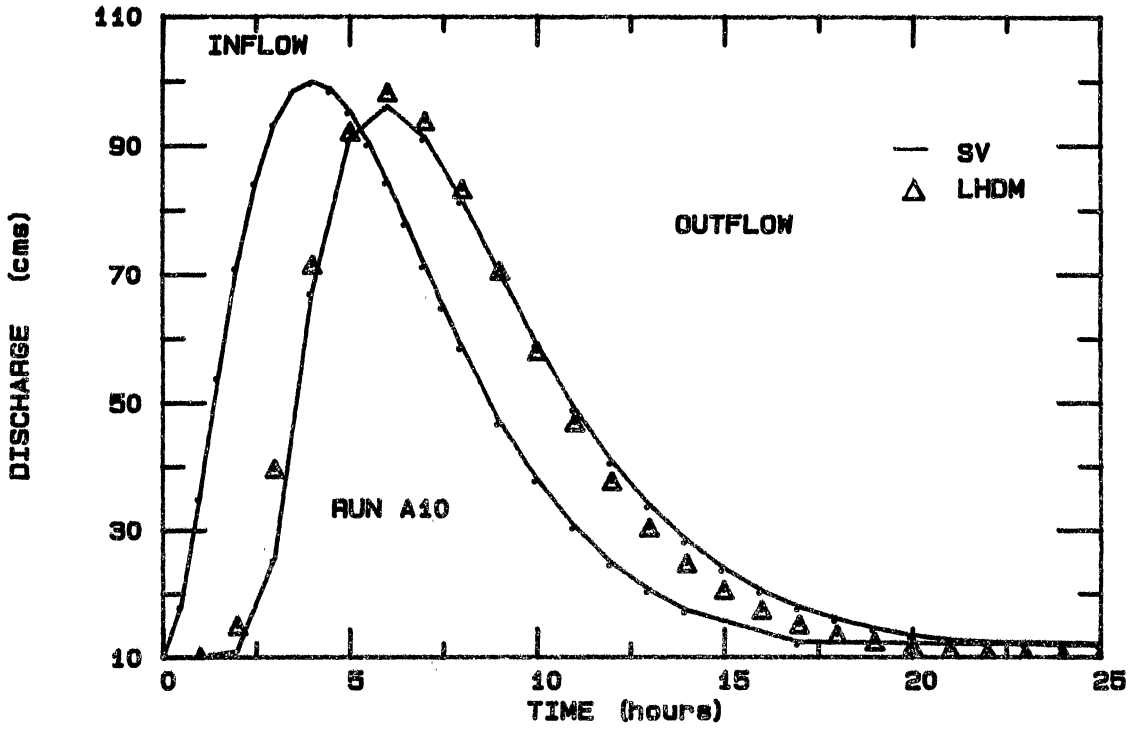
INFLOW
OUTFLOW
SV
LHDM
RUN A10
DISCHARGE (cms)
TIME (hours)
110
90
70
50
30
10
0
5
10
15
20
25

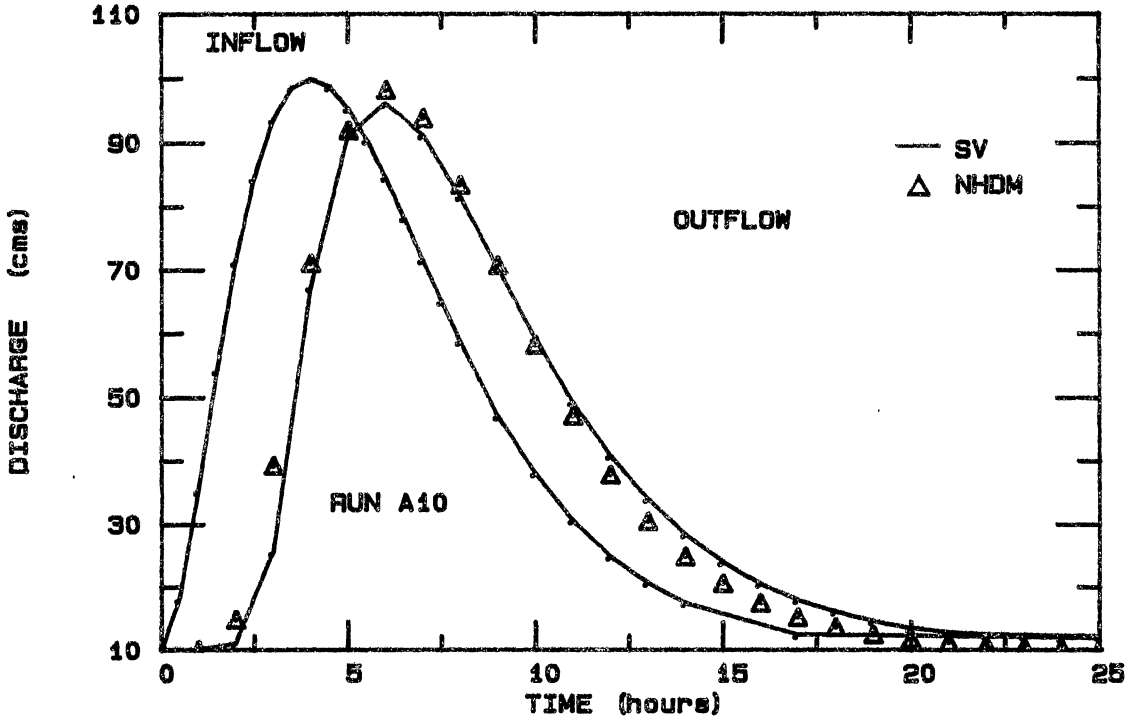
INFLOW
OUTFLOW
SV
NHDM
RUN A10
DISCHARGE (cms)
TIME (hours)
110
90
70
50
30
10
0
5
10
15
20
25

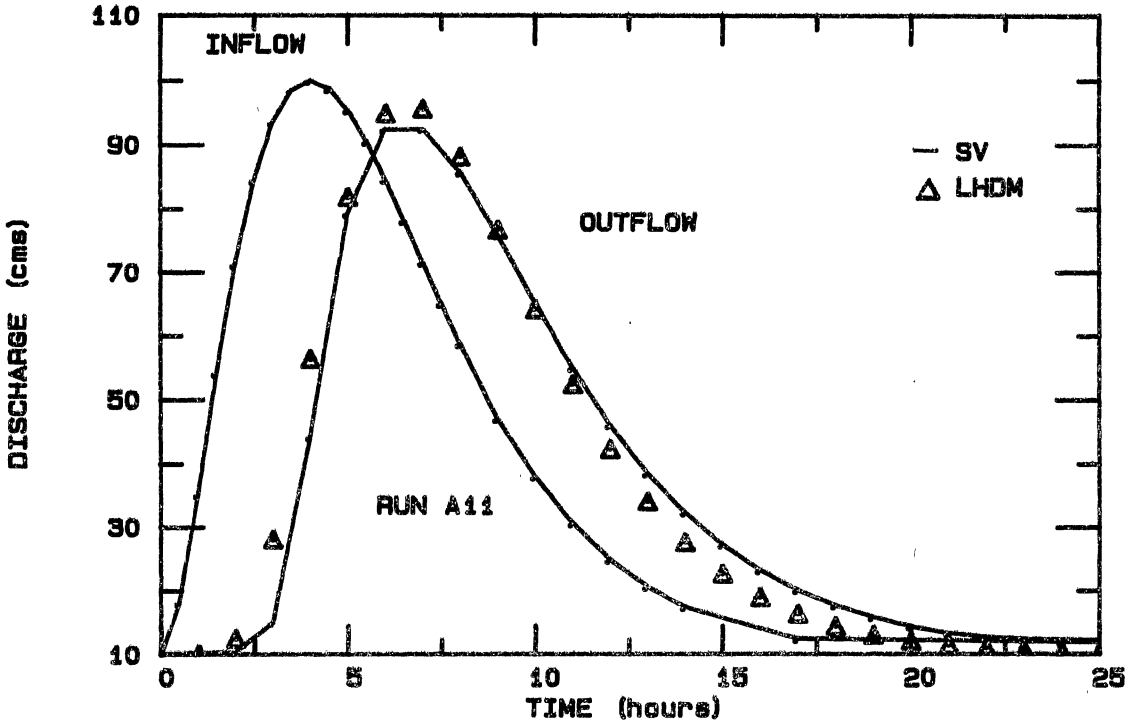
INFLOW
OUTFLOW
RUN A11
SV
LHDM
DISCHARGE (cms)
TIME (hours)
110
90
70
50
30
10
0
5
10
15
20
25

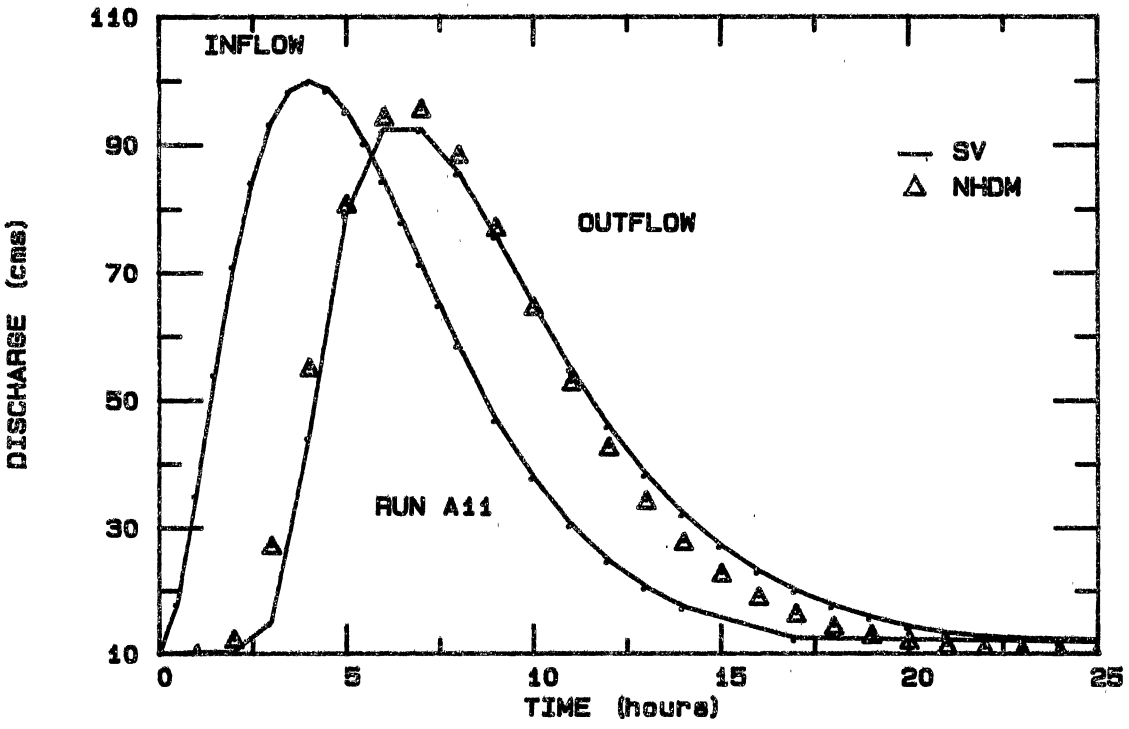
INFLOW
OUTFLOW
RUN A11
SV
NHDM
DISCHARGE (cms)
TIME (hours)
110
90
70
50
30
10
0
5
10
15
20
25

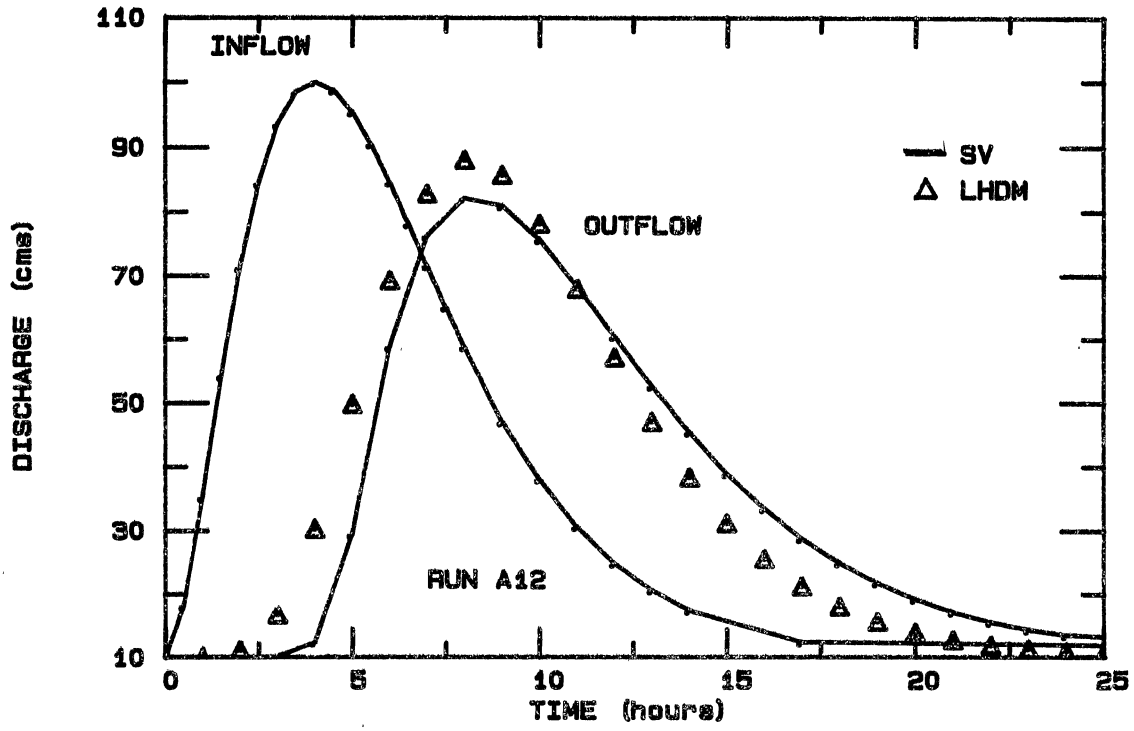
INFLOW
OUTFLOW
SV
LHDM
RUN A12
DISCHARGE (cms)
TIME (hours)
110
90
70
50
30
10
0
5
10
15
20
25

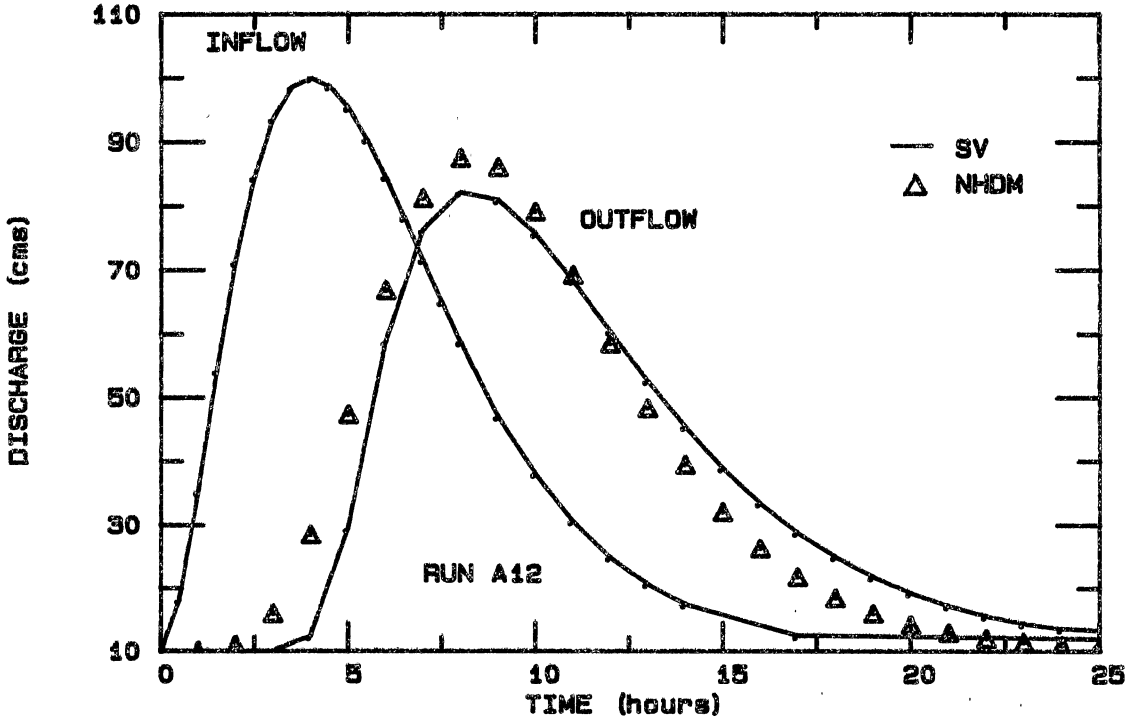
INFLOW
OUTFLOW
SV
NHDM
RUN A12
DISCHARGE (cms)
TIME (hours)
110
90
70
50
30
10
0
5
10
15
20
25

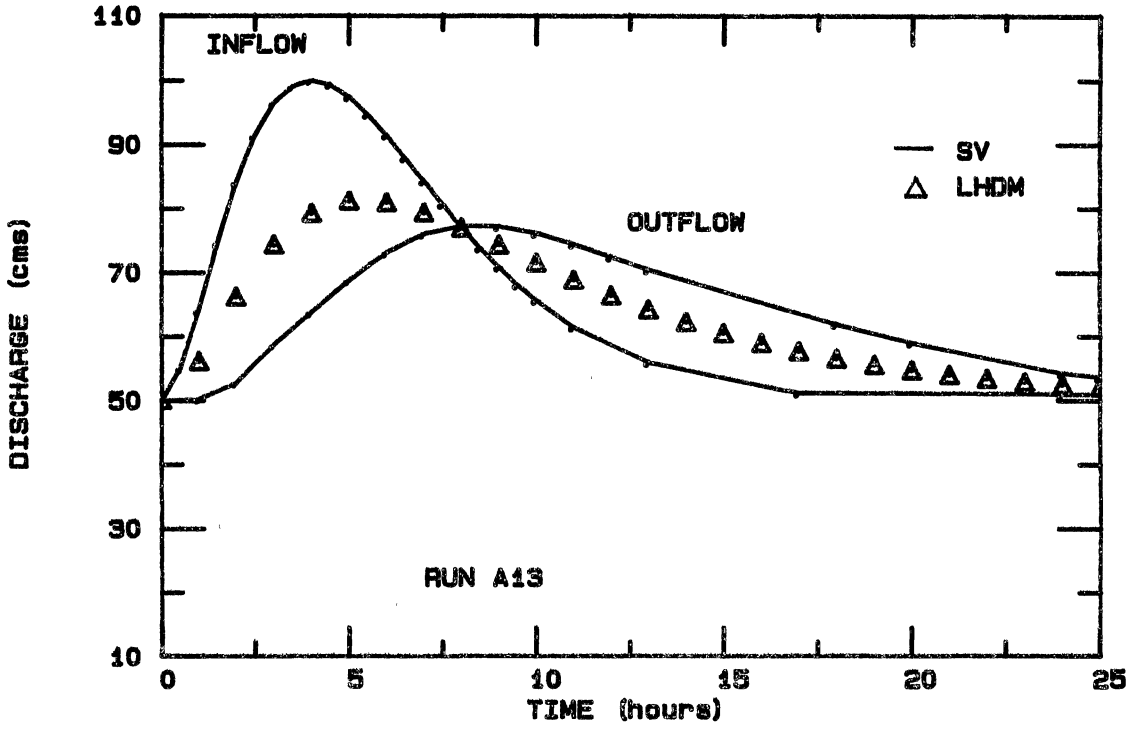
INFLOW
OUTFLOW
SV
LHDM
RUN A13
DISCHARGE (cms)
TIME (hours)
110
90
70
50
30
10
0
5
10
15
20
25

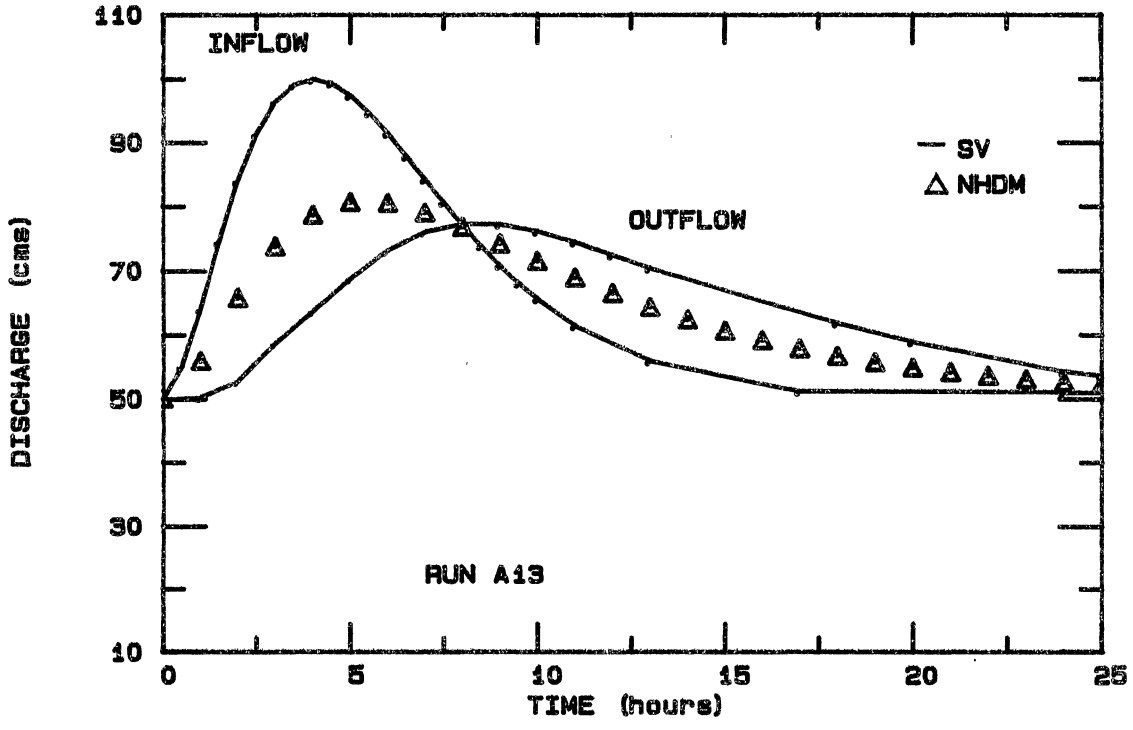
INFLOW
OUTFLOW
SV
NHDM
RUN A13
DISCHARGE (cms)
TIME (hours)
110
90
70
50
30
10
0
5
10
15
20
25

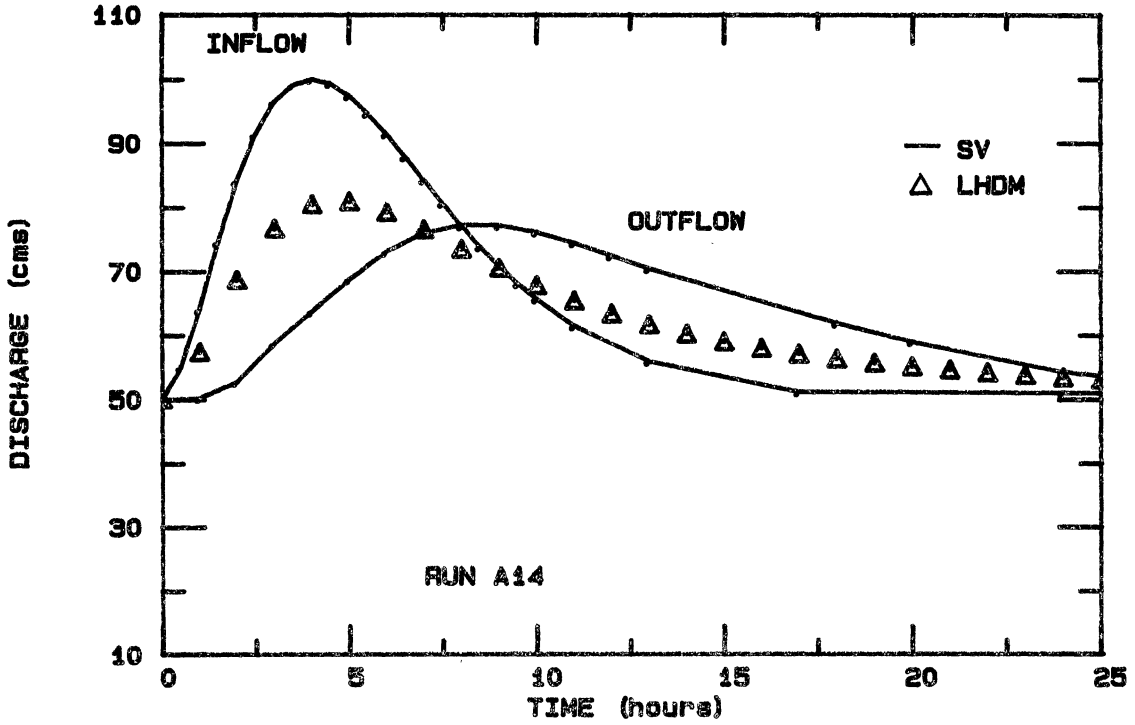
INFLOW
OUTFLOW
SV
LHDM
RUN A14
DISCHARGE (cms)
TIME (hours)
110
90
70
50
30
10
0
5
10
15
20
25

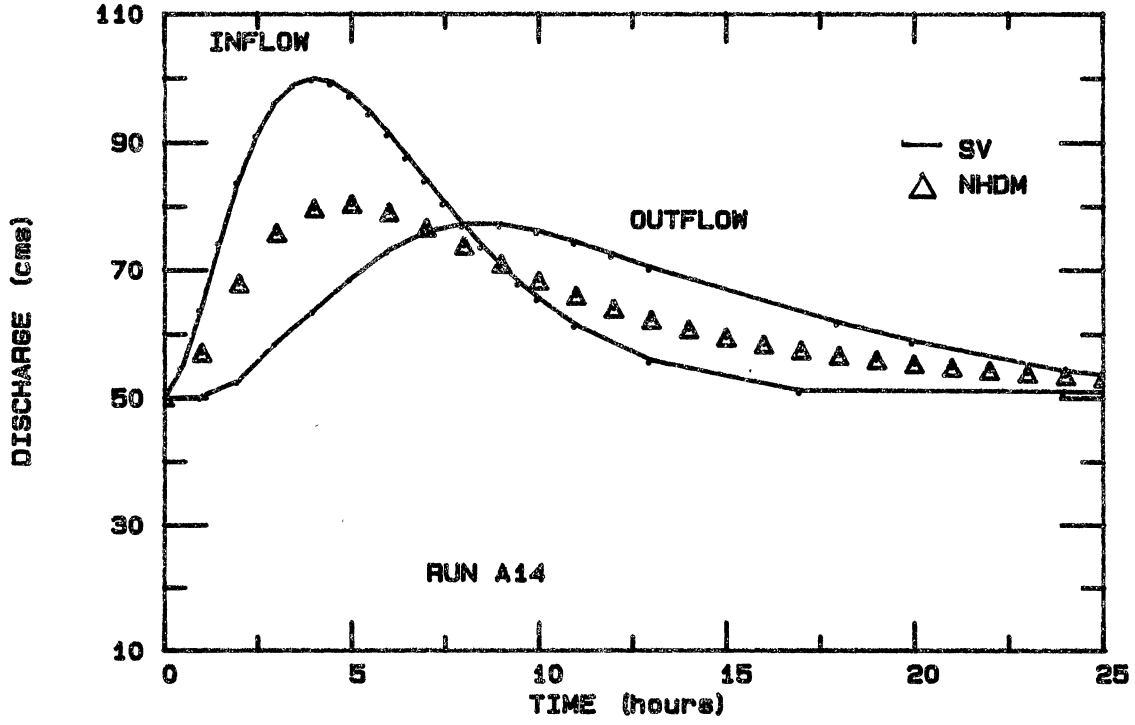
INFLOW
OUTFLOW
SV
NHDM
RUN A14
DISCHARGE (cms)
TIME (hours)
110
90
70
50
30
10
0
5
10
15
20
25

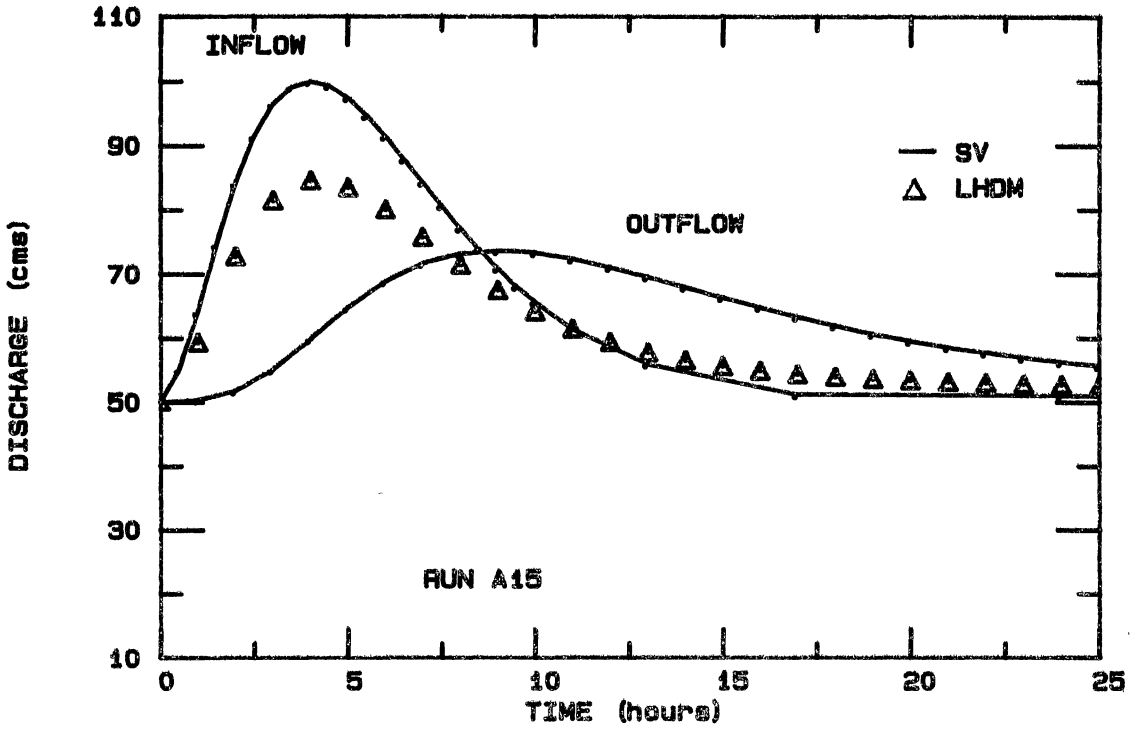
INFLOW
OUTFLOW
SV
LHDM
RUN A15
DISCHARGE (cms)
TIME (hours)
110
90
70
50
30
10
0
5
10
15
20
25

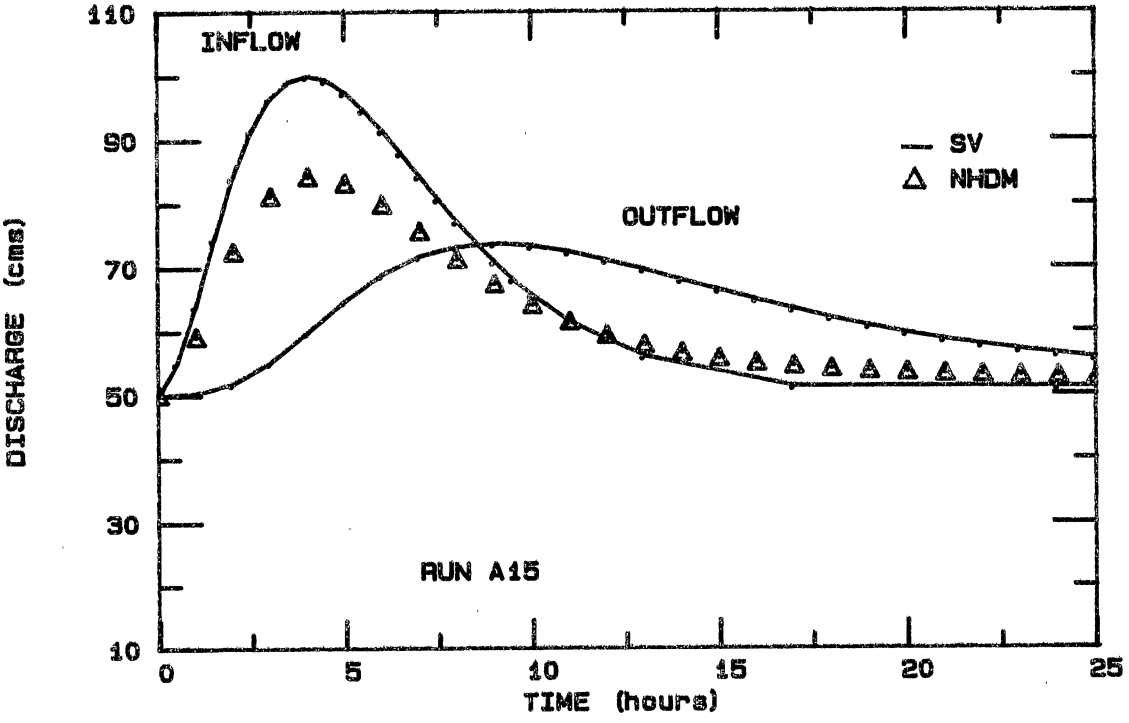
INFLOW
OUTFLOW
SV
NHDM
RUN A15
DISCHARGE (cms)
TIME (hours)
110
90
70
50
30
10
0
5
10
15
20
25

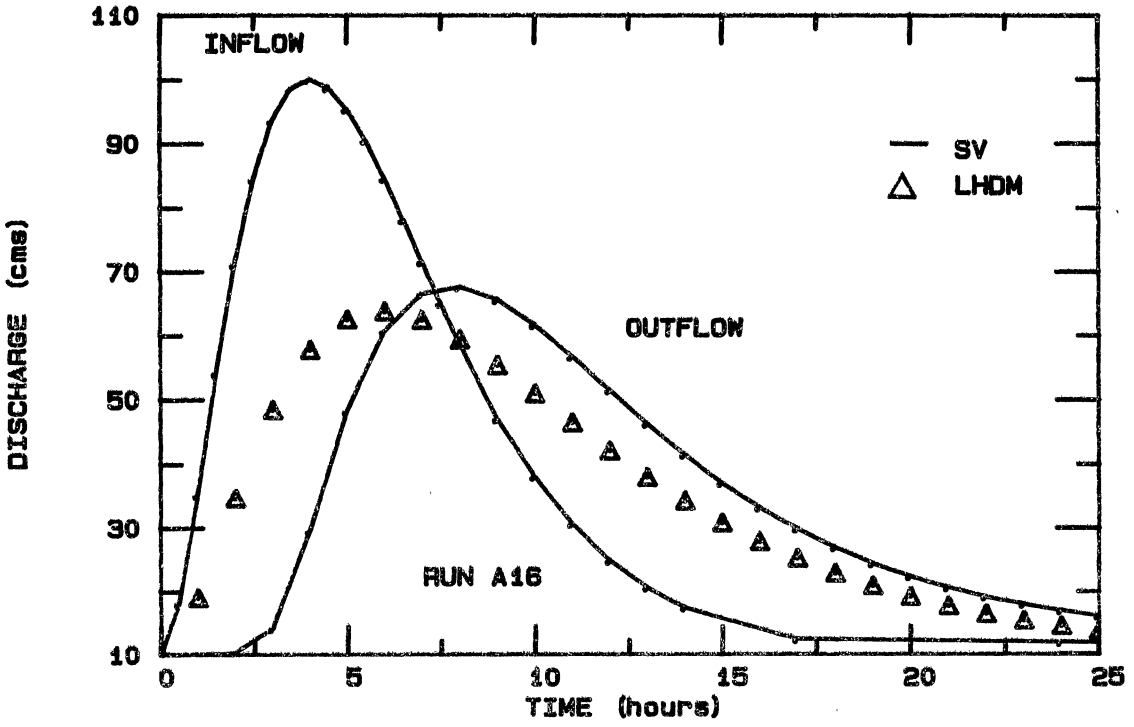
INFLOW
OUTFLOW
SV
LHDM
RUN A16
DISCHARGE (cms)
TIME (hours)
110
90
70
50
30
10
0
5
10
15
20
25

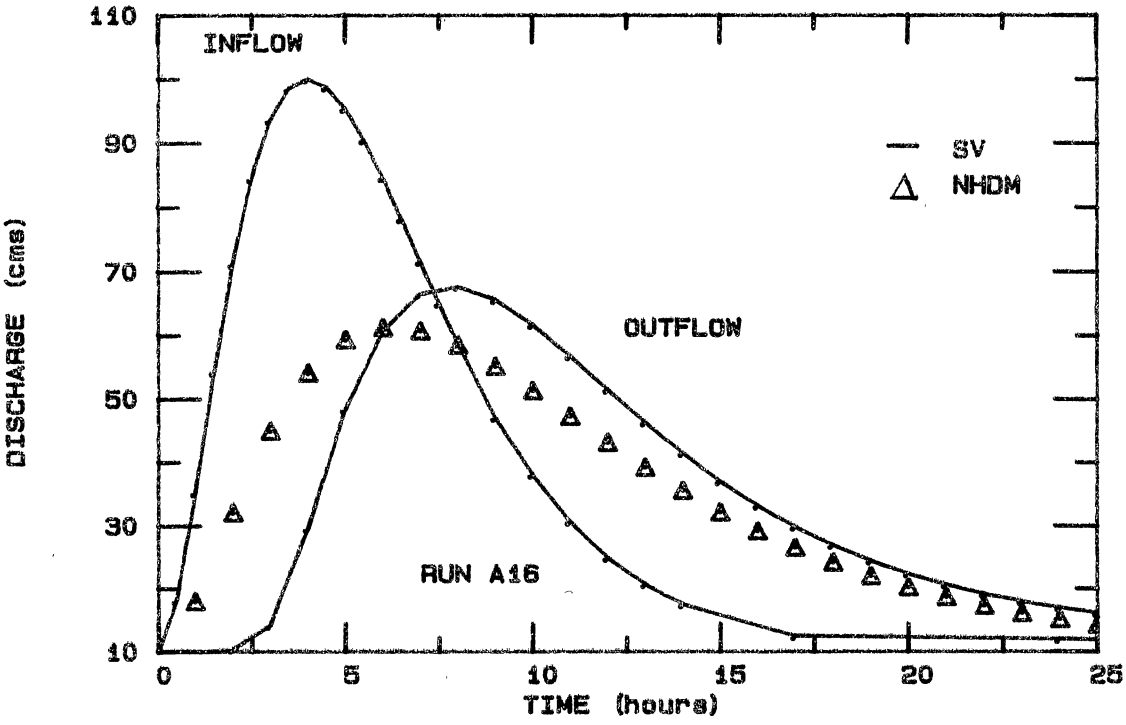
INFLOW
OUTFLOW
SV
NHDM
RUN A16
DISCHARGE (cms)
TIME (hours)
110
90
70
50
30
10
0
5
10
15
20
25

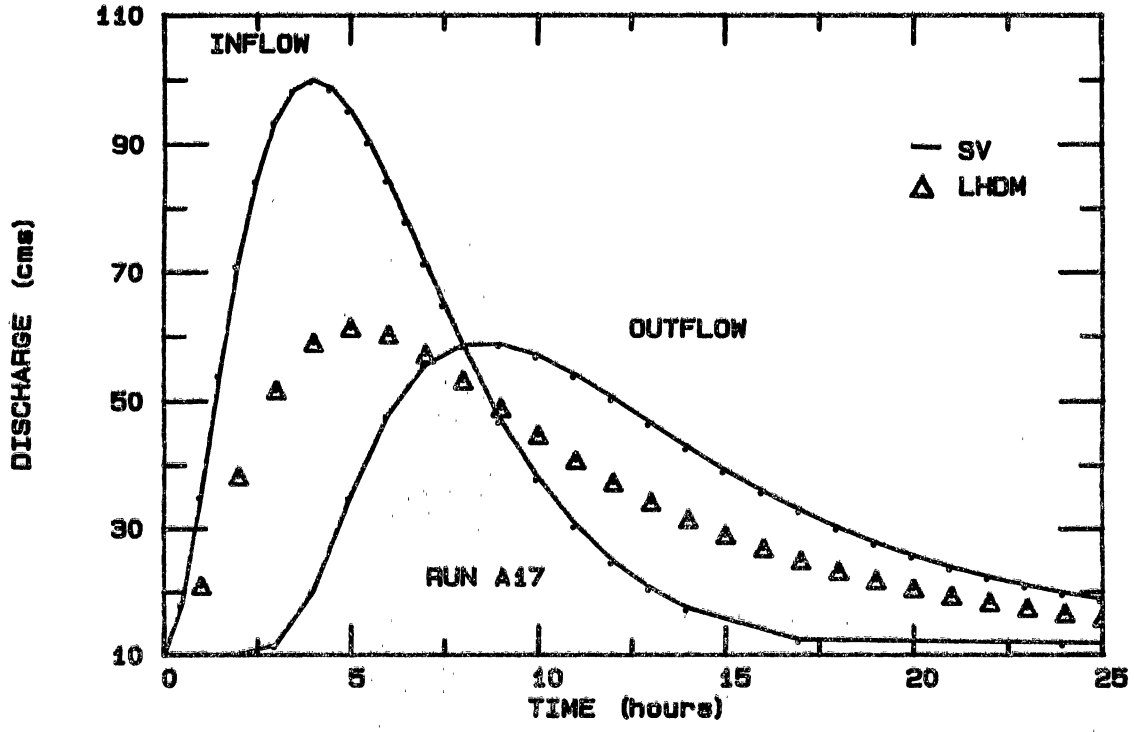
INFLOW
OUTFLOW
RUN A17
SV
LHDM
DISCHARGE (cms)
TIME (hours)
110
90
70
50
30
10
0
5
10
15
20
25

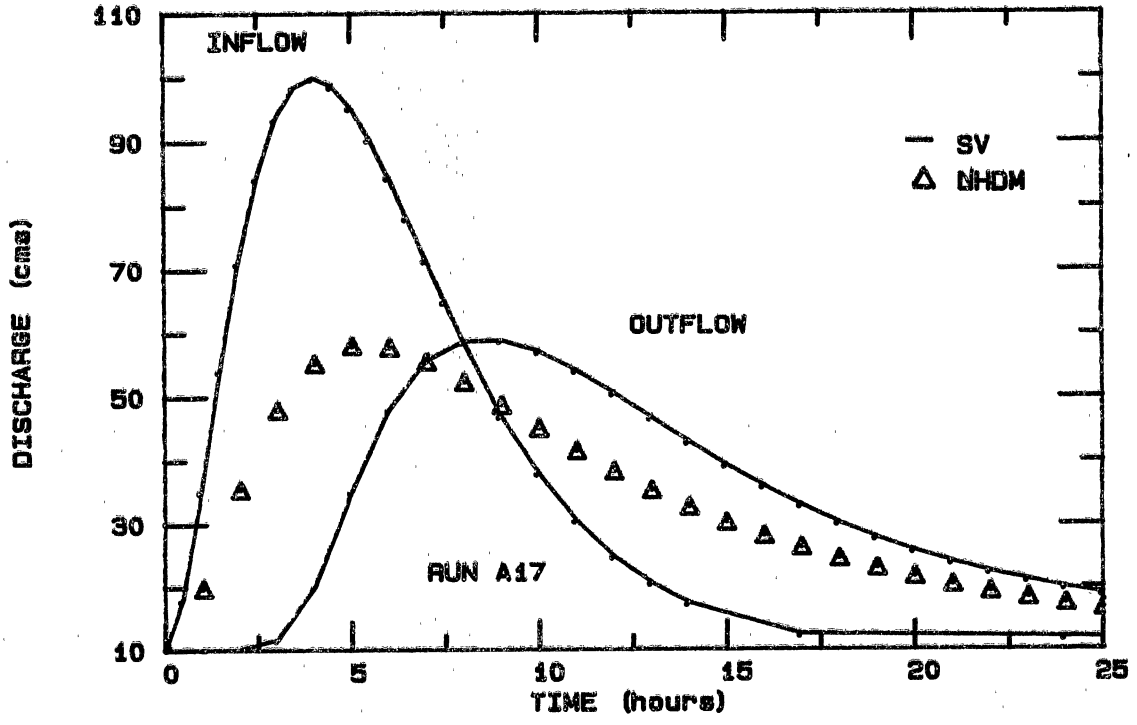
INFLOW
OUTFLOW
RUN A17
SV
NHDM
DISCHARGE (cms)
TIME (hours)
110
90
70
50
30
10
0
5
10
15
20
25

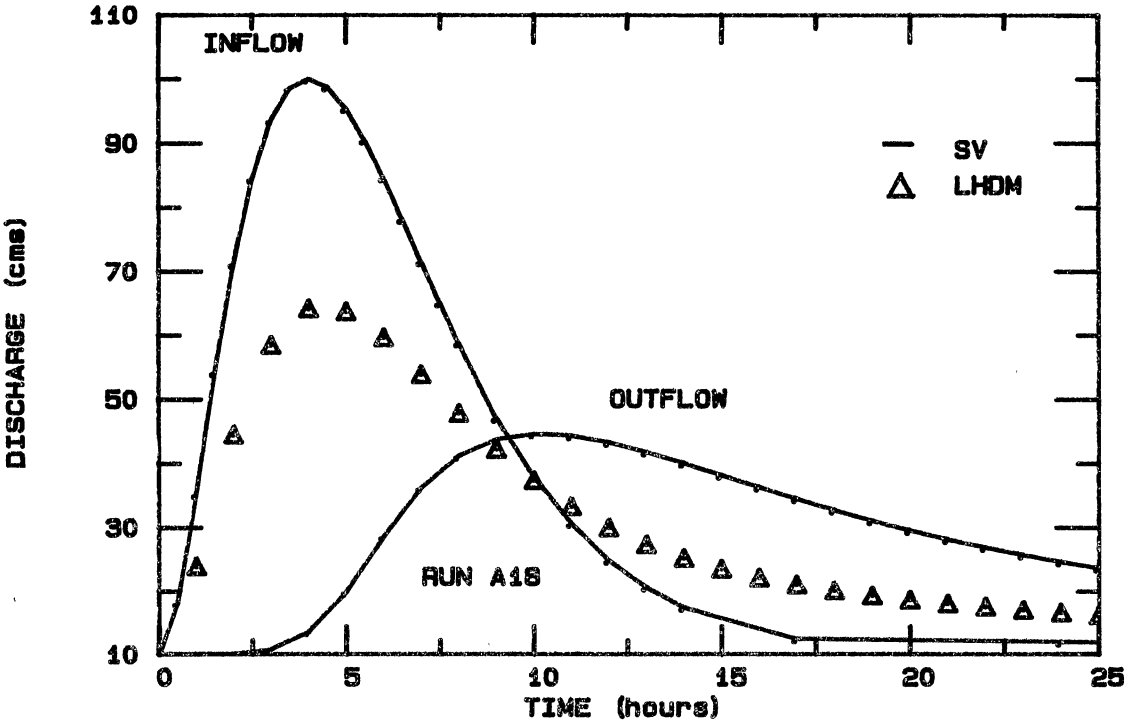
INFLOW
OUTFLOW
RUN A18
SV
LHDM
DISCHARGE (cms)
TIME (hours)
110
90
70
50
30
10
0
5
10
15
20
25

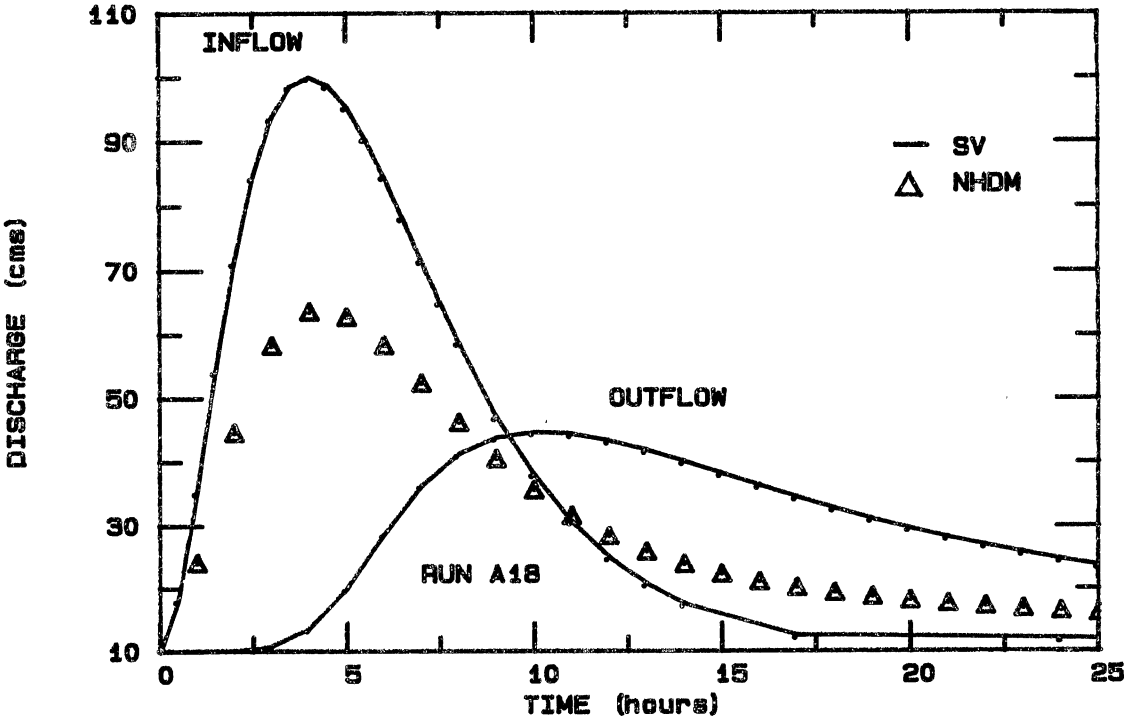
INFLOW
OUTFLOW
RUN A18
SV
NHDM
DISCHARGE (cms)
TIME (hours)
110
90
70
50
30
10
0
5
10
15
20
25

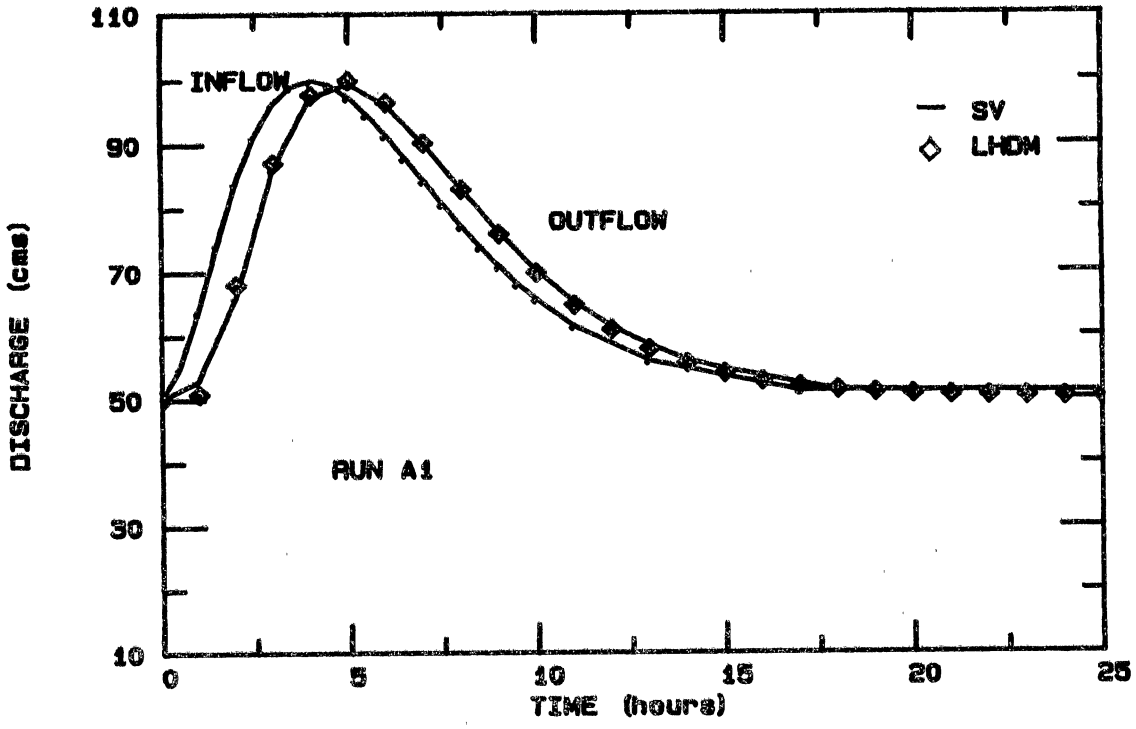
110
90
70
50
30
10
0
5
10
15
20
25
DISCHARGE (cms)
TIME (hours)
INFLOW
OUTFLOW
SV
LHDM
RUN A1

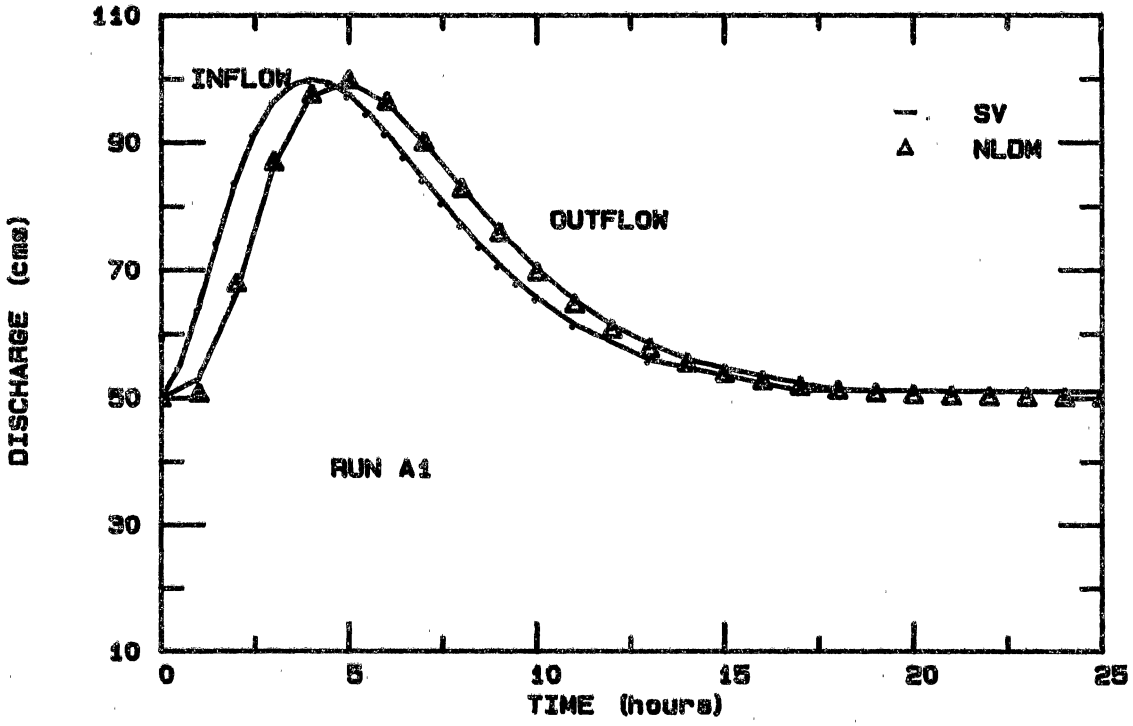
110
90
70
50
30
10
0
5
10
15
20
25
DISCHARGE (cms)
TIME (hours)
INFLOW
OUTFLOW
SV
NLDM
RUN A1

APPENDIX C

SERIES IV RECTANGULAR PLOTS

LHDM - LINEAR HYDRODYNAMIC MUSKINGUM METHOD

NHDM - NONLINEAR HYDRODYNAMIC MUSKINGUM METHOD

SV - SAINT VENANT EQUATIONS

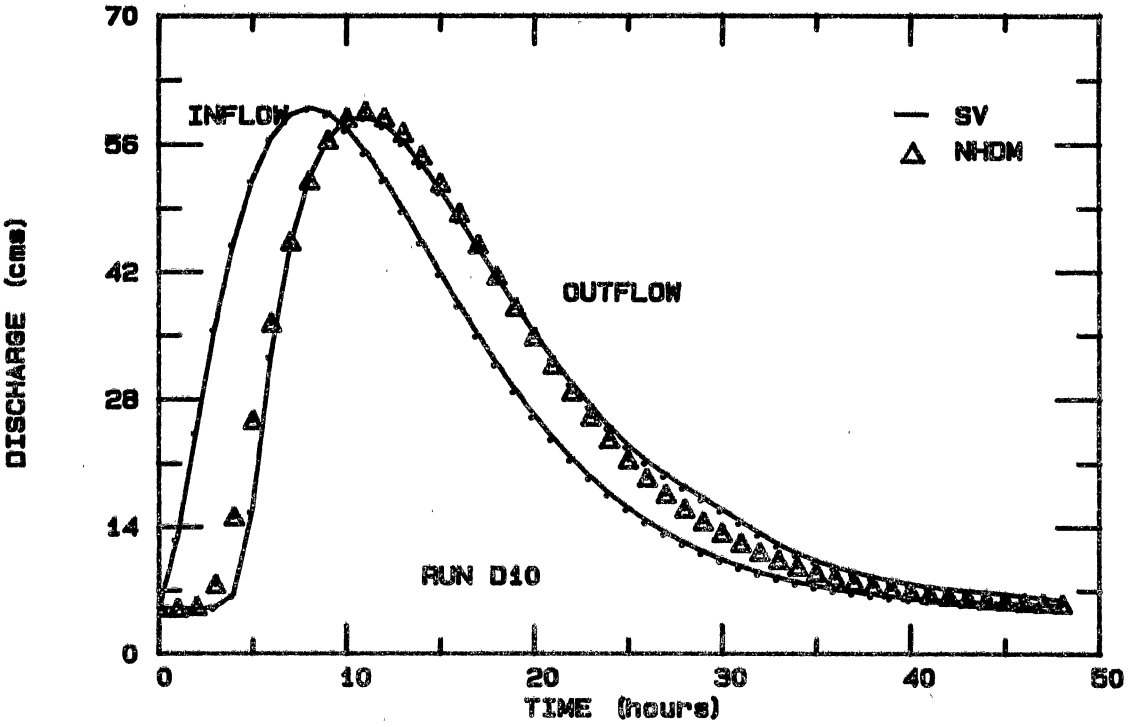
70
56
42
28
14
0
DISCHARGE (cms)
INFLOW
OUTFLOW
SV
NHDM
RUN D10
0
10
20
30
40
50
TIME (hours)

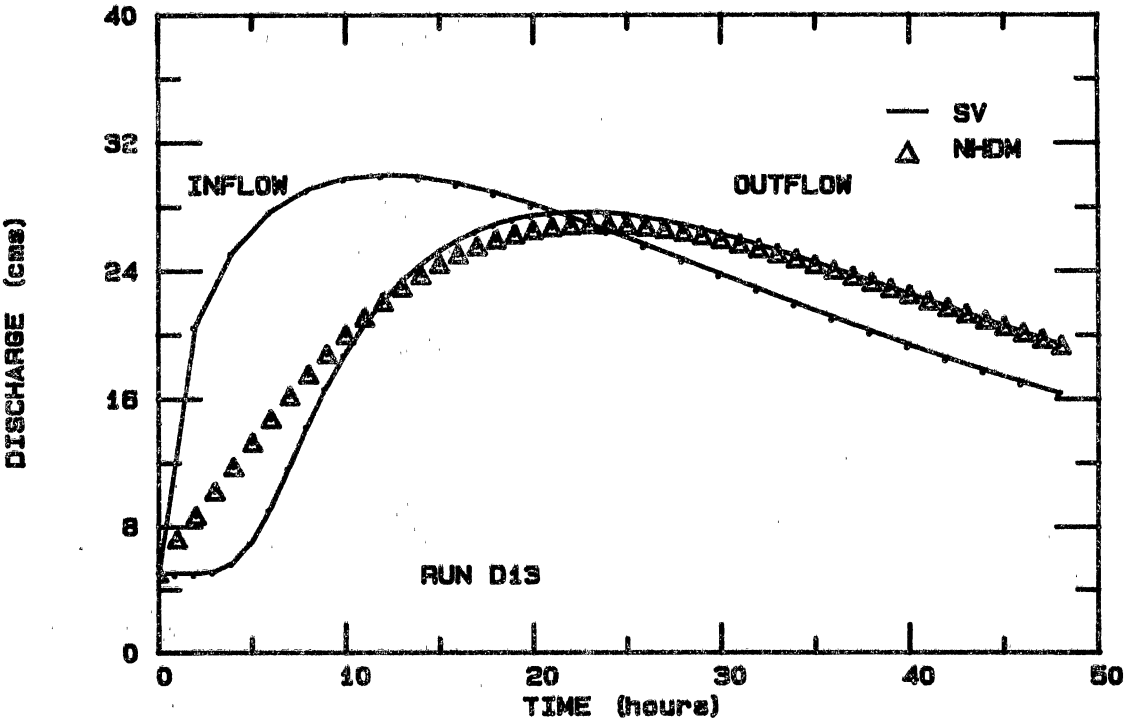
40
32
24
16
8
0
DISCHARGE (cms)
INFLOW
OUTFLOW
SV
NHDM
RUN D13
0
10
20
30
40
50
TIME (hours)

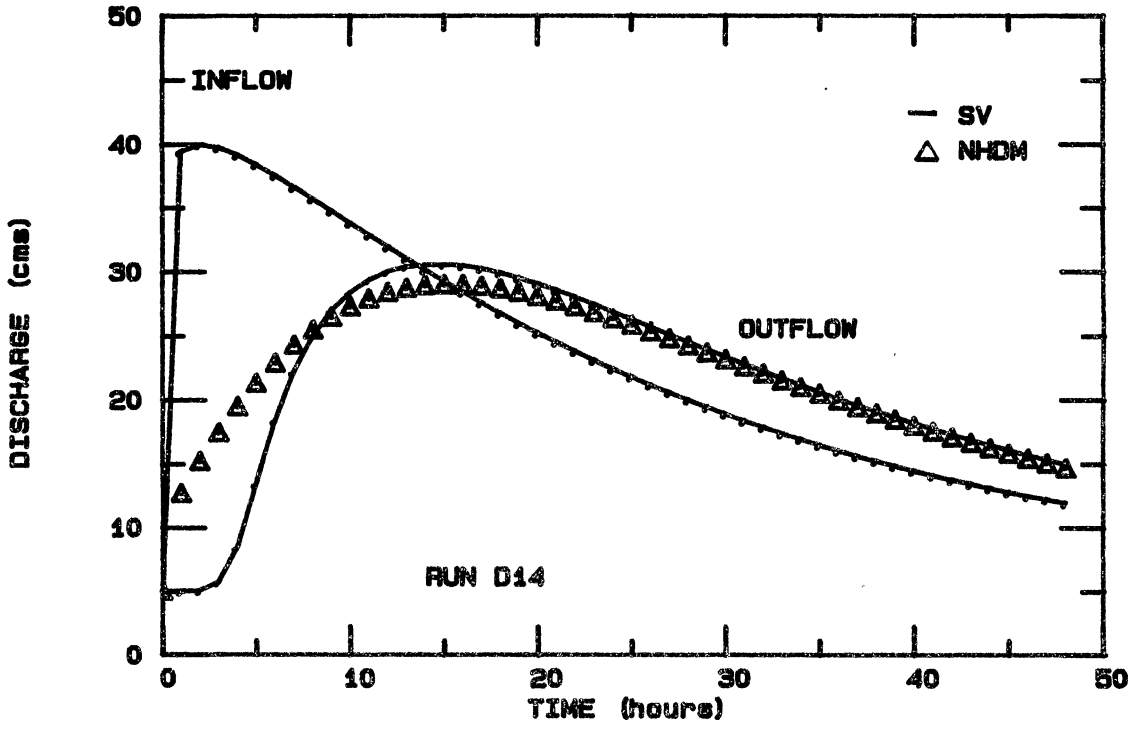
INFLOW
SV
NHDM
OUTFLOW
RUN D14
DISCHARGE (cms)
TIME (hours)
0
10
20
30
40
50

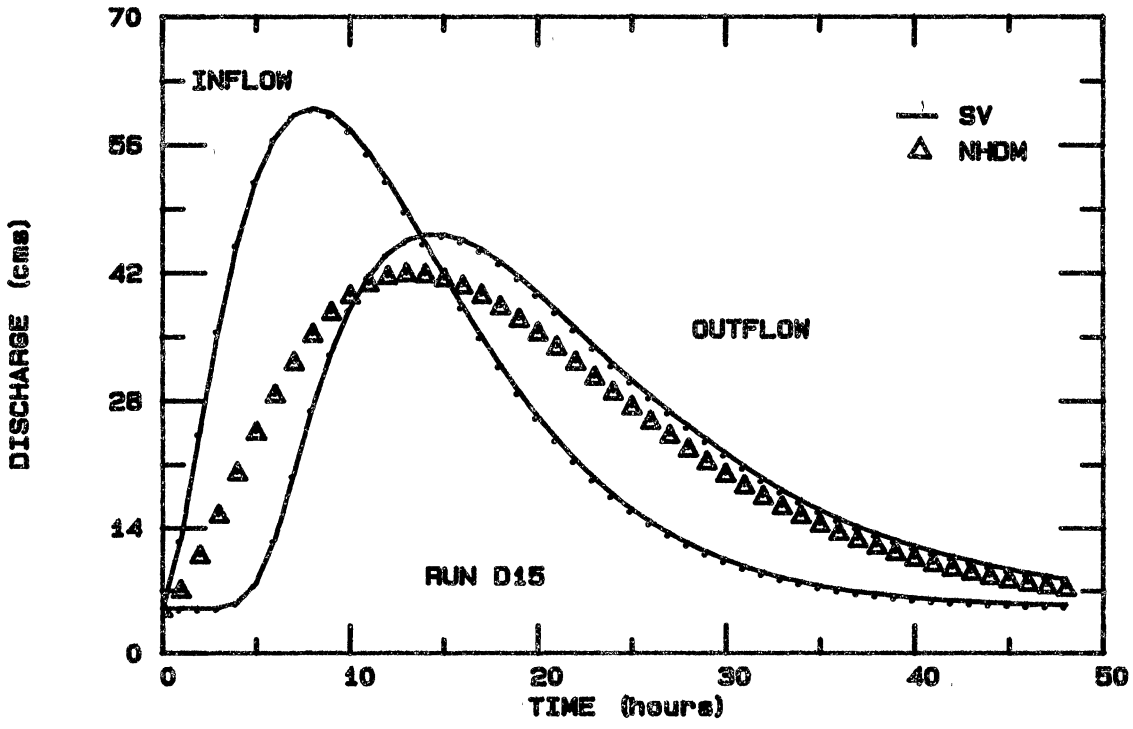
INFLOW
SV
NHDM
OUTFLOW
RUN D15
DISCHARGE (cms)
TIME (hours)
0
14
28
42
56
70
10
20
30
40
50

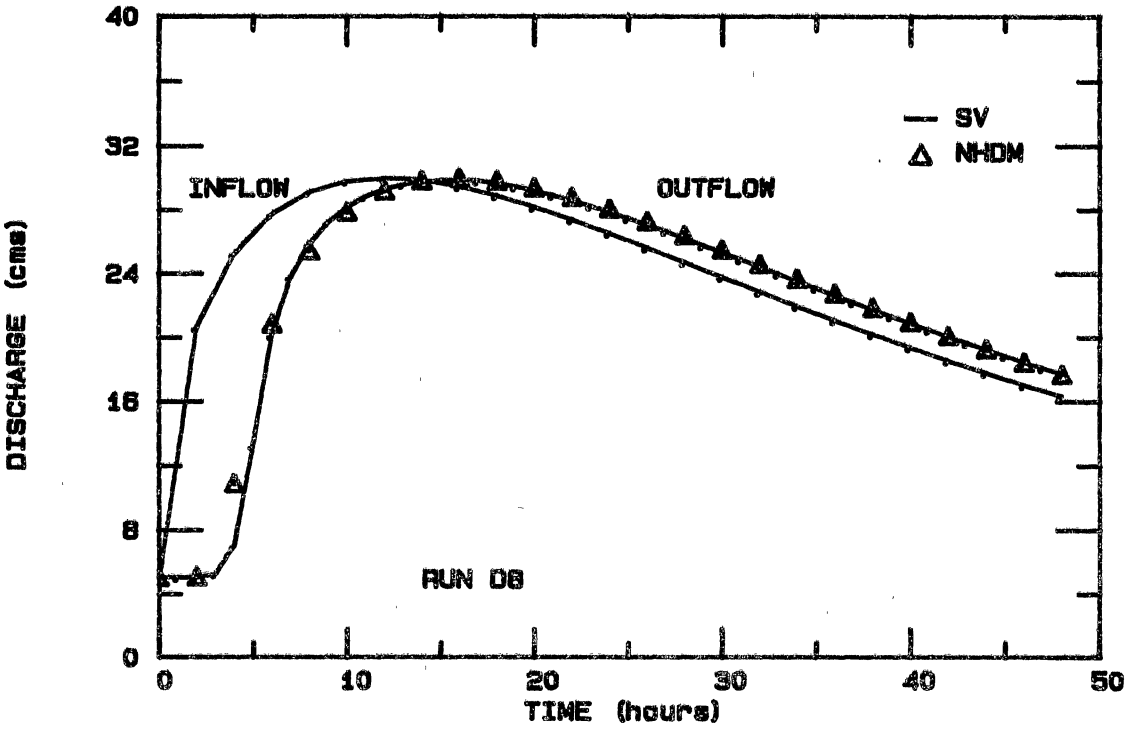
DISCHARGE (cms)
TIME (hours)
INFLOW
OUTFLOW
SV
NHDM
RUN D8
0
8
16
24
32
40
0
10
20
30
40
50

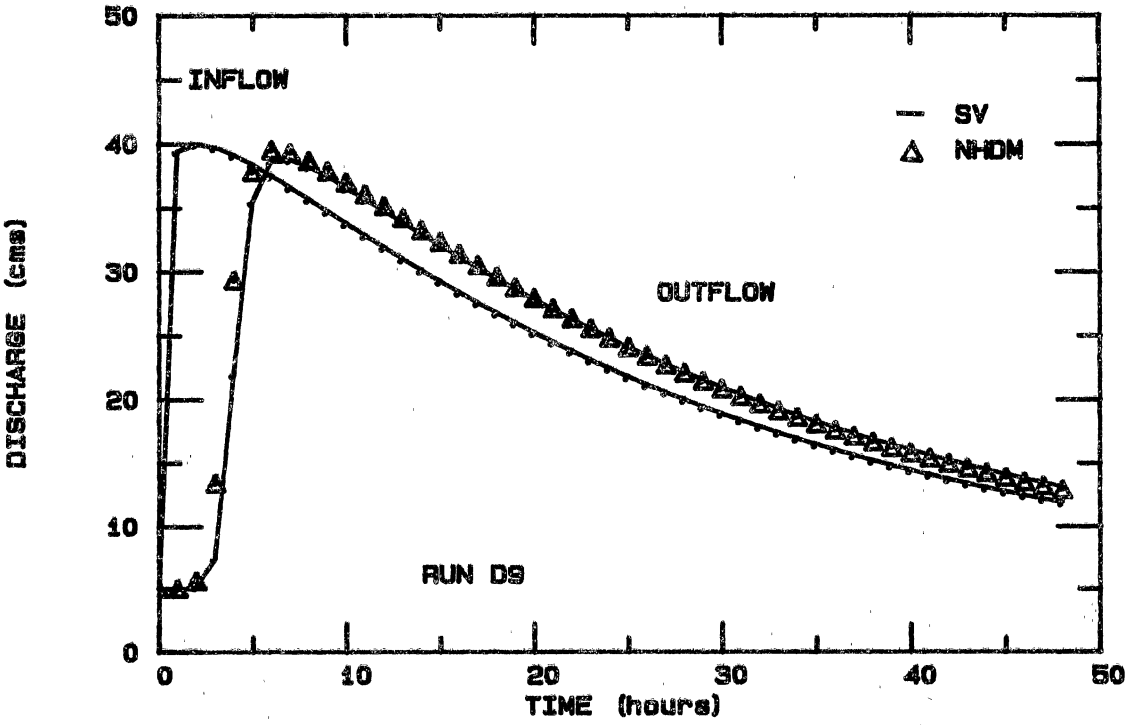
DISCHARGE (cms)
TIME (hours)
INFLOW
OUTFLOW
SV
NHDM
RUN D9
0
10
20
30
40
50
0
10
20
30
40
50

APPENDIX D

SERIES IV TRIANGULAR CHANNEL PLOTS

LHDM - LINEAR HYDRODYNAMIC MUSKINGUM METHOD

NHDM - NONLINEAR HYDRODYNAMIC MUSKINGUM METHOD

SV - SAINT VENANT EQUATIONS

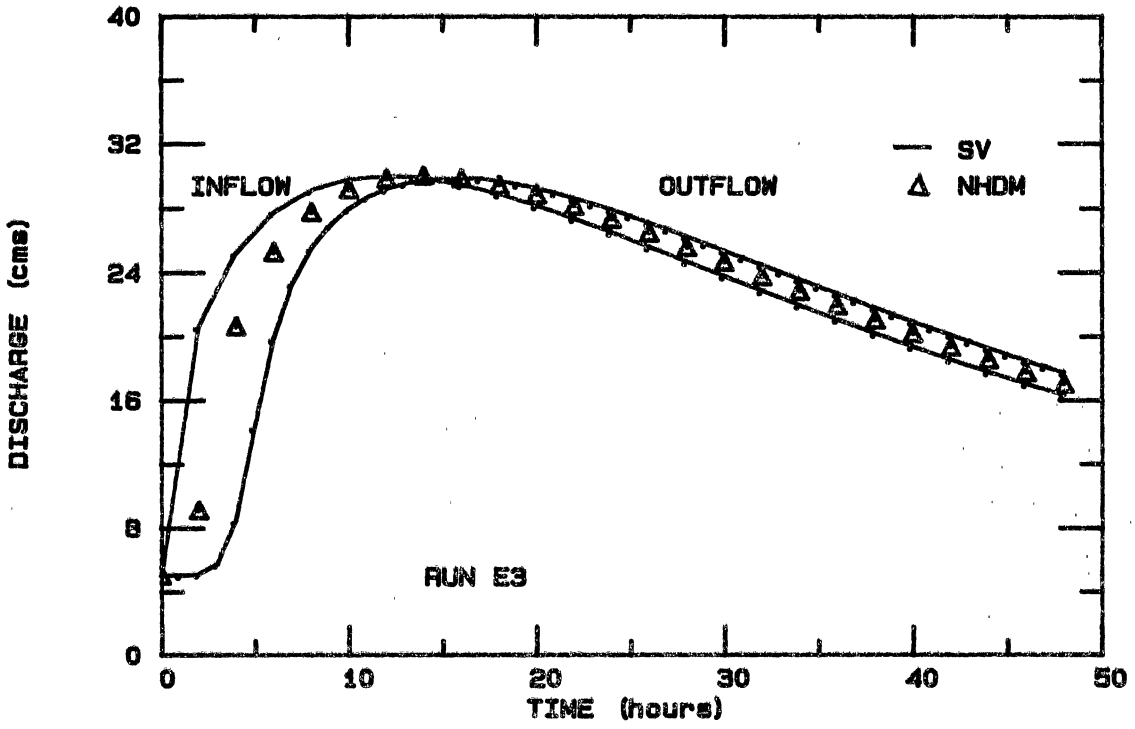
DISCHARGE (cms)
40
32
24
16
8
0
INFLOW
OUTFLOW
SV
NHDM
RUN E3
0
10
20
30
40
50
TIME (hours)

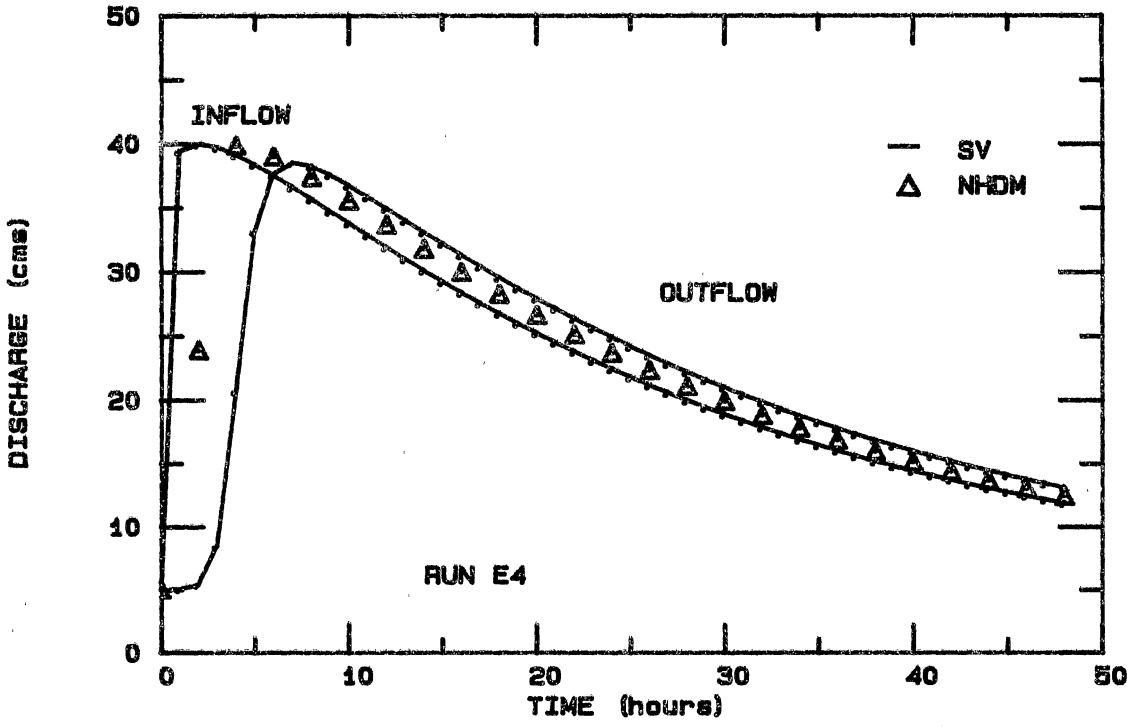
DISCHARGE (cms)
50
40
30
20
10
0
INFLOW
SV
NHDM
OUTFLOW
RUN E4
0
10
20
30
40
50
TIME (hours)

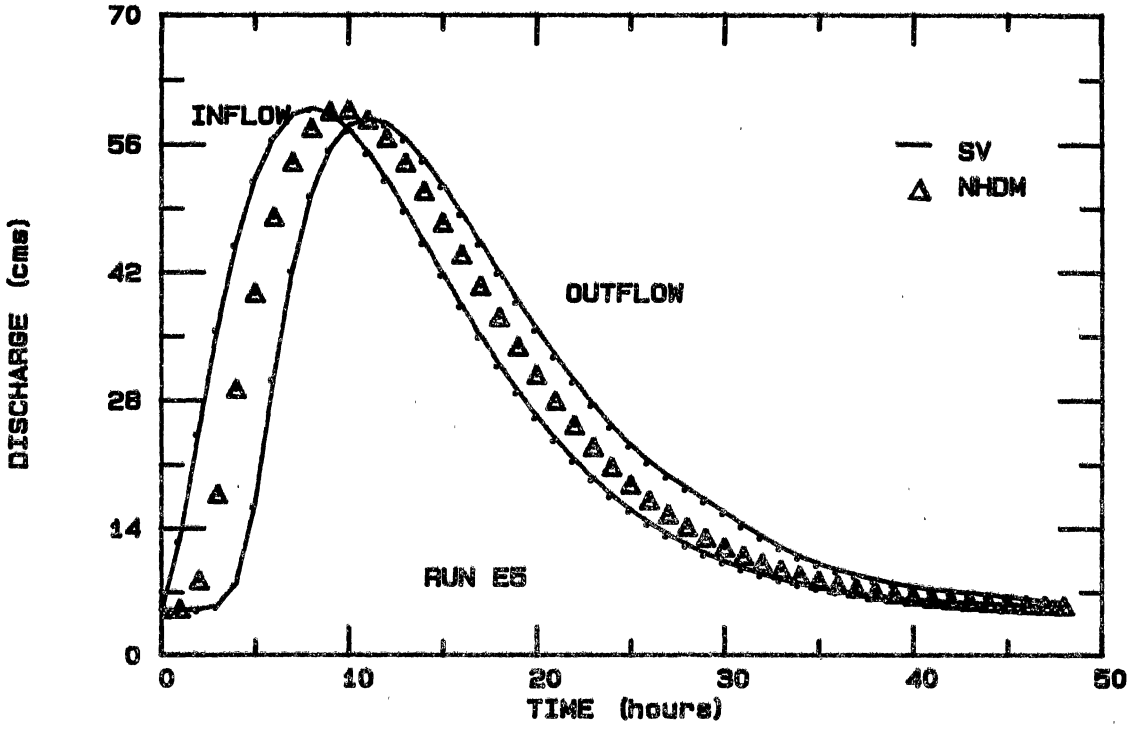
70
56
42
28
14
0
DISCHARGE (cms)
INFLOW
OUTFLOW
SV
NHDM
RUN E5
0
10
20
30
40
50
TIME (hours)

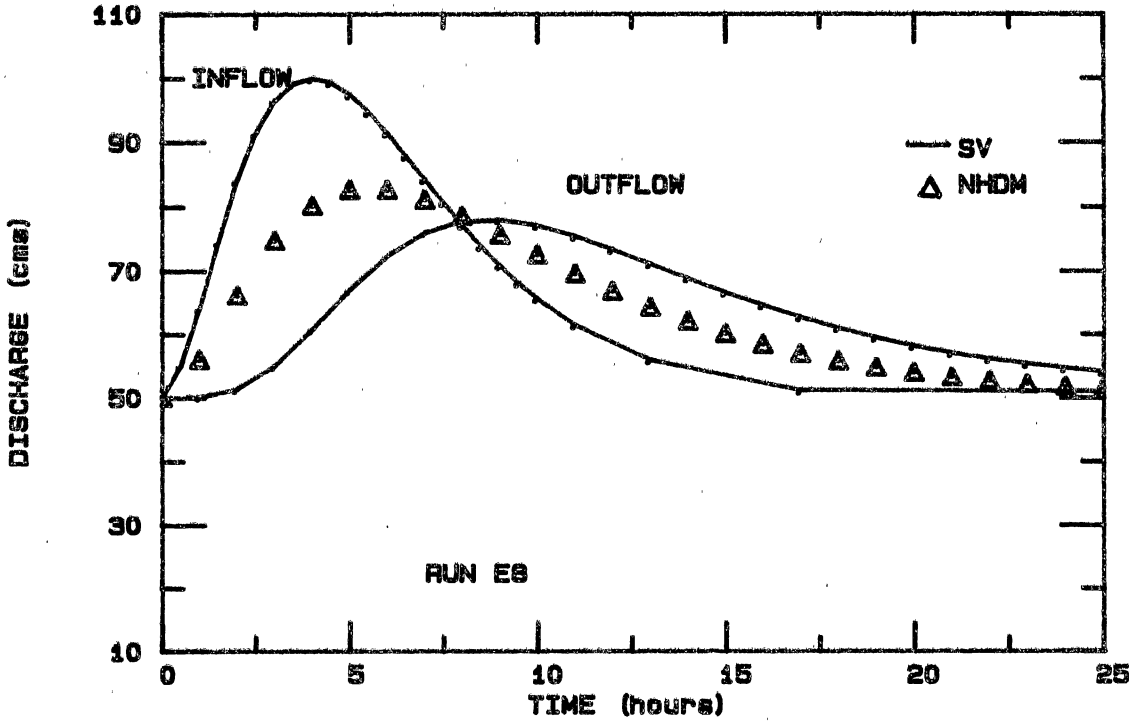
110
90
70
50
30
10
DISCHARGE (cms)
INFLOW
OUTFLOW
SV
NHDM
RUN E8
0
5
10
15
20
25
TIME (hours)

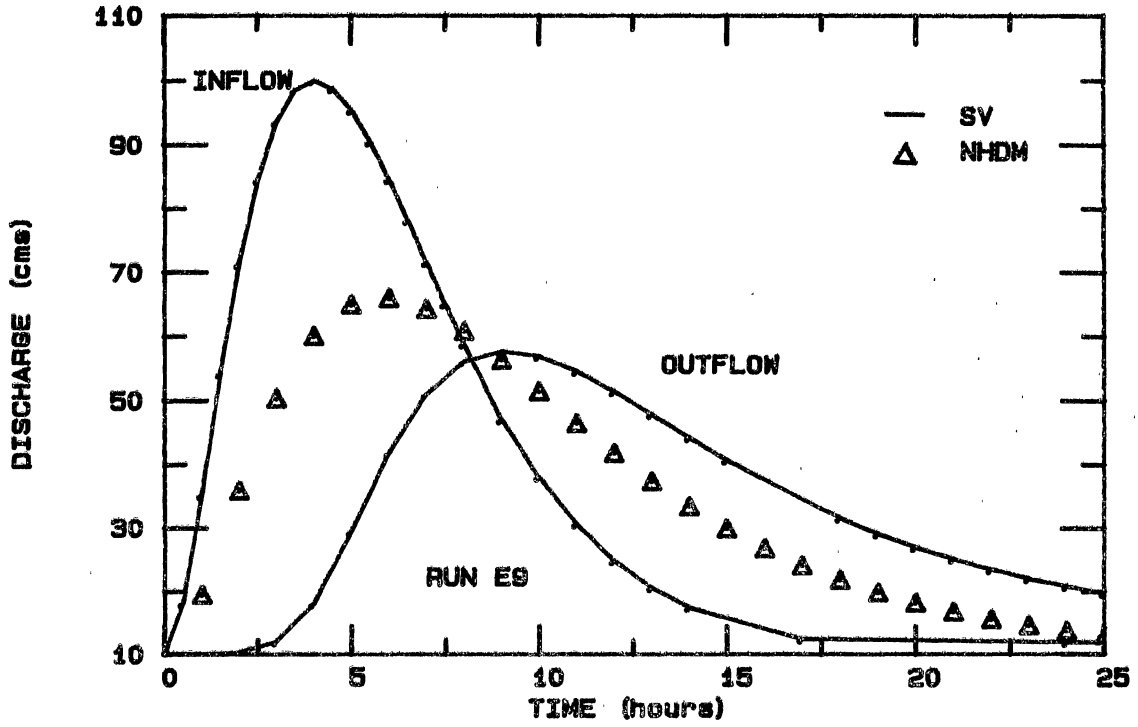
110
90
70
50
30
10
DISCHARGE (cms)
INFLOW
OUTFLOW
SV
NHDM
RUN E9
0
5
10
15
20
25
TIME (hours)

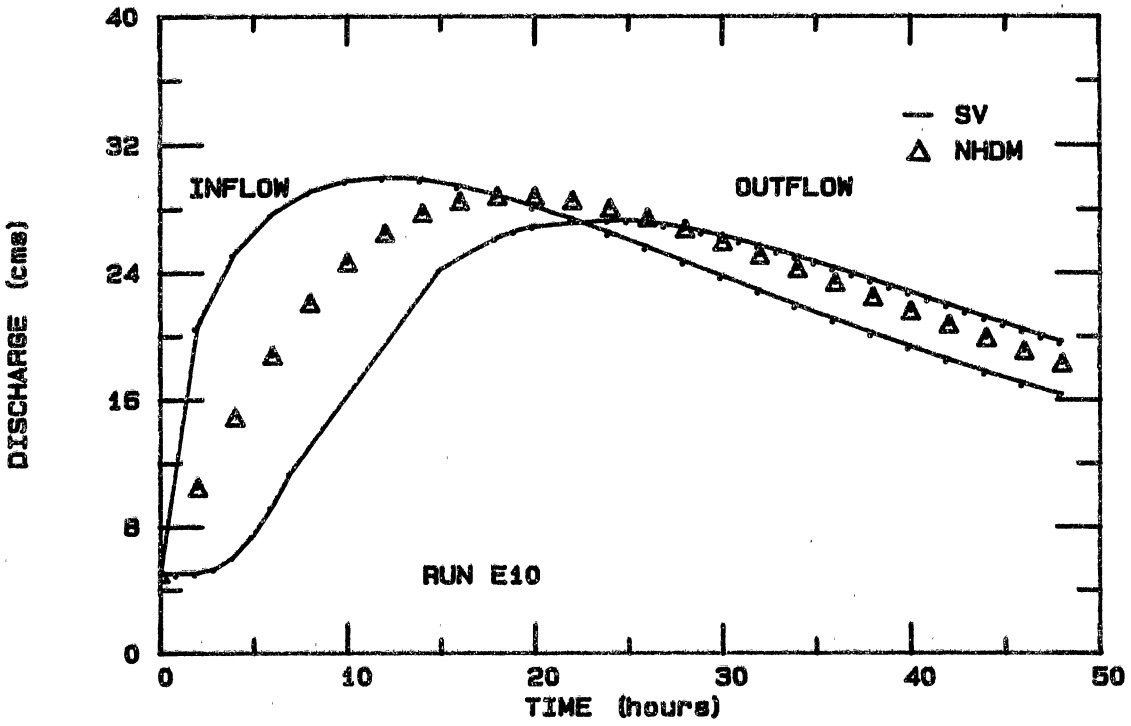
40
32
24
16
8
0
DISCHARGE (cms)
INFLOW
OUTFLOW
SV
NHDM
RUN E10
0
10
20
30
40
50
TIME (hours)

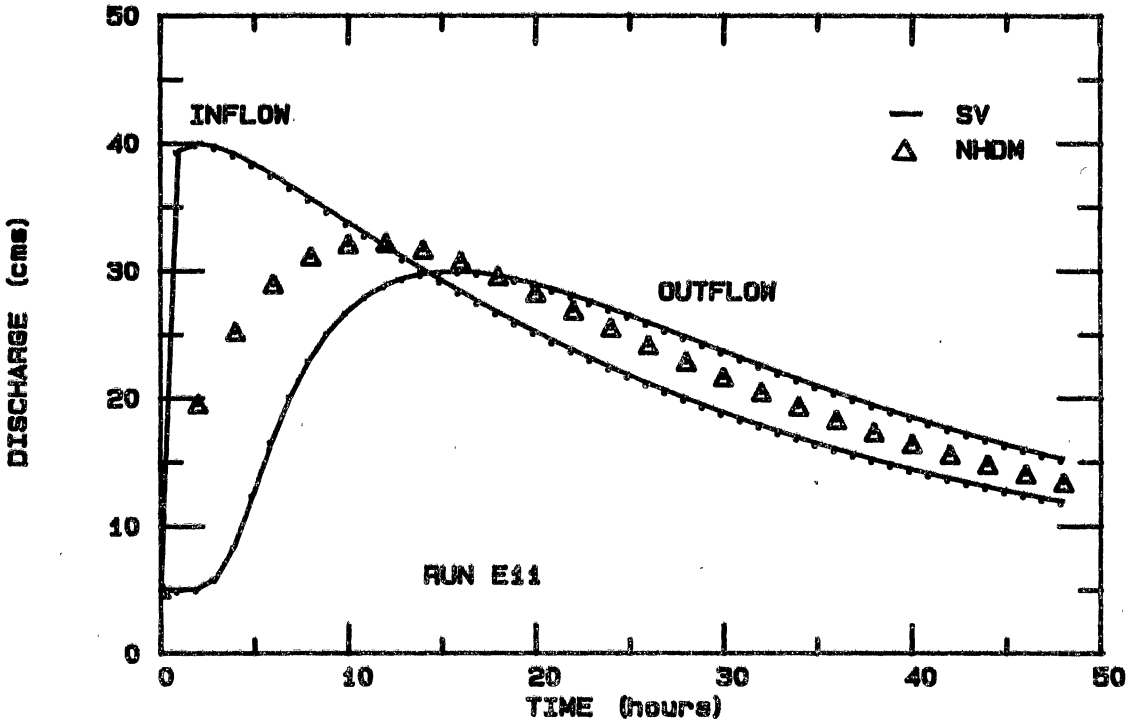
INFLOW
OUTFLOW
SV
NHDM
RUN E11
DISCHARGE (cms)
TIME (hours)
0
10
20
30
40
50

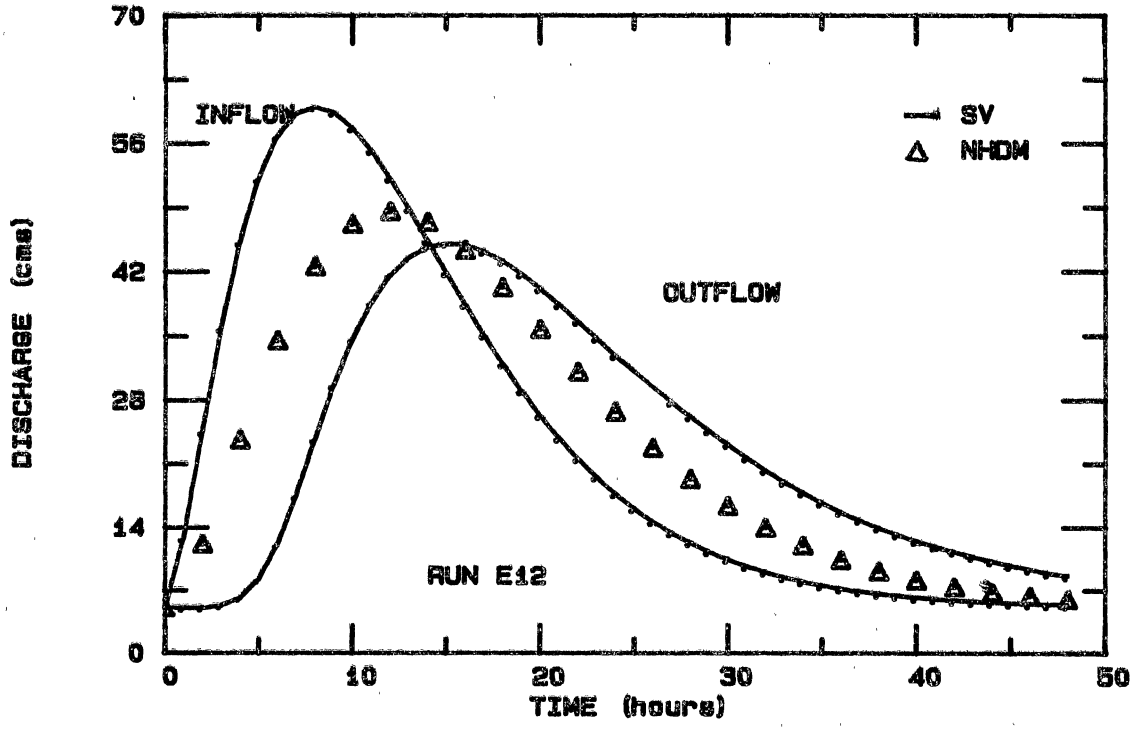
INFLOW
OUTFLOW
SV
NHDM
RUN E12
DISCHARGE (cms)
TIME (hours)
0
14
28
42
56
70
10
20
30
40
50

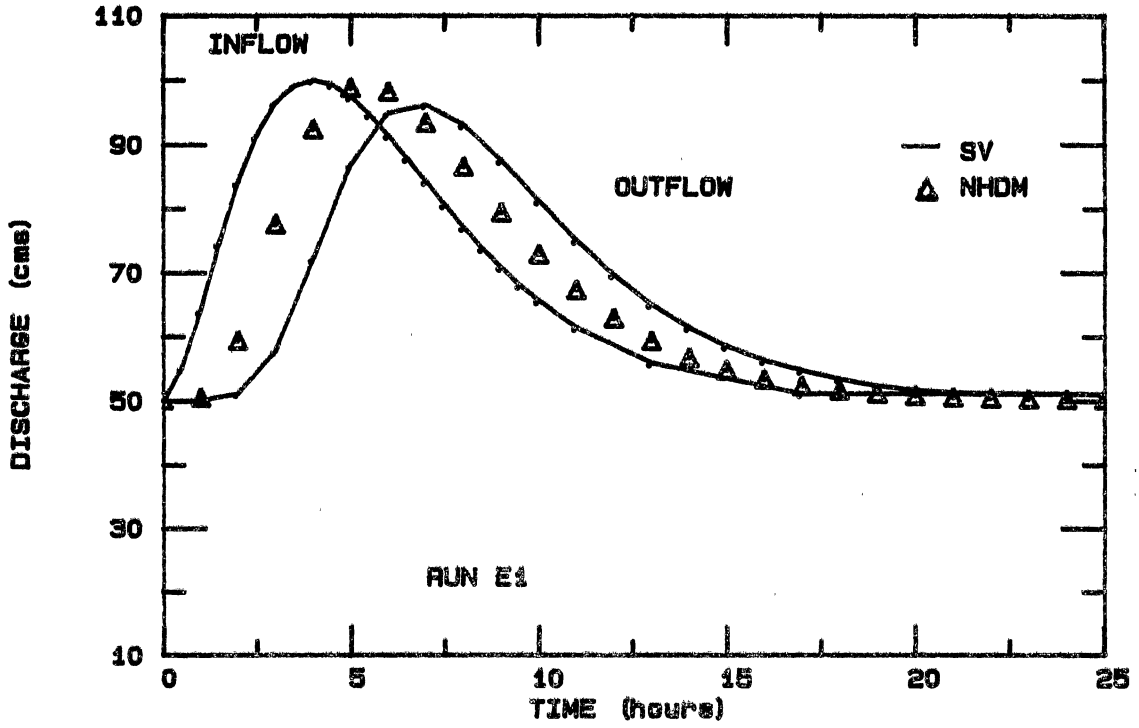
INFLOW
OUTFLOW
SV
NHDM
RUN E1
DISCHARGE (cms)
TIME (hours)
110
90
70
50
30
10
0
5
10
15
20
25

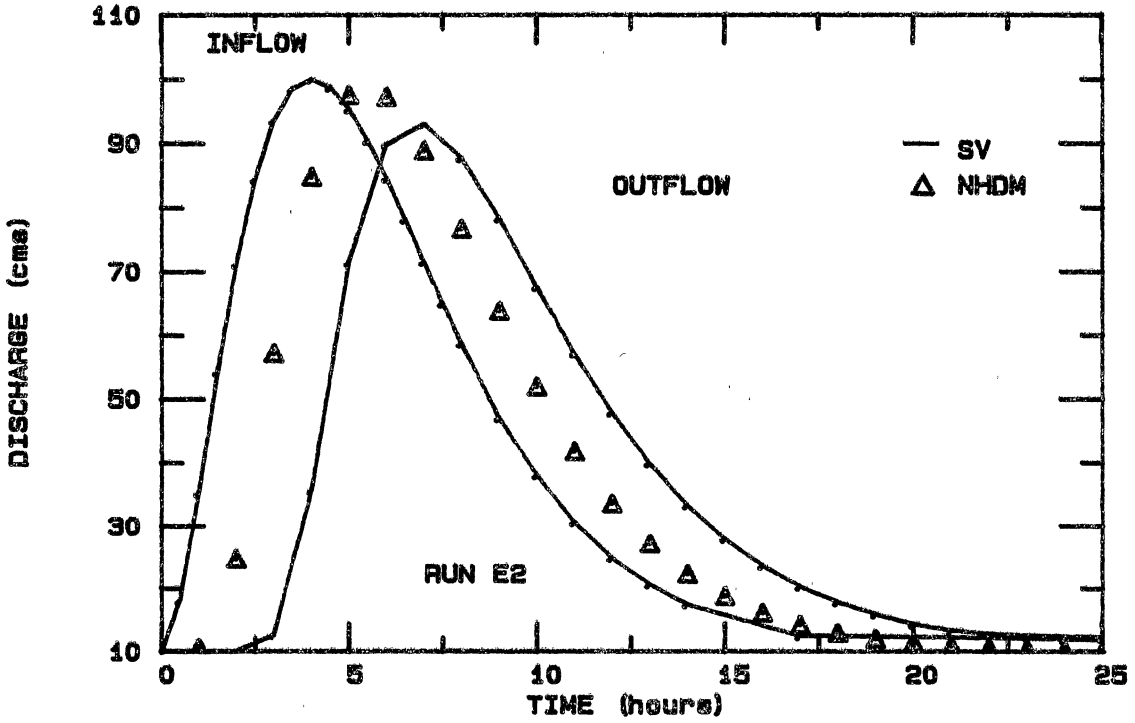
INFLOW
OUTFLOW
SV
NHDM
RUN E2
DISCHARGE (cms)
TIME (hours)
110
90
70
50
30
10
0
5
10
15
20
25

APPENDIX E

FINITE ELEMENT FORMULATION

FINITE ELEMENT FORMULATION

Nwagozie and Tyagi (1984) presented a finite element solution to the Saint Venant equations. Their derivation is similar to the derivation used by Smith (1977), varying only in the selection of shape functions. Nwagozie and Tyagi (1984) selected linear shape functions for all variables to keep calculations simple and to minimize computational cost. Smith (1977) used a quadratic shape function to describe flow rate. An error was found in Nwagozie and Tyagi's finite element equations. The second term of the finite element momentum equation was incorrect. The correct formulation is presented here. This derivation is also intended to present the reader with some understanding of the finite element model used for the evaluation of the Hydrodynamic Muskingum method.

Linear functions are selected for the description of depth, flow rate and velocity. A two node element is used with the variables being defined at the ends. The depth, y, is defined as follows,

$$y = N^{e}_{i}\ y_i + N^{e}_{i+1}\ y_{i+1} \qquad (A.1)$$

where N^{e}_{i} and N^{e}_{i+1} are basis functions for element e, at nodes i and i+1, respectively, given by,

$$N_i = (1-x/L) \qquad (A.2)$$

$$N_{i+1} = (x/L) \qquad (A.3)$$

L is the element length and x is the distance down the element. Similar relationships can be written for velocity, flow rate and friction slope.

Applying Galerkin's principle (Zienkiewicz, 1971) to equations 2.1 and 2.2 yields,

$$\sum_{1}^{K-1} \int_{0}^{1} N^T \left(\frac{\partial v}{\partial t} + y\frac{\partial v}{\partial x} + v\frac{\partial y}{\partial x} - q \right) dx = 0 \qquad (A.4)$$

$$\sum_{1}^{K-1} \int_{0}^{1} N^T \left(\frac{\partial v}{\partial t} + v\frac{\partial v}{\partial x} + \frac{Vq}{y} + g\left(\frac{\partial y}{\partial x} + S_f - S_o\right)\right) dx = 0 \qquad (A.5)$$

where K is the total number of nodal points and N^T is the transpose of the shape function. Equations A.4 and A.5 can be evaluated over the length of an element giving the following nonlinear, finite element equations for the continuity and momentum equations, respectively,

$$\frac{L}{6}\begin{bmatrix}2 & 1\\ 1 & 2\end{bmatrix}\begin{Bmatrix}y_1\\ y_2\end{Bmatrix} + \frac{1}{6}\begin{bmatrix}v_2-4v_1 & 2v_2+v_1\\ -v_2-2v_1 & 4v_2-v_1\end{bmatrix}\begin{Bmatrix}y_1\\ y_2\end{Bmatrix} - \frac{Lg}{2}\begin{Bmatrix}1\\ 1\end{Bmatrix} = 0 \qquad (A.6)$$

$$\frac{L}{6}\begin{bmatrix}2 & 1\\ 1 & 2\end{bmatrix}\begin{Bmatrix}v_1\\ v_2\end{Bmatrix} + \frac{1}{6}\begin{bmatrix}-2v_1-v_2 & 2v_1+v_2\\ -v_1-2v_2 & v_1+v_2\end{bmatrix}\begin{Bmatrix}v_1\\ v_2\end{Bmatrix}$$
$$+\frac{Lg}{2}\begin{bmatrix}2 & 1\\ 1 & 2\end{bmatrix}\begin{Bmatrix}(v/y)_1\\ (v/y)_2\end{Bmatrix} + \frac{g}{2}\begin{bmatrix}-1 & 1\\ -1 & 1\end{bmatrix}\begin{Bmatrix}y_1\\ y_2\end{Bmatrix} + \frac{gL}{6}\begin{bmatrix}2 & 1\\ 1 & 2\end{bmatrix}\begin{Bmatrix}Sf_1\\ Sf_2\end{Bmatrix} - \frac{gS_oL}{2}\begin{Bmatrix}1\\ 1\end{Bmatrix}$$
$$= 0 \qquad (A.7)$$

where y and v are the time derivatives. The element equations A.6 and A.7 can now be assembled into matrix equations (Zienkiewicz, 1971) containing the total number of elements, N. A dimensionless time weighting factor can be incorperated in the forward difference scheme of the time derivative.

The matrix equations can then be solved by imposing an upstream and a dowmstream boundary condition. The upstream boundary condition can be defined using the inflow hydrograph. The downstream boundary condition can be defined using a rating curve or a simplified version of equation 2.2, containing only the pressure, friction, and gravity terms.

A Newton-Raphson iterative method in conjunction with the Gauss elimination technique can be used to solve the system of linear algerbraic equations .

VITA

John Lawrence Ruffini

Candidate for the Degree of

Master of Science

Thesis: THE APPLICABILITY OF HYDRODYNAMICALLY DERIVED MUSKINGUM FLOOD ROUTING COEFFICIENTS.

Major Field: Agricultural Engineering

Biographical:

Personal Data: Born in Toowoomba, Australia, December 1960, the son of Raul and Vivienne M. Ruffini.

Education: Graduated from Saint Mary's Christian Brothers College, Toowoomba, Australia, in December 1978; recieved Bachelor of Engineering with a major in Agricultural Engineering from Darling Downs Institute of Advanced, Toowoomba, Australia, in March 1983; completed requirements for the Master of Science Degree at Oklahoma State University in December 1985.

Professional Experience: Research Assistant, Department of Agricultural Engineering, Oklahoma State University, August, 1984 to August, 1985.

Professional Organizations: American Society of Agricultural Engineers.